New Jersey Institute of Technology

Digital Commons @ NJIT

Dissertations
Electronic Theses and Dissertations

Fall 1-31-2001

Numerical modeling and optimization of waterjet based surface decontamination

Konstantin Babets
New Jersey Institute of Technology

Recommended Citation

ABSTRACT

NUMERICAL MODELING AND OPTIMIZATION OF WATERJET-BASED SURFACE DECONTAMINATION

by

Konstantin Babets

The mission of this study is to investigate the high-pressure waterjet based surface decontamination. Our specific objective is to develop a practical procedure for selection of process conditions at given constraints and available knowledge. This investigation is expected to improve information processing in the course of material decontamination and assist in the implementation of the waterjet decontamination technology into practice. The development of a realistic procedure for processing of a chaotic and non-accurate information constitutes the main accomplishment of this study.

The research involved acquisition of representative information about removal of brittle, elastic and viscous deposits. As a result an extended database representing jet based decoating has been compiled and feasibility of the damage free decontamination of various surfaces including highly sensitive ones is demonstrated. Artificial Intelligence techniques (Fuzzy Logic, Artificial Neural Networks, Genetic Computing) have been applied for processing of the acquired information and a realistic procedure of such an application has been developed and demonstrated. This procedure enables us to integrate available information about surface in question and existing numerical models. The developed procedure allows a user to incorporate both qualitative (linguistic) and quantitative (crisp) information into a process model and to predict operational conditions

for treatment of an unknown surface using a readily detectable single experimental parameter that characterizes a deposit/substrata combination. The suggested technique is shown to perform reliably in the case of incomplete and chaotic information, where the traditional regression based methods fail.

Numerical simulations of the two-phase flow inside a waterjet nozzle are conducted. Numerical solutions of the partial differential equations of the two-phase turbulent jet flow are obtained using FLUENT package. The numerical prediction of jet velocity profiles and the interface between the two phases (water - air) inside a nozzle are in good agreement with experimental data available in the literature. Thus the current problem setup and the results of simulations can be applied to improvement in the nozzle design.

A realistic procedure for the design of the jet based surfaces decontamination developed, as a result of this study, is applied for optimization of the removal of the paint, rust, tar and rubber from the steel surface.

NUMERICAL MODELING AND OPTIMIZATION OF WATERJET-BASED SURFACE DECONTAMINATION

by
Konstantin Babets

A Dissertation
Submitted to the Faculty of the
New Jersey Institute of Technology
in Partial Fulfillment of the Requirements for the Degree of
Doctor of Philosophy in Mechanical Engineering

Department of Mechanical Engineering

January 2001

APPROVAL PAGE

NUMERICAL MODELING AND OPTIMIZATION OF WATERJET-BASED SURFACE DECONTAMINATION

Konstantin Babets

Dr. Ernest S. Geskin, Dissertation Advisor   Date
Professor of Mechanical Engineering, NJIT

Dr. Avraham Harnoy, Committee Member   Date
Professor of Mechanical Engineering, NJIT

Dr. Zhiming Ji, Committee Member   Date
Associate Professor of Mechanical Engineering, NJIT

Dr. Raj Sodhi, Committee Member   Date
Associate Professor of Mechanical Engineering, NJIT

Dr. Haim Grebel, Committee Member   Date
Professor of Electrical and Computer Engineering, NJIT

BIOGRAPHICAL SKETCH

Author: Konstantin Babets

Degree: Doctor of Philosophy in Mechanical Engineering

Undergraduate and Graduate Education:

- Doctor of Philosophy in Mechanical Engineering,
  New Jersey Institute of Technology, Newark, NJ, 2001

- Engineer-Specialist in Mining Engineering,
  Krivoy Rog Technical University, Krivoy Rog, Ukraine, 1996

Major: Mechanical Engineering

Presentations and Publications:

Babets, K., Geskin E.S. and Goldenberg B., "Experimental and Numerical Investigation of Waterjet Rust Removal", Submitted to Journal of Metallurgical and Material Transactions, B.

Babets, K., Geskin E.S., "Artificial Intelligence in Open Pit Mining Applications", Stand-by Presentation at World Mining Congress, 2000. October, Las Vegas, Nevada.

Babets, K., Geskin E.S., "Optimization of Jet Based Material Decontamination", Submitted to International Journal of Applied Thermodynamics.

Geskin, E.S., Shishkin, D., Babets, K., "Ice, Cryogenic and Polymer Added Jets", Chapter in the Book, "Abrasive Water Jet, A View on Future", 2000. Published by Institute for Industrial Technologies and Automation.

Babets, K., Geskin E.S., "Optimization of Energy Utilization in the Course of Material Processing", 2000. International Symposium on Advanced Thermodynamics and Energy Utilization ECOS 2001.

Babets, K., Geskin E.S., "Application of Soft Computing Techniques for Optimization of the Waterjet Based Surface Processing", 2000. International Conference on Jetting Technology, 6-8 September, Ronneby, Sweden.

Geskin, E.S., Goldenberg, B., Shishkin, D., Babets, K., "Development of the Ice Based Surface Processing Technology", 2000. International Conference on Jetting Technology, 6-8 September, Ronneby, Sweden.

Geskin, E.S., Goldenberg, B., Shishkin, D., Babets, K., "Ice Based Surface Decontamination", 2000. Fourth U.S. Department of Energy International Decommissioning Symposium, June 12-16, Knoxville, TN.

Babets, K., Geskin, E.S., "Application of Fuzzy Logic for Modeling of the Waterjet Paint Stripping", 2000. An International Journal of Machining Science and Technology, Volume 4, Number 1.

Geskin, E.S., Goldenberg, B., Shishkin, D., Babets, K., Petrenko, O., "Ice Based Decontamination of Sensitive Surfaces", 2000. NSF Design & Manufacturing Grantees Conference, January 2-6, Vancouver, Canada.

Babets, K., Geskin, E.S., Shishkin, D., "Application of Artificial Intelligence for Waterjet Modeling and Optimization", 1999. Second International Symposium on Mineral Resources Quality Control, Yalta, Ukraine.

Babets, K., Geskin, E.S., "Fuzzy Logic Model of Waterjet Depainting: Grapho – Analytical Approach", 1999. 10th American Waterjet Conference, August, Houston, TX.

Babets, K., Geskin, E.S., Chaudhuri, B., "Neural Network Model of Waterjet Depainting Process", 1999. 10th American Waterjet Conference, Houston, TX, August

Babets, K., Geskin, E.S., "Optimization of Jet Based Material Decontamination", 1999. International Symposium on New Applications of Water Jet Technology, Ishinomaki, Japan, October 19-21.

Geskin, E.S., Shishkin, D., Babets, K., "Application of Ice Particles for Precision Cleaning of Sensitive Surfaces", 1999. 10th American Waterjet Conference, August, Houston, TX.

Geskin, E.S., Shishkin, D., Babets, K., "Investigation of Icejet Machining", 1999. NSF Design & Manufacturing Grantees Conference, January 5-8, Long Beach, California.

Geskin, E.S., Tismenetskiy, L., Shishkin, D., Babets, K., "Development of Icejet Machining Technology", 1996. First International Symposium on Mineral Resources Quality Control, Krivoy Rog, Ukraine.

This dissertation is dedicated to
my wife Irene and daughter Natalie

ACKNOWLEDGMENT

The author wishes to express his sincere gratitude to his advisor, Dr. E. S. Geskin, for his remarkable guidance, constant supervision, friendship, and moral support throughout this research.

Special thanks to Dr. Harnoy, Dr. Ji, Dr Sodhi, and Dr. Grebel for serving as members of the dissertation committee, having kindly read through the original manuscript, and providing many valuable suggestions. Additionally, sincere thanks to Dr. Boris Goldenberg, Mr. D. Shishkin and Mr. O. Petrenko for their timely help and suggestions in this study.

The author is grateful to the Department of Mechanical Engineering, New Jersey Institute of Technology for providing TA funding for this research.

Also thanks are due to Mr. A. Logan (Church and Dwight Corp, Arm and Hammer division) for providing experimental materials and device.

The author also appreciates the encouragement and help from his friends: Andrey Titov, Nickolai Markarian, Ruslan Mudriy.

And finally, grateful thanks and deep appreciation to the author's wife, Irene, his father Eugene, mother Svetlana, sister Irene and baby Natalie - for their support, encouragement and love through all these years. I could not have done it without you.

TABLE OF CONTENTS

Chapter   **Page**

TABLE OF CONTENTS
(Continued)

Chapter   **Page**

TABLE OF CONTENTS
(Continued)

LIST OF TABLES

LIST OF FIGURES

LIST OF FIGURES
(Continued)

xv

LIST OF FIGURES
(Continued)

LIST OF FIGURES
(Continued)

CHAPTER 1

INTRODUCTION

Today's rapidly developing and changing technologies and industrial products and practices frequently carry with them the increased generation of materials that, if improperly dealt with, can threaten both public health and the environment. Therefore the increasing attention is now being paid to the process, defined as material cleaning. In this work the term "cleaning" determines various surface decontamination technologies, e.g. sterilization, derusting, decoating, degreasing etc. Cleaning involves removal of undesirable substances from substrate surface without alteration of the surface geometry and properties. There is an enormous variety of cleaning operations ranging from street cleaning to decontamination of the space craft parts prior to assembly. Current cleaning technologies are extremely low energy efficient and environmentally non-friendly. Conventionally, removal of a soil attached to a surface involves flooding the surface with a solvent, most often water, with or without a detergent, and subsequent dumping of the solvent, with or without recycling. In most cases a solvent is delivered to the surface as a fluid stream. The soil is entrained by the fluid mechanically or chemically and carried out by the off-stream. An object can be submerged into solvent or if the surface is an enclosure (tank, vessel), the solvent fills the space surrounded by the surface in question. Solvents can be delivered by a cleaning tissue, jet, etc.

Cleaner technologies based on physical decoating are commercially available or are being developed to replace solvent strippers. These technologies take advantage of the differences in physical properties between the coating and the substrate to destroy the

bonding and/or abrade the coating from the underlying substrate. Among available coating removing techniques the most promising ones appear to be the blasting technologies. These include but not limited to: plastic media blasting, wheat starch blasting, sodium bicarbonate wet blasting, high pressure water blasting and cryogenic blasting. It is clear that the water blasting constitutes the most effective technology. Water is readily available, comparatively inexpensive, and induces no damage to environment. The complete separation of water and debris facilitates material recovery. Therefore complete pollution prevention is feasible.

The deposit removal by an impinging waterjet is the most realistic replacement to chemical strippers. The principal advantages of the waterjet are the feasibility of the decontamination of a wide variety of surfaces and potential for complete recycling of cleaning water and off-products. In most cases the waste stream generated in the course of waterjet cleaning constitutes a mechanical mixture of water and debris. The debris generated during water cleaning are not contaminated by solvents or other foreign substances and can be at least partially reused. Waterjets have been customarily used for various cleaning applications such as street and car washing, scale, paint and rust removal, etc. Commercial waterjet cleaning equipment including the equipment for cleaning of tanks is manufactured by a number of companies. Moreover, there are a number of contractors routinely providing waterjet cleaning services. The existing commercial technologies however, do not assure completeness of the deposit removal and the water consumption is extremely high. Because of these and some other shortcomings of waterjet cleaning, the use of solvents remains to be the principal precision cleaning technique.

The current research is therefore concerned with experimental and numerical investigation of the waterjet based surface decontamination. This study will outline the effective ranges of the application of this technology and identify the key process variables responsible for the effective and competitive application of the waterjet technology for decontamination of various types of materials.

CHAPTER 2

ALTERNATIVE DECONTAMINATION TECHNIQUES

2.1 Overview of Existing Cleaning Technologies

Cleaner technologies based on physical coating removal are commercially available or are being developed to replace solvent strippers. Physical coating removal technologies take advantage of differences in physical properties between the coating and the substrate to destroy the bonding and/or abrade the coating from the underlying substrate. Protecting the underlying substrate from damage while achieving good coating removal is a major concern.

Cleaner coating removal technologies are developing rapidly to fill a variety of process needs. Cleaner coating removal technologies use one or more of four general types of physical mechanisms (USPA, 1994):

- Abrasive technologies wear the coating off with scouring action.

- Impact technologies rely on particle impact to crack the coating to remove it.

- Cryogenic technologies use extreme cold to make the coating more friable and induce differential contraction to debond the coating.

- Thermal technologies use heat input to oxidize, pyrolyze, and/or vaporize the coating.

Many cleaner organic coating removal applications combine these methods. The abrasion and impact mechanisms typically occur together in technologies emphasizing one mechanism over the other. For example, sodium bicarbonate stripping relies mainly on abrasion with some removal by impact. On the other hand, plastic media blasting

4

(PMB) relies mainly on impact to crack and remove the coating but includes some abrasive action. The cryogenic technologies use a coolant, such as liquid nitrogen, to provide a cooling mechanism supplemented with PMB or other technology using an impact removal mechanism. Thermal technologies burn the organic coating to form an ash but often are followed by ash or soot removal with a technology providing an impact mechanism.

2.2 Plastic Media Blasting

The plastic media blasting (PMB) coating removal process eliminates the use of solvent strippers. The process uses nontoxic plastic media for coating removal and stripping process, thus eliminating generation of wastewater.

The PMB process uses low-pressure air or centrifugal wheels to project plastic media at a surface. The blast particles have sufficient impact energy, coupled with hardness and geometry. To chip away or erode the coating. The sharp-faceted particles fracture on impact, leaving new sharp edges to allow continued use for stripping.

Applications of PMB removal include but not limited to powder coatings, urethanes, military chemical agent resistant coatings, epoxies, high solids, polyamid, acrylic lacquers, polysulfide sealants, fluorocarbon films.

2.3 Wheat Starch Blasting

The process uses nontoxic, biodegradable media for coating removal and does not generate volatile organic air emissions. The wheat starch blasting media are made from

renewable agricultural products Wheat starch blasting is a completely dry stripping process.

Wheat starch blasting sues low-pressure air to propel particles at the painted surface. The coating is stripped away by a combination of impact and abrasion. Although wheat starch blasting sues generally similar equipment and techniques to PMB, the process has somewhat different operating characteristics and stripping action.

Wheat starch blasting is known mainly for its gentle stripping action. Therefore most of the testing and application has been on sensitive substrates such as thin aluminum, particularly sort alloys or anodized surfaces (e.g., commercial aircraft skins), sensitive composites (e.g., automobile fiberglass or plastic or aircraft radomes).

2.4 Burnoff Coating Removal

Burnoff coating removal technologies use a combination of volatilization, pyrolysis, and oxidation to remove organic coating materials. Thermal methods completely avoid the use of solvents for coating removal but generate potentially contaminated offgas and wastewater streams. Burnoff systems use temperatures of 370 deg C (700 deg F) or higher to volatilize and/or burn the organic coating material. Burnoff coating removal is commonly used for high-volume, noncritical parts such as the hooks, racks, overspray collectors, or other similar parts. Burnoff methods can be used to remove both conventional and power coatings.

2.5 Carbon Dioxide Pellet Cryogenic Blasting

Carbon dioxide (CO2) stripping generates a smaller amount of waste than all of the available technologies and some of the emerging thermal technologies. Upon impacting the surface being cleaned or decoated, the CO2 pellets disintegrate and sublime, that is, they pass directly from solid to gaseous state without appearing in the liquid state, thus not generating a spent media residue.

CO2 pellet blasting applies a blast medium much the same way, as does PMB. Compressed air or liquid nitrogen thrusts small CO2 pellets at a coated surface. The CO2 pellets remove the coating by a combination of impact, embrittlement, thermal contraction, and gas expansion. The CO2 pellet technology is primarily useful in food processing automotive manufacturing electronics, aerospace.

2.6 High-Pressure Water Blasting

High-pressure water blasting eliminates the use of chemical strippers containing HAPs. However, wastewater is generated that contains paint debris. The stripping water can be recycled to reduce waste volume. Unlike dry stripping processes, water stripping does not generate dust.

High-pressure waterjet stripping removes coating with a stream of water projected from specially designed nozzles at pressures of 15,000 psi to 50,000 psi or more. High-pressure pumps supply water to a system of stationary or rotating nozzles that spray the water stream onto the coated surface. The coating is removed by the kinetic impact of the water stream.

2.7 Liquid Nitrogen Cryogenic Blasting

The liquid nitrogen cryogenic coating stripping process eliminates solvent use and results in no ash or residual to clean. Liquid nitrogen is used to cool the part and to help propel plastic bead blasting media. The process does not use air to propel the media, so neither dust nor wastewater is generated.

The cryogenic technology takes advantage of extreme cold to embrittle and shrink the coating. The liquid nitrogen is sprayed on items to be stripped, thus chilling the coating, causing greater thermal contraction of the coating than of the substrate. Tensile stresses thus develop within the coating and make it brittle. High velocity, nonabrasive plastic pellets (media) are then blasted by centrifugal throw wheels to make the coating crack, debond, and break away from the substrate.

Liquid nitrogen cryogenic coating removal works well for removal of heavy coating buildups such as those that accumulate on coating line fixtures.

2.8 Laser Cleaning

Laser cleaning requires using laser and an inert gas to clean and prepare surfaces. It is relatively inexpensive for variety of applications, works at variable throughput within those applications and uses no scarce resources such as water. It uses and emits no toxic chemicals such as acids or basis. Laser cleaning relies simply on ultraviolet light and inexpensive inert gases such as nitrogen or argon. It presents minimal risk with proper handling. Laser cleaning removes the smallest contamination and also a lot of gross materials, and is amenable to incorporation into flexible tooling of high reliability and long life.

CHAPTER 3

LITERATURE SURVEY

A number of investigations of waterjet cleaning and decoating have been reported. Up to date most of the information about the correlation between process parameters and process output was based on various experimental studies. The process parameters in question include water pressure, nozzle traverse rate, nozzle type and size, standoff distance, type of abrasive, if any. The results of the studies are summarized as follows.

Water pressure determines jet velocity and turbulent properties, which influence the jet cleaning. When water pressure increases, material removal rate, cleaning width and depth also increase (Galecki and Vicker, 1982; Haferkamp, et al., 1992; Kang et al. 1993; Xu and Summers; 1994; Leu, et al., 1994; Geskin, et al., 1995, 1996, Meng, et al, 1995, 1996). Also it was found that there exists a threshold pressure, below which no material removal occurs no matter how large a water flow rate is and how long a process may take. (Erdmann-Jesnitzer, et al., 1980; Midden, et al., 1990; Wu and Kim, 1995).

Experimental studies on the effects of traverse rate on water jet cleaning show that the width or depth of material removal decrease with an increase of travel speed (Hashish and duPlessis, 1978; Saunders and Barton, 1986, Singh, et al., 1994; Leu, et al., 1994; Xu and Summers, 1994; Wu and Kim, 1995; Hlavac, 1995; Geskin, et al., 1995; Meng et al., 1995, 1996a, 1996b, 1996c). These experimental results show that width or depth of material removal decrease with the increase of travel speed. An increase of travel speed may result in a decrease of energy delivered per unit of coating area. Singh,

9

et al., (1992) have discussed the complete coating removal envelope at various travel speeds for a given standoff distance and pressure. In this study traverse speed during decoating was divided into three regions: incomplete coating removal, complete coating removal, and substrate damage.

There are two types of commonly used nozzles in waterjet material decontamination. These are the round-jet nozzles and the flat-jet nozzles. Round shape nozzles produce a jet with minimized divergence to reach a good efficiency at a greater distance from the nozzle. Contrary to this, the flat-jet enlarges only in one direction, the divergence orthogonal to this direction is minimal. Flat jets are being used at smaller distances from a nozzle to load larger area (Louis and Schicor, 1982). Harbaugh and Fincher (1993) designed a specific nozzle for complex surfaces with improved jet coherency and as a result higher level of delivered energy. This effect was attained due to the combination of flat and round nozzles with translation and rotation along the centerline. A similar application was once mentioned by Saunders and Barton (1986). A long cohesive jet is used to form a jet with minimal energy loss. Fan jets work better at low cleaning rates and shorter distances for removal of larger areas (Wu and Kim, 1995; Xu et al., 1994). Multiple orifices of smaller sizes, which may be preferable to single-orifice of larger size work more effectively (Waston, 1993; Harbaugh, 1993; Gracey, 1989, Babets (current work, 2000).

At a given pressure larger nozzles are more efficient than smaller ones. Experimental results have shown, that width and depth of decoating, and thus material loss increases with the increase of nozzle diameter (Wu and Kim, 1995, Babets, (present

work)). Similar results were also shown in the experimental studies of Watson, (1993); Leu, et al., (1994); Geskin, et al., (1995, 1996) and Meng, et al., (1995, 1996a, 1996b).

A new concept of critical cleaning standoff distance was first reported by Leu et al., (1994), then discussed by Geskin, et al., (1995, 1996) and Meng et al. (1995, 1996a). This concept implies that there exist a standoff distance, above which the cleaning becomes ineffective. A similar concept of effective standoff distance was also used in the selection of the standoff distance in jet cleaning (Wu and Kim, 1995). Experimental observations have shown that there exists an optimal standoff distance at which the volume of material removal is the greatest at a given travel speed (Louis and Schikorr, 1982; Kang, et al., 1993). Also it was shown that the cleaning rate increases with an increase of the standoff distance until it reaches the maximum at a certain standoff distance. After that the cleaning rate declines with increased standoff distance (Hashish and duPlessis, 1978; Galecki and Vickers, 1982; Haferkamp, et. Al., 1984; Leu, et al., 1994; Xu and Summers, 1994; Geskin, et al., 1995, Wu and Kim, 1995, Babets et al., (1999). The optimal standoff distance is related to coating and substrate materials, jet structure and properties, operational parameters such as nozzle size, water pressure, travel speed, etc.. Meng, et al., (1996b, 1996c) firstly introduced mathematical models for the evaluation of the optimal standoff distance for the cases of stationary and moving waterjet cleaning.

Duration of the jet-surface interaction is in order of 0.0001~0.001 seconds. This time is too short for completion of chemical reaction. The chemical should therefore be applied to the surface prior to impact (Summers, 1993). Nut a surfactant added in the jet can provide corrosion inhibition on the cleaned surface (Hall, 1986). The effect of the

surfactant (1% FC-722) was tested and reported by Geskin, et al., (1995), which proved that good cleaning performance could be achieved by this method.

The use of high temperature water as opposed to cold water is more effective in removing the grease (Summers, 1982), and temperature influence on the jet cleaning or material removal process was mentioned by Neusen and Schramm, 1978; Louis and Shikorr, 1982). Improvement of nozzle geometry (l/d ratio and conical angle) may influence jet cleaning or material removal rate (Minden, et al., 1990, Bury, et al., 1974).

Meng in (1996a, 1996b, 1996c) made an attempt to develop a mathematical model for prediction of water jet depainting based on the Springier theory of material erosion by a liquid impact. The rate of depainting was estimated by the balance of available momentum of impinging droplets and the momentum required for the paint separation. Springier's equation determining dimple formation was used to estimate a required momentum while a semi empirical equation of the development of a turbulent jet enabled us to estimate available momentum in the impingement zone. The suggested mathematical model included an empirical variable, which needs to be determined by special experiments.

It is expedient however to construct model of cleaning process using process characteristics acquired in the course of routine operations. Statistical techniques, conventionally used for construction of the empirical correlations are not effective in this case. The form of the correlation needed for the construction of regression equations is not known *a priori*. Also the available qualitative (linguistic) information accumulated in the course of technology application cannot be sufficiently utilized by the statistical

techniques. It is necessary to select a practical procedure to process all available quantitative and qualitative information.

The goal of the current research is in the focus on the information processing problems in the course of waterjet based material processing. The ultimate goal, however, is to develop a simple and practical technique for prediction of the results of cleaning, that will facilitate the implementation of waterjet based cleaning into the industrial practice.

CHAPTER 4

OBJECTIVES AND MOTIVATION

4.1 Objectives

The mission of this study is the investigation of the jet based material decontamination. Our specific objective is to develop a practical numerical procedure for selection of the optimum process parameters at given process constraints and available knowledge about process conditions. We will use Artificial Intelligence and Finite Element techniques to achieve this goal.

The specific goals of current research can be summarized as following:

- Experimental feasibility study of jet surface cleaning. These case studies help us to understand the possibilities of the application of jets for surface cleaning. Also they help us understand the peculiarities of jet based cleaning technology, such as wide variety of cleaning situations, availability of qualitative information, but not quantitative, etc. These peculiarities dictate the need for a special approaches in process modeling.

- Construction of the prediction model of a jet cleaning based on the principals of the Fuzzy Logic.

- Construction of the prediction model of a jet cleaning based on the principals of the Artificial Neural Networks.

- Construction of the prediction model of a jet cleaning based on the integration of a conventional Clustering and the Neural Network Driven Fuzzy Reasoning techniques.

- Selection of the optimal process characteristics by Genetic Algorithms.

- Numerical study of the flow formation in a nozzle. (Application of the Finite Element Method).

- Numerical study of the two-phase flow in the cutting head. .(Application of the Finite Element Method).

- Development of the Generic Procedure for selection of the cleaning technology.

4.2 Motivation

Water jet cleaning is characterized by a large number of variables, representing mechanical and geometrical properties of the surface, properties of the deposit, deposit distribution and adhesion to the substrate surface, geometry and dynamics of the waterjet, conditions of the removal of the water and debris. The history of the substrate prior to cleaning is usually very complicated and information about this history is rather limited. It is necessary to maximize the use of the available information in order to develop an effective cleaning technology. The various artificial intelligence (AI) techniques enable us to achieve this most efficiently.

CHAPTER 5

COMPUTATIONAL TECHNIQUES

5.1 Introduction

In data /information processing the objective is to gain the understanding of a complex phenomena through "modeling" of the system either experimentally or analytically. Then after a model of a system has been obtained, various procedures (e.g. sensitivity analysis, statistical regression, etc.) can be used to gain a better understanding of the system. There are, however situations in which the phenomena involved are very complex and not well understood and for which the first principle models are not effective. Even more often, experimental measurements are difficult and/or expensive. These difficulties lead us to explore the application of Soft Computing (A.I.) techniques as a way of obtaining models based on experimental measurements. The field of Soft Computing is comparatively new, and it includes fuzzy logic, neural networks, expert system, cellular automata, chaotic systems, wavelets, complexity theory, anticipatory systems among others. But only fuzzy logic, neural networks and genetic algorithms have reached the stage of development, where they are used for real world problems (Michalewicz, 1996).

Fuzzy logic systems address the imprecision of the input and output variables directly by defining them with fuzzy sets (fuzzy numbers), that generally expressed in linguistic terms. Moreover they allow for very complex and nonlinear systems to be described in vary simple terms, thus making them easier to understand. Another

important feature of fuzzy systems is their ability to accommodate the existing expert knowledge of a process into a model by expressing it in terms of fuzzy rules.

Neural Networks on the other hand model a system by using sets of input-output data to train some generic model of a system. Neural Networks are very good at modeling very complex nonlinear relationships with large number of input and output variables, and in classification problems. Models based on neural networks also easy to optimize, since although the model itself is not given in terms of explicitly defined function, the gradient of this function can be found numerically. Artificial neural networks are most likely to be superior to other modeling methods under the following conditions (Masters, 1993):

- The data on which conclusions are based is "fuzzy", and subject to possibly large error.

- The data exhibits significant unpredictable nonlinearity.

- The data is chaotic.

- The relationship between different groups of data is hidden.

The combination of the above two techniques often results in greater flexibility and/or more clear representation of a model then when they are used separately. This combination is often referred to as neuro-fuzzy model of a system. Neuro-fuzzy approach also allows overcoming some traditional problems in using fuzzy logic or neural networks, such as the problem of defining a membership function, extracting fuzzy rules, etc.

Optimization of a system is an essential part of any analysis, but conventional optimization techniques (i.e. gradient based) are not quite effective in case of A.I. based

models. The reason is that in most cases the model is not given in terms of mathematical function, therefore a gradient is quite problematic to find. Genetic Algorithms represent a computational method from the area of Evolutionary Computing, and they are very effective in finding a near optimum solution for any kind of model.

Figure 5.1 summarizes the above overview and suggests a choice of a modeling technique based on the type of the information available about the process. Usually, the information available for waterjet coating removal involves some numerical data acquired in the course of simple routine experiments and supplemented by an expert knowledge. The expert knowledge is expressed in simple linguistic expressions such as "FAST traverse rate AND MODERATE impact pressure result in HIGH stripping rate and INSIGNIFICANT substrate damage", or "LOW nozzle traverse rate AND VERY HIGH impact pressure AND SMALL standoff distance result in LOW stripping rate and HIGH substrate damage". If the process in question does not involve many input and output variables, the most effective modeling technique is fuzzy logic. This approach is represented by the path 1-2-4-6-9-12 on the flow chart on Figure 5.1.

If available experimental information about the waterjet decoating involves a limited number of numerical data, a statistical technique combined with ANOVA table should be used (path 1-3-5-13, Figure 5.1). But as the number of input and output variables increases or if the empirical information is acquired from different sources, the conventional regression analysis is less effective. The major disadvantage of the multiple regression, however, is the necessity to have a preliminary information about the form of the regression equation. If the use of a standard statistical technique is too complicated or

ineffective, the artificial neural networks can be used for process modeling (Figure 5.1, path 1-2-4-8-11-13).

When the available knowledge is represented by a limited numerical data and limited linguistic information, the fuzzy rules cannot be accurately defined. Application of neural networks also becomes ineffective, since it requires fairly large amount of experimental data. Neuro-fuzzy modeling is proved to be sufficiently reliable and accurate for such systems. The use of various modeling techniques is illustrated in the following chapters of this work.

Of course, there are many more other "well-behaved" and reliable standard fitting methods, which will do a good job in modeling a process. And the use of those methods is in no way disparaged. The basic idea is to introduce the new and generally reliable techniques for modeling and optimization of waterjet coating removal process.

5.2 Architecture of Fuzzy Logic Modeling

In general a fuzzy logic modeling consists of the Fuzzy Preprocessing and Fuzzy Processing modules (Figure 5.2).

Fuzzy preprocessing involves representation of all available information in a form suitable for application of fuzzy logic technique. In fuzzy preprocessing module the knowledge pertaining to the process is obtained from various sources, such as experimental and empirical data, expert knowledge, linguistic formulation, etc. is utilized for process representation.

This module consists of three independent modules:

- Knowledge acquisition module

- Fuzzy vocabulary

- Fuzzy associative memory (FAM).
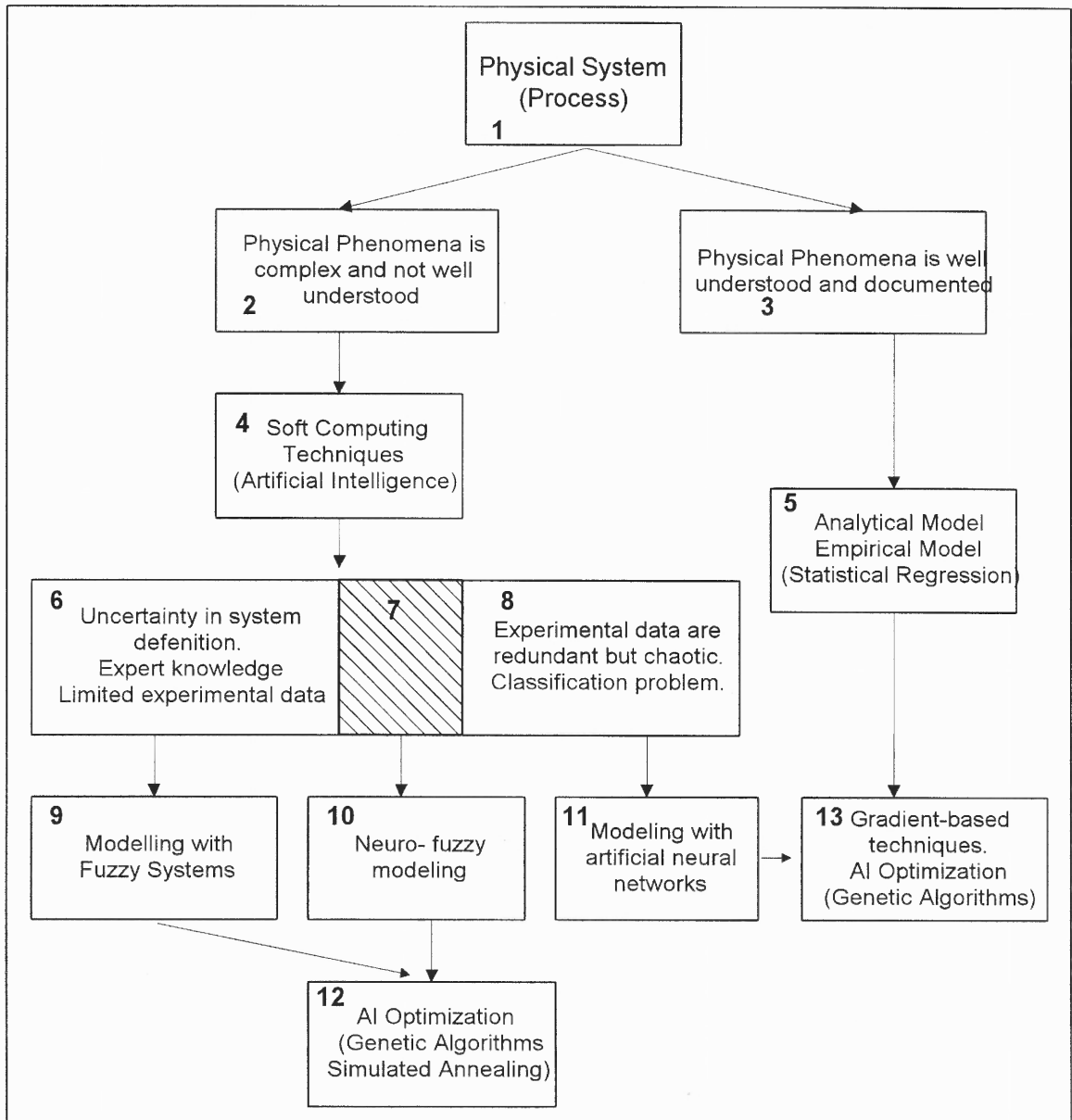
Figure 5.1 Choice of Modeling Technique
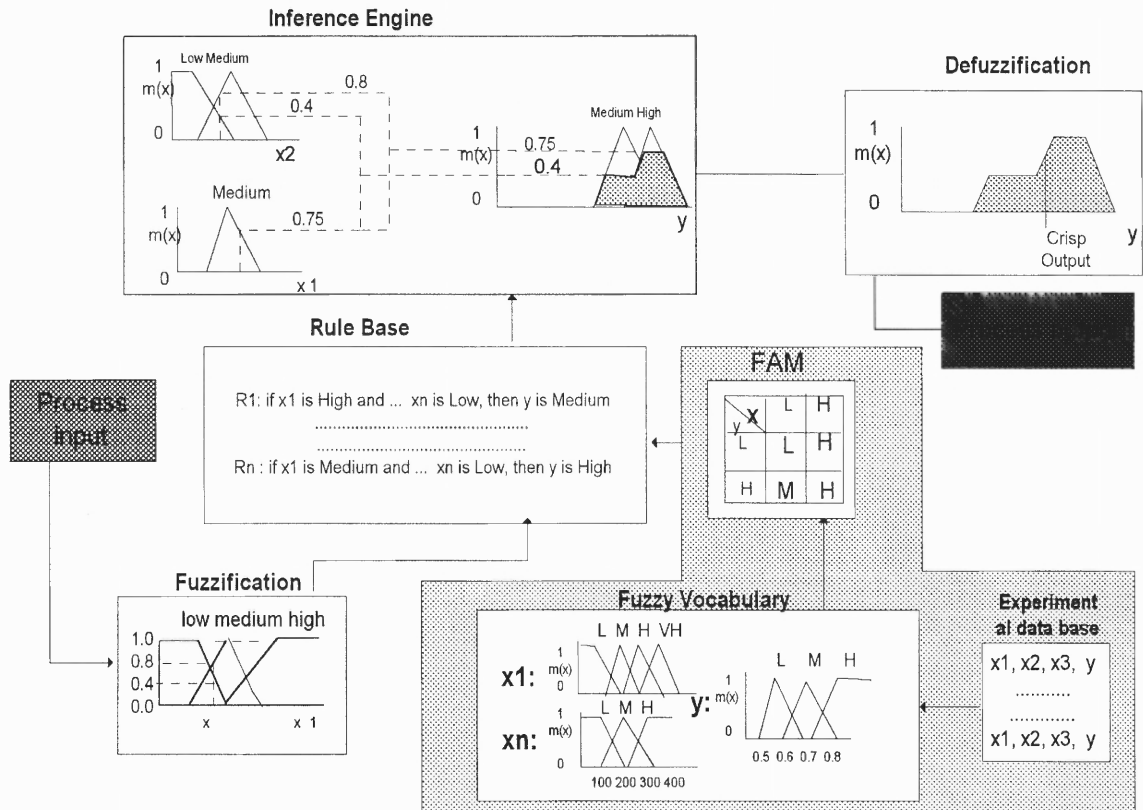
Figure 5.2 Architecture of Fuzzy Logic Modeling

The knowledge acquisition module constitutes a bank of all available pertinent information, crisp or linguistic, which can be stored in a computer memory. There is always a wealth of knowledge that cannot be formalized but nevertheless provides a significant insight about a process. In fact one of the major advantages of the fuzzy logic technique is its ability to utilize this knowledge. The fuzzy vocabulary module enables us to represent all available crisp information in a form acceptable by the fuzzy logic technique. In short, a crisp value of a process variable is replaced by a fuzzy set. The acquired knowledge is translated into a fuzzy language using the following few steps. The first step is identification of the ranges of the change of input and output variables. Then the interval of the change of each variable is divided into a set of subintervals and

each of the subintervals is assigned a membership function, and is given an appropriate linguistic name. This combination of a subinterval, its membership function, and its linguistic name constitutes a fuzzy set. Fuzzy sets of one particular variable usually overlap. The degree of overlap reflects fuzziness in the definition of fuzzy sets. The aggregation of all subintervals of one process variable on a single coordinate axis is called the Universe of Discourse of that variable. Figure 5.3 shows a typical example of Fuzzy Universe of Discourse for process parameter Water Pressure.
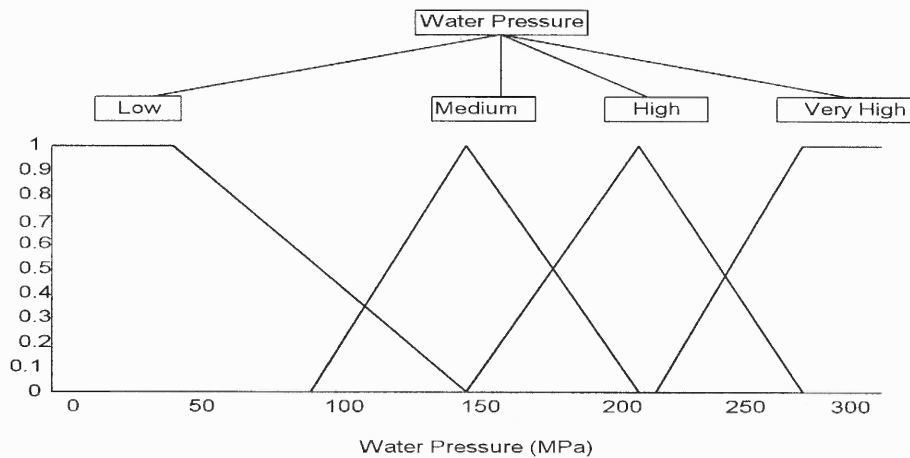
Figure 5.3 Example of Fuzzy Universe of Discourse

It is clear that construction of the fuzzy vocabulary involve in addition to the information acquired in the memory also a knowledge which cannot be stored, for example, an expert opinion.

Finally, the fuzzy logical equations or fuzzy rules relating variables defined by the fuzzy vocabulary are constructed in the FAM module. The fuzzy vocabulary provides a just representation of the process variables. The relationships themselves are constructed on the base of all available information, stored in the computer memory or provided by

an expert. In the field of fuzzy logic the most common way to express human knowledge is to form it into natural language expressions of the type:

IF premise (antecedent), THEN conclusion (consequent)

This form is commonly referred to as **IF-THEN** rule- based form. It represents the inference such that if we know the antecedent then the consequent can be inferred or derived. The constructed IF-THEN equations relate process variables stored in the fuzzy vocabulary. At the same time these equations express empirical or heuristic knowledge, derived from sources such as experiments or human experience, linguistically in this rule-based format. FAM contains a set of the fuzzy logical equations, which in the final analysis summarize all available knowledge about the process in question and present it in the form available for fuzzy modeling.

Modeling itself is carried out by the Fuzzy Processing Module, which converts the input information about a selected process manifestation into the information about output variables. The prior knowledge accumulated in FAM constitutes the base of these conversions. The Fuzzy Processing Module consists of the following independent modules:

- Process input module

- Fuzzification module

- Inference module

- Defuzzification module

Process input module enables us to store the pertinent input information. The fuzzification module converts the stored crisp data into fuzzy logic type information. For each crisp input data this module identifies a corresponding fuzzy set and the degree of

the belonging to this set. Due to the overlapping of the fuzzy sets, each input can be assigned to several fuzzy sets. The example of this operation is given in Figure 5.4.
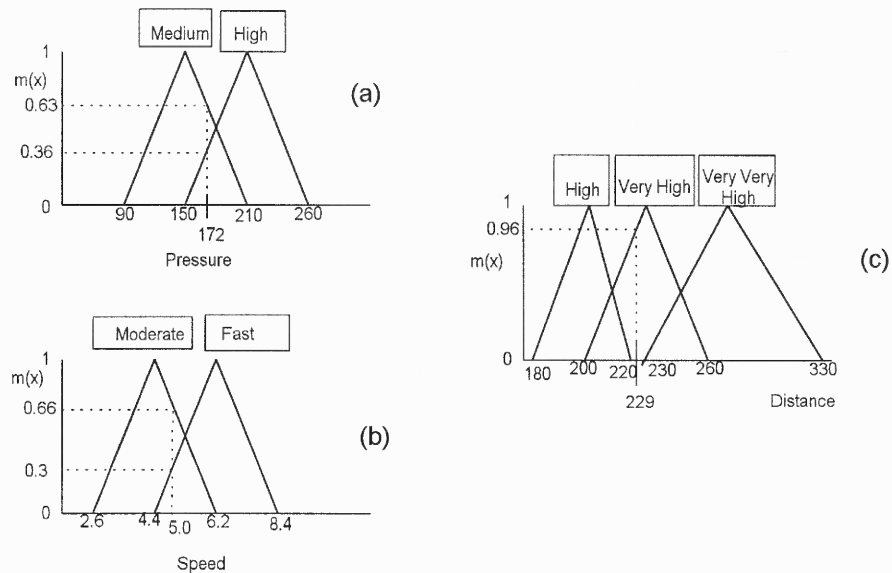
Figure 5.4 Fuzzification Module

Here a hypothetical process has a set of three control variables: {Pressure, Distance, Speed} and a set of output parameters, consisting of a single variable {Output}. Application of a set of crisp input values of {172, 229, 5} to Fuzzy Universes of Discourse of these control variables converts this crisp input set into four fuzzy input sets (since crisp input values can belong to more then one fuzzy value, but with different degree of membership): {Medium, Very High, Moderate}, {Medium, Very High, Fast}, {High, Very High, Moderate}, {High, Very High, Fast}.

The fuzzy input information developed in the fuzzification module is fed into the inference module. Here fuzzy rules pertinent to the information in hand are selected

(fired) and used to infer fuzzy values of output variables. It is clear that an each equation (fuzzy rule) generates a single fuzzy value of the output variable. Therefore we are interested in evaluating the following linguistic correlation:

{**Pressure, Distance, Speed**}-→ {**Output**},

expressed in terms of multiple fuzzy relations. In this hypothetical example we would deal with four such relations.

Fuzzy rules give us only linguistic correlation between sets of the input parameters and the output variable, instead we would like to estimate to what degree a rule's consequent (part to the right from the **then** statement) is true. In order to do so we apply the fuzzy inference technique. There are several methods of inference in fuzzy systems: We selected the min-max method, which involves comparatively simple numerical manipulations. In fuzzy min-max implication each rule is evaluated separately. Therefor continuing with this hypothetical example we evaluate each input fuzzy set, or conversely each rule, according to Figure 5.5 (a).

The result of this evaluation is a fuzzy region of the output variable and its degree of belonging to this region. In order to evaluate the degree of the truth (belonging) of the consequent of a rule we examine the degrees of truth of each antecedent and assign to the consequent the minimal one. Then these individual solution regions are aggregated into a final solution region (Figure 5.5 (b)), which determines the fuzzy value of the output variable. Analytically the above steps can be expressed with the help of the following equations.

$$\mu cfs[xi] \leftarrow \min (\mu pt(1), \mu pt(2), \mu pt(n)]) \qquad (5.1)$$

which indicates that the consequent fuzzy (cfs) set is modified by taking the minimum of predicate propositions.

And $\qquad \mu$sfs [xi] $\leftarrow$ max (μsfs [xi], μcfs [xn]) $\qquad$ **(5.2)**

Which shows that the solution fuzzy set (sfs) is updated by taking the maximum of either

the truth value of a solution fuzzy set or that the fuzzy set modified in equation.
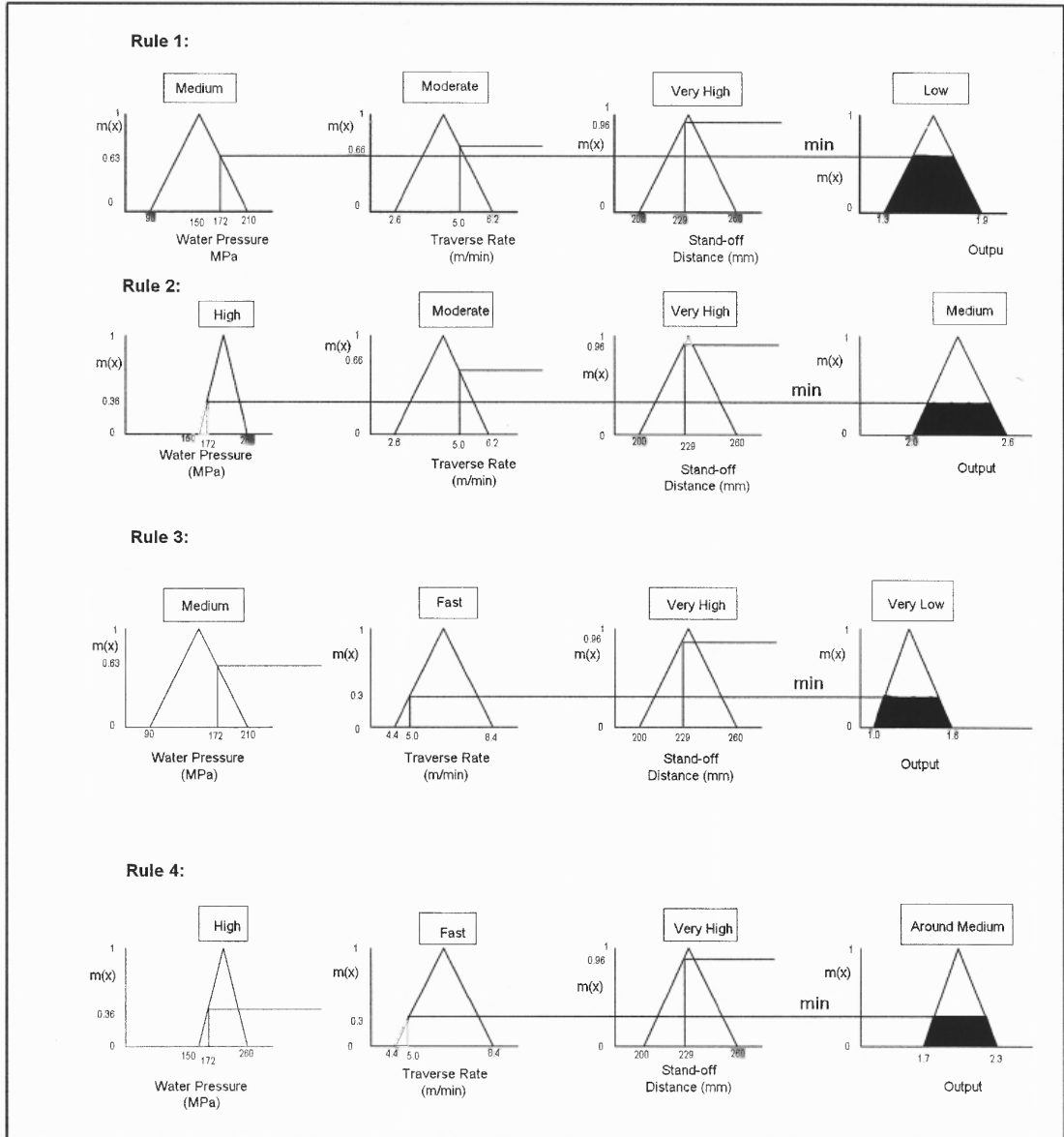
Figure 5.5 (a) Fuzzy Min-Max Implication
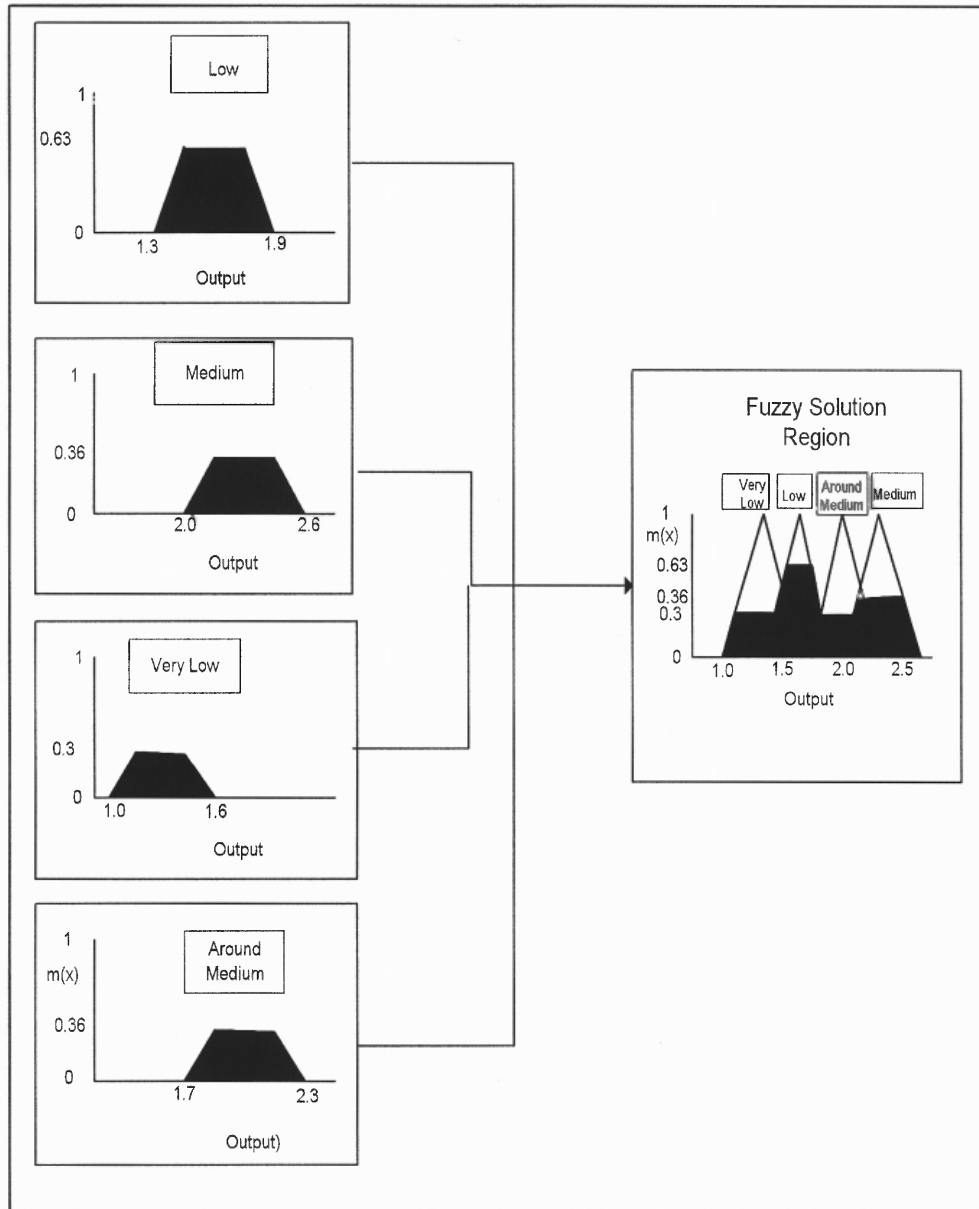
Figure 5.5 (b) Fuzzy Min-Max Implication

Finally, the defuzzification module converts the fuzzy output of the inference module in a conventional crisp result (Figure 5.6). The most commonly used defuzzification technique is the centroid method given by the following equation (Cox, 1994):

$$z = \frac{\sum\limits_{i=0}^{n} d_i \mu_y(d_i)}{\sum\limits_{i=0}^{n} \mu_y(d_i)} \qquad (5.3)$$

Here d is the value of the width of strip at some point, and μ(d) is the truth membership value for that point.
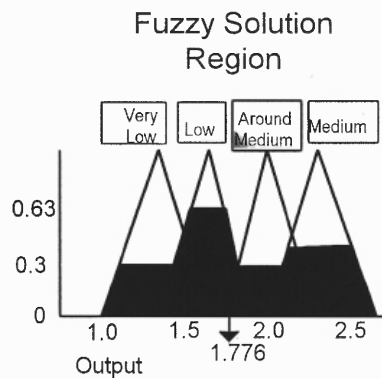
Figure 5.6 Centroid Defuzzification

5.3 Artificial Neural Networks

5.3.1 Introduction to Artificial Neural Networks

An artificial neural network consists of many interconnected identical elementary processing units or neurons, in architecture inspired by the structure of the cerebral cortex of the brain. A neuron is a simple processing unit (Figure 5.7), which consists of two parts. The first part simply sums up all the weighted inputs from other neurons, while the second part modifies this aggregated signal by applying an activation function to it. The input signals X1, X2, X3…, Xn are being sent to processing units through the network's connections.
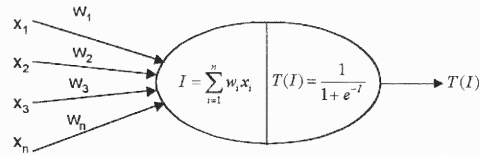
Figure 5.7 Schematic of Artificial Neuron

The connections between neurons in a network are assigned the so- called weights (wn), which modify input signal, making it either positive or negative, which corresponds to acceleration or inhibition of the signal in a biological neuron.

The working of a neuron is summarized with following equations.

$$I = \sum_{i=1}^{n} w_i x_i \quad \text{Sum of wighted inputs} \tag{5.4}$$

$$T = T(I) \qquad \text{Activation function}$$

Equation 5.4 shows that an input of a neuron is the sum of weighted outputs from the neurons in the proceeding layer. Equation 5.4 shows that a neuron generates an output by applying activation function to its aggregated input.

The most widely used activation function is the logistic sigmoid, given by:

$$\Phi(I) = \frac{1}{1 + e^{-\alpha I}} \tag{5.5}$$

The activation function limits the values of the output of an artificial neuron to values between two asymptotes (0-1 in this case). This limitation is very useful in keeping the output within a reasonable dynamic range.

The neurons in a network are usually arranged in layers (Figure 5.8). The number of layers in the network depends on a problem complexity. Within the network the information from a neuron in the preceding layer goes through the network connections to all neurons in the next layer. Each connection has its weight associated with the importance of this particular connection. Training or learning is the process of adjusting the internal parameters of a network (weights) to reach its optimum performance. During training (learning) process these weights are adjusted according to some particular algorithm, thus memorizing a functional relationship between input and output variables. The architecture of the backpropagation-training algorithm is shown in Figure 5.9. In this study the experimental database representing the process was divided into training data set and checking data set.
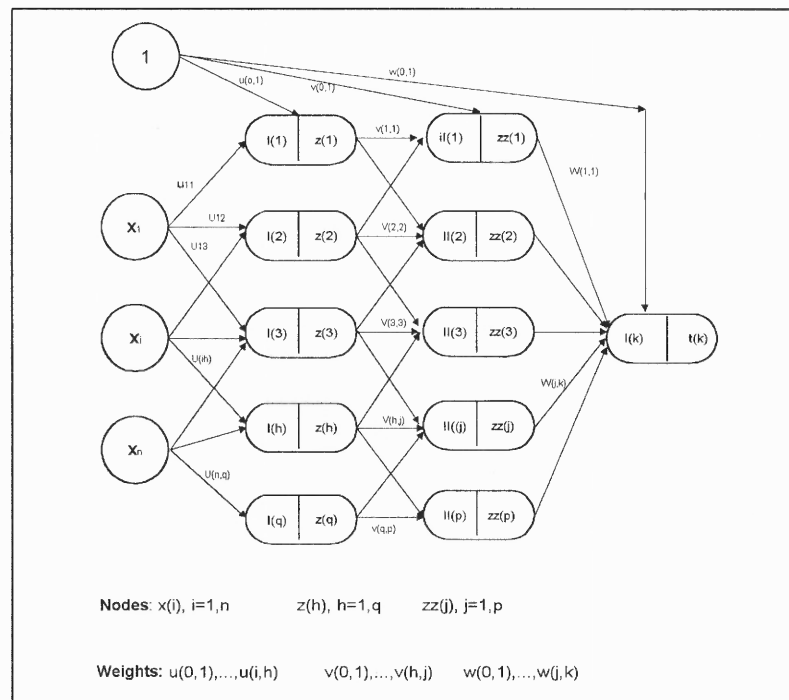
Figure 5.8 Artificial Neural Network

The data in each set were represented in form of input – output pairs. In a supervised learning an input pattern (combination of the input parameters), presented to the network, generates a random output. This generated output is compared to the desired target value to define an error. This error is then backpropagated to adjust the weights in order to minimize this error function. These new weights are then assigned to a network and the procedure is repeated for a new input – output pair. This procedure is repeated until all training data pairs are used. After each iteration the error is stored, to accumulate the total error. After all training data pairs are used (one epoch) the total error (the error accumulated through one epoch) is compared to some specified error tolerance. If the tolerance is not met the procedure is repeated. If the tolerance is satisfied the procedure is stopped and the weights adjusted after the last iteration constitute the output of the training. These weights are assigned to the network and the network is considered to be trained. To check the network performance the checking data set is used. After the network is checked to perform satisfactory it is used as the model of the process, i.e. for process prediction, sensitivity analysis, optimization, etc.

5.3.2 Neural Network Model of a Process

The network architecture used to represent an example process is shown in Figure 5.8. For this problem the three-layer network was chosen. The input layer consisted of three neurons X1, X2, X3. The output layer consisted of one neuron which corresponded to the process output variable T. Two hidden layers were used in the current network's architecture. A classical feed forward algorithm with backpropagation of error is used in the network training.
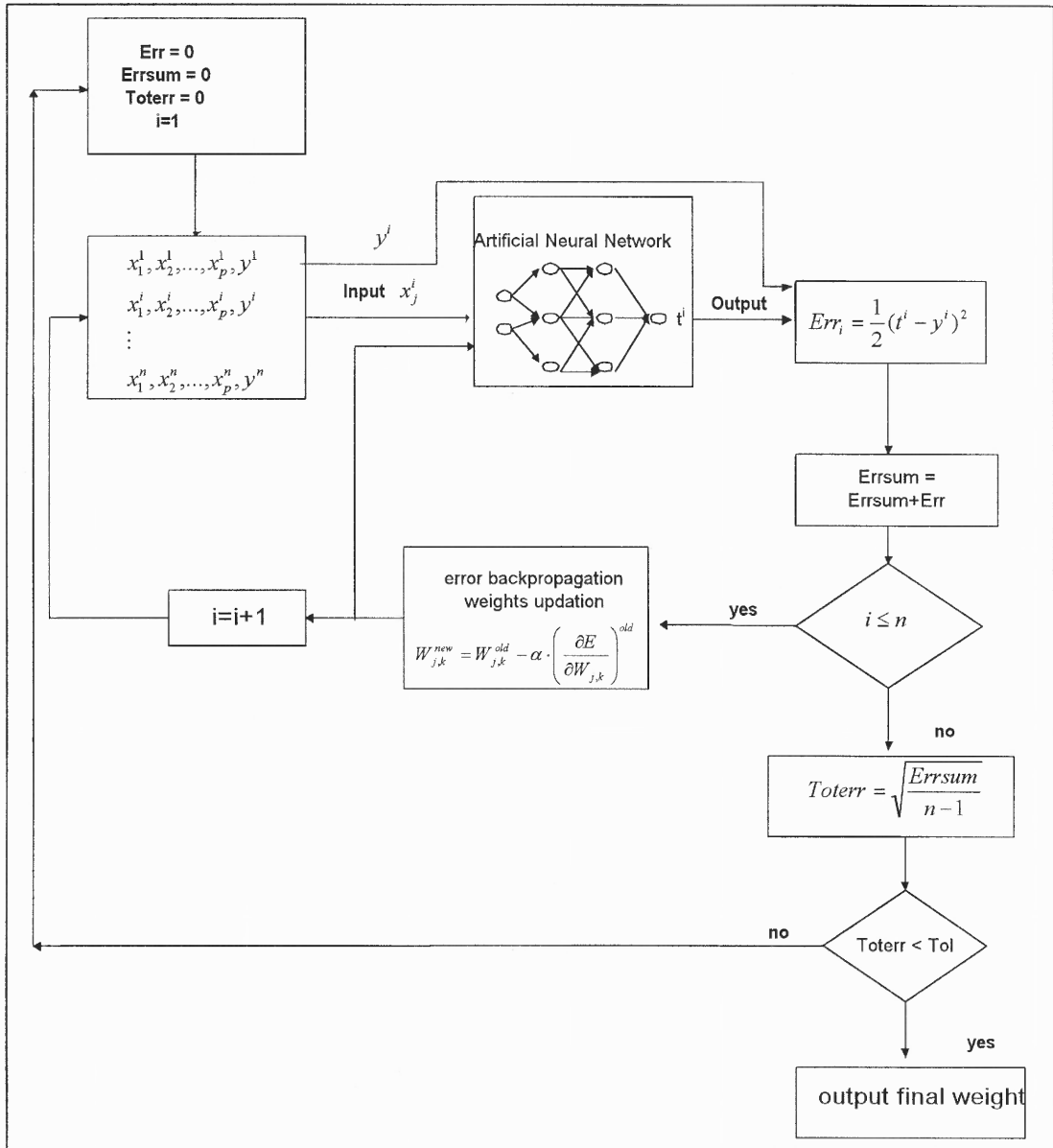
Figure 5.9 Backpropagation Training Algorithm

For a multilayer neural network with two hidden layers, three input neurons, one output

neuron and a notation given in Figure 5.8, the following set of algebraic equations apply:

First hidden layer :

$$I_{(h)} = U_{0,h} + \sum_{i=1}^{3} U_{i,h} \cdot X_i$$

$$Z_{(h)} = \frac{1}{1 + e^{-I_h}} \quad for \ h = 1,5$$

(5.6)

Second hidden layer :

$$II_{(j)} = V_{0,j} + \sum_{h=1}^{5} V_{h,j} \cdot Z_{(h)}$$

$$ZZ_{(j)} = \frac{1}{1 + e^{-II_j}} \quad for \ j = 1,5$$

(5.7)

Output layer

$$I_{(k)} = W_{0,k} + \sum_{j=1}^{5} W_{j,k} \cdot ZZ_{(j)}$$

$$T_k = \frac{1}{1 + e^{-I_k}} \quad for \ k = 1$$

(5.8)

The error is then computed as :

$$E = 0.5 \cdot \sum_k \left[Y_k - T_k \right]^2 \quad for \ k = 1$$

(5.9)

where Tk is the network's output and Yk is the experimental value of the output variable. The Equations 5.7-5.9 are the standard representation of signal propagation in a feed forward neural network. After the error is defined it is propagated backwards to define new weights. A weight updating is then performed according to the formulae (5.10), where the expressions in the brackets are the partial derivatives of the error function (Equation 5.9) with respect to weights on different connections, and η is a some small constant, termed the learning constant.

$$W_{j,k}^{new} = W_{j,k}^{old} - \eta \cdot \left(\frac{\partial E}{\partial W_{j,k}} \right)^{old}$$

$$V_{h,j}^{new} = V_{h,j}^{old} - \eta \cdot \left(\frac{\partial E}{\partial V_{h,j}} \right)^{old}$$

(5.10)

and

$$U_{i,h}^{new} = U_{i,h}^{old} - \eta \cdot \left(\frac{\partial E}{\partial U_{i,h}} \right)^{old}$$

Since error is a function of weights then these partial derivatives are evaluated as follows:

$$\frac{\partial E}{\partial U_{i,h}} = \frac{\partial E}{\partial T_k} \frac{\partial T_k}{\partial I_k} \frac{\partial I_k}{\partial ZZ_{(j)}} \frac{\partial ZZ_{(j)}}{\partial II_{(j)}} \frac{\partial II_{(j)}}{\partial Z_{(h)}} \frac{\partial Z_{(h)}}{\partial I_{(h)}} \frac{\partial I_{(h)}}{\partial U_{i,h}} =$$

$$-\left[Y_k - T_k \right] \cdot T_k \cdot \left(1 - T_k \right) \cdot W_{j,k} \cdot ZZ_{(j)} \cdot \left(1 - ZZ_{(j)} \right) \cdot V_{h,j} \cdot 1 - Z_{(h)} \cdot X_i$$

(5.11)

where E is given by Equation 5.9, T_k and I_k are given by (5.8). In the similar manner the rest of the desired derivatives are presented:

$$\frac{\partial E}{\partial V_{h,j}} = \frac{\partial E}{\partial T_k} \frac{\partial T_k}{\partial I_k} \frac{\partial I_k}{\partial ZZ_{(j)}} \frac{\partial ZZ_{(j)}}{\partial II_{(j)}} \frac{\partial II_{(j)}}{\partial V_{h,j}} =$$

$$-\left[Y_k - T_k \right] \cdot T_k \cdot \left(1 - T_k \right) \cdot W_{j,k} \cdot ZZ_{(j)} \cdot \left(1 - ZZ_{(j)} \right) \cdot Z_{(h)}$$

(5.12)

for h = 1,5, j = 1,5, k = 1

$$\frac{\partial E}{\partial W_{j,k}} = \frac{\partial E}{\partial Y_k} \frac{\partial Y_k}{\partial I_{y,k}} \frac{\partial I_{y,k}}{\partial W_{j,k}} = -\left[T_k - Y_k \right] \cdot Y_k \cdot \left(1 - Y_k \right) \cdot ZZ_j \text{ , for } j = 1,5 \text{ and } k = 1.$$

(5.13)

The new weights are then substituted into the network and this procedure is repeated iteratively until the network is trained. After the network is trained its performance is verified using a testing data set. At this point only the feed forward part of the algorithm is applied. When the network is verified to perform satisfactory it can be used as the

model of the process, for sensitivity analysis, optimization, or for prediction of an output, once an input is specified.

5.3.3 Sensitivity Analysis

In performing sensitivity analysis we are interested in evaluation of the degree of influence of different input variables on the process output. In other words, if we slightly perturb input, how would output react? And what input variable influences output(s) the most. For the network with two hidden layers, using the notation of Fig. 5.8 the desired gradients are found in the following manner (2):

$$\sigma_i = \frac{\partial T_k}{\partial X_i} = \frac{\partial T_k}{\partial I_{(k)}} \frac{\partial I_{(k)}}{\partial ZZ_{(j)}} \frac{\partial ZZ_{(j)}}{\partial II_{(j)}} \frac{\partial II_{(j)}}{\partial Z_{(h)}} \frac{\partial Z_{(h)}}{\partial I_{(h)}} \frac{\partial I_{(h)}}{\partial X_i} =$$

$$T_k \cdot [1 - T_k] \cdot \sum_{j=1}^{5} W_{j,k} \cdot ZZ_{(j)} \cdot (1 - ZZ_{(j)}) \cdot \sum_{h=1}^{5} V_{h,j} \cdot$$

$$Z_{(h)} \cdot (1 - Z_{(h)}) \cdot U_{i,h}$$

$$\text{(5.14)}$$

for i = 1,3, j = 1,5, h = 1,5

5.3.4 Modifications of Conventional Training Algorithm

The backpropagation -training algorithm discussed above has been proven itself as a reliable technique for training a traditional three or four layer network with nonlinear activation functions (logistic sigmoid (Equation 5.5), for instance). The convergence speed of the algorithm depends greatly on the choice of network parameters, such as number of layers, number of neurons in a layer, choice of activation function. The optimum combination of these parameters would, in most cases, result in excellent network training in less time. But, even with poor choice of network parameters, it is still

possible to train a network to perform satisfactory using the traditional backpropagation of error algorithm, though the training could be extremely slow.

In the past few years a fair number of modifications of the basic algorithm was suggested. The most important once, include the alternative weight update procedure, and the incorporation of linear regression into a network training process.

5.3.4.1 Momentum. In backpropagation with momentum, the weight change is in direction that follows the direction of the current gradient and the previous gradient. This is a modification of the gradient descent whose advantage arises when some training data is significantly different from the majority of data, or even incorrect. Thus the gradient descent in the wrong direction is averted. In order to implement the backpropagation with momentum algorithm the weights from the previous iteration(s) should be saved. And the weight update formulae (5.10) now become:

$$V_{h,j}^{(t+1)} = V_{h,j}^t - \eta \cdot \left(\frac{\partial E}{\partial V_{h,j}} \right)^t + \mu \cdot \left[V_{h,j}^t - V_{h,j}^{(t-1)} \right]$$

$$U_{i,h}^{t+1} = U_{i,h}^t - \eta \cdot \left(\frac{\partial E}{\partial U_{i,h}} \right)^t + \mu \cdot \left[U_{i,h}^t - U_{i,h}^{t-1} \right]$$

$$W_{j,k}^{t+1} = W_{j,k}^t - \eta \cdot \left(\frac{\partial E}{\partial W_{j,k}} \right)^t + \mu \cdot \left[W_{j,k}^t - W_{j,k}^{(t-1)} \right]$$

(5.15)

where, t- current training step, μ- momentum coefficient. The momentum coefficient μ is constrained to be in the range from 0 to1, exclusive of endpoints. Momentum allows the net to make reasonably large weight adjustments as long as the corrections are in the same general direction.

5.3.4.2 Batch Weight Updating. Yet another modification of conventional backpropagation algorithm makes use of what is called the batch weight updating. In this techniques the weight correction terms of the net are accumulated for several iterations, and weights are updated after the specified number of iterations. This procedure has a smoothing affect on the correction term, though sometimes it may increase chances of convergence to local minima.

5.3.4.3 Training with Regression. One reason that conventional backpropagation is slow to converge is that the error propagates back through non-optimum last hidden layer weights, thus resulting in far-from optimum changes in the other layer weights. This could be avoided if the last layer's weights are not generated randomly, but rather approximated with regression. This approach was shown to speed the training of a network greatly (40 fold), in some cases. The training algorithm is initiated by randomly generating all the weights on network connections, with the exception of the weights connecting the last hidden layer and the output layer. A training sample from the training data set is chosen and passed forward through the network's connections, until it reaches the last hidden layer. At this point the inverse activation of the desired output for each output neuron is calculated, based on the activation method for the output layer neurons. In the case of the linear activation method for the output neurons (i.e. Equation 5.9 is given by $\Phi(I) = I$), the inverse activation of the desired output equals to the output itself. If we now treat the last hidden layer's outputs as independent variables, and have a known desired input to an output neuron as the dependent variable, we have a regression

problem. And the weight vector connecting the last hidden layer and the output layer represents the unknown regression coefficients.

Thus, for a network with n hidden layer neurons (including the bias), and m data samples in the training data set we obtain:

$$\mathbf{A}\,\boldsymbol{\beta} = \mathbf{Y}, \tag{5.16}$$

where:

$\mathbf{A}$ (n x m)- is the matrix of network's last hidden layer activations for each training data sample in the training data set.

$\mathbf{Y}$ (m x 1) – a column vector of the measured dependent variable inverse activations.

$\boldsymbol{\beta}$ (n x 1) – a column vector of coefficients to be estimated (weights connecting the second hidden layer and the output layer).

Equation 5.16 can be solved for the weight vector using the general least square procedure.

$$\boldsymbol{\beta} = (\mathbf{A}'\mathbf{A})^{-1}\mathbf{A}'\mathbf{Y} \tag{5.17}$$

At this point the state of the training of the neural network is far more advanced then after the first iteration of the conventional backpropagation, because the optimal weights for the last hidden layer were computed with linear regression. And, thus, the mean squared error is minimized with extremely high precision. We now proceed with conventional backpropagation algorithm as described earlier. This combination of the conventional backpropagation with optimum calculation of the last hidden layer's weights by linear regression was proven to speed up the training process greatly and results in a network with better generalization capabilities. After this initial pass through the network the next training input-output pair is chosen, and the above steps repeated. As the training

proceeds, the features of model of the system under study are embedded in the weights that connect the input layer to the hidden layer (and interconnect hidden layers if more then one is used).

In the above-discussed algorithm the weight values produced by regression can contain very large values (5- 6 orders of magnitude), that could result in poor network generalization abilities. Moreover the algorithm can fail if the matrix A in Equation 5.17 is numerically close to singular. A zero pivot element may be encountered during the solution of linear equations (5.17), which results in very large magnitudes of the fitted parameters (weights in this case). The solution to this problem lies in application of the technique known as matrix SVD (Singular Value Decomposition). The matrix A in(5.16) is broken down into its singular value decomposition given by:

$$A = U W V^T \qquad (5.18)$$

where, U (m x n) - matrix of principal components (orthonormal basis for the subspace

spanned by the columns of A

W (n x n) - diagonal matrix of singular values.

V (n x n) – orthonormal matrix of right singular values.

In this method, only the most relevant information is retained to compute the weights. The least important information is discarded, because it is most likely resulted from noise. This is achieved by altering the diagonal matrix of singular values W. If a singular value in this matrix is less then a cutoff value, the value is changed to zero in the inverse matrix. The weights are then calculated as:

$$A=VS^{-1}U^{T}T \tag{5.19}$$

This method, though takes longer to implement, can not (at least theoretically) fail. Thus it constitutes a reliable technique to use in conjunction with linear regression in training of a neural network.

5.4 Integrated Neuro- Fuzzy Reasoning

5.4.1. T-H Method

Fuzzy reasoning realizes the flexibility of the reasoning corresponding to human logical reasoning. Therefore it has been proven effective when the conventional modeling techniques fail. However two problems of conventional fuzzy reasoning has not been solved yet: the method of determining membership functions and the adaptation of the reasoning to the environment. The problem of determining the membership function is even more appealing in case of multidimensional fuzzy space, where membership function design by experience or intuition is merely impossible. The second problem of conventional fuzzy reasoning is the lack of the adaptation of the existing rules to changing environment. In other words a low cost learning function is desired. The following method proposed by Hideyuki Takagi and Isao Hayashi (Takagi and Hayashi, 1991) solves the above stated problems by using learning functionality and nonlinearity of Neural Networks.

The T-H method consists mainly from three parts. These are outlined below and explained on the basis of the hypothetical example (Figure 5.10).

Part 1. The existing database is divided into two data sets- training (TDS) and checking data set (CDS). The number n of fuzzy rules (R) for the database is decided, and it is

divided into n classes using a conventional clustering technique. Thus the number of classes equals to the number of inference rules (R) (Figure 5.10(a)).

Part 2. After the number of inference rules has been established, and the data in both TDS and CDS are classified as either belonging to a class or not in a conventional Boolean way, a NN is used to learn the functional relationship between coordinates of a data point in TDS and its corresponding crisp (Boolean) membership in $R(i)$, $i=1,..n$. The CDS is then used to verify the network performance. After the classification network is verified to perform satisfactory it can be used for estimation of fuzzy membership in all $R(i)$, $i=1,..n$, for any data point (Figure 5.10(a). More rigorously we obtained the NN for membership estimation and fuzzy classification, which is used to determine the IF parts (conditional parts of the rules).

Part 3. The RHS parts of the rules are determined by using separate neural network with supervised learning, for each rule from part 1. Rules are usually of Sugeno-type. Sugeno type rules are where the output is a function of the inputs.

For instance the induced rule would be:

$$\text{If } (x_1, x_2) \text{ is } A^s, \text{ then } y^s = NN_s (x_1, x_2)$$

where NN_s (x_1, x_2) is a neural network that determines the output of the sth rule. Thus for each rule (class) R a neural network is created. Each class is represented in terms of the input-output pairs { X_i, Y} of the TDS. The network for each class Ri is trained until it is able to reproduce the functional relationship between input-output pairs in the TDS for that particular class. The CDS is then used to check the performance of the Net. Thus the

antecedent part (part after **then** statement) of the rule R_i can now be inferred by the corresponding Neural Network (NN_i.).

The steps above determine the **IF /Then** parts of each inference rule. The system identification process for the fuzzy model is then completed. The final control value y_i can now be determined according to the following:

$$y_i^* = \frac{\sum_{s=1}^{r} \mu_{A^s}(x_i) \cdot u_s(x_i)}{\sum_{s=1}^{r} \mu_{A^s}(x_i)}, i = 1,2 \dots n \tag{5.20}$$
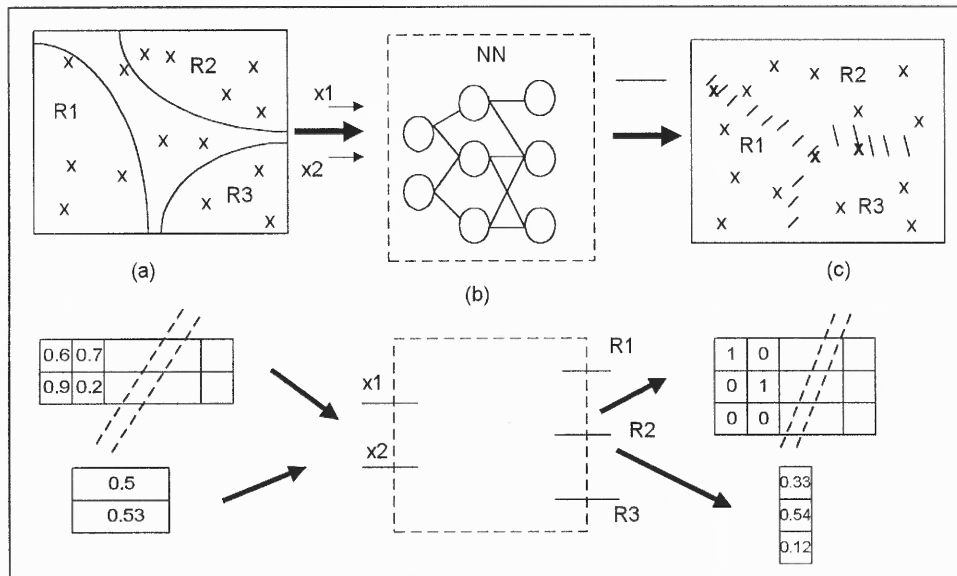
Figure 5.10 Design of Membership Function with NN.

(a) Input data space; (b) NN to determine membership values; (c) Data Space, partitioned into fuzzy rules. (From Takagi and Hayashi, 1991)
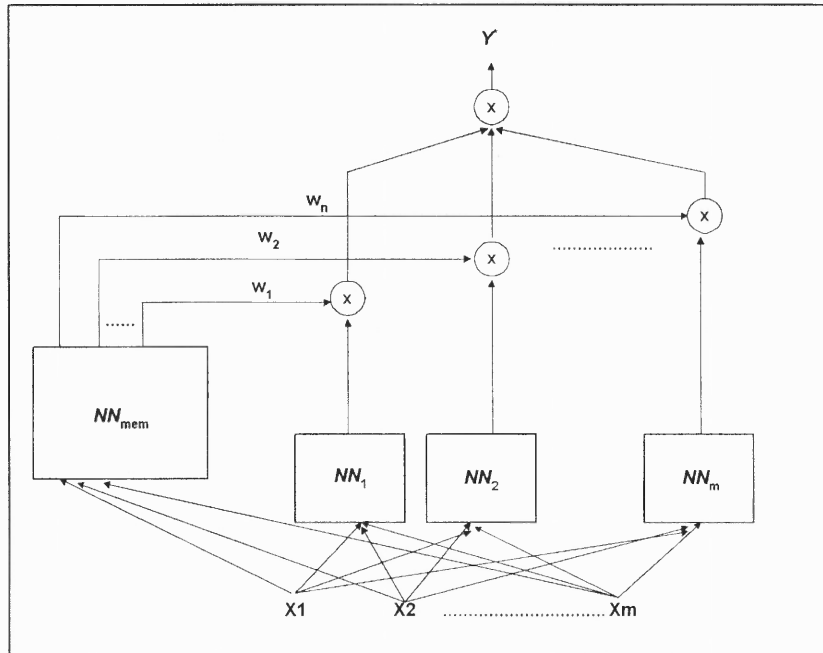
Figure 5.11 NN Driven Fuzzy Reasoning System.

NNmem is the NN that decides the membership values for each rule. NN1-NNm- NNs that determine the outputs yi for each rule. W1- Wm – membership values. (From Takagi and Hayashi, 1991)

5.5 Genetic Algorithms

5.5.1 Introduction to Genetic Algorithms

Genetic Algorithms were initiated and developed in early 70s by John Holland. He used the concept of Darwin's theory of evolution, which stressed the fact that the existence of all living things is based on the rule of "survival of the fittest" (Ross, 1995). Darwin also postulated that new breeds of living things come into existence through the process of reproduction, crossover, and mutation of the existing organisms. Evolution takes place in chromosomes, the genetic units that encode the features of living creatures. Natural selection is a process by which nature causes those chromosomes that encode

better characteristics (by some criteria) to reproduce more often, compared to the chromosomes that encode poorer characteristics (Michalewicz, 1992). Thus the next generation of chromosomes comes with better characteristics then the previous one. These evolutionary principals constitute the base for the computational technique-Genetic Algorithms.

5.5.2 Basic Concepts of Genetic Algorithms

Genetic algorithms found numerous applications nowadays. One of the most often applications of Genetic Algorithms is in optimization problems. Genetic algorithms have many advantages compared to standard optimization techniques (gradient based, etc). Genetic Algorithms do not rely on the analytical properties of the function being optimized (existence of a derivative). We start by generating the initial population of the chromosomes (bit strings), which encode information pertinent to the problem at hand. The information is to be encoded in a binary form (usually). Next step is to define an evaluation function (fitness) for the problem. Evaluation function is nothing else but a criterion according to which we evaluate how fit is a chromosome in the population. After all of the chromosomes are evaluated for their fitness we select the best ones according to our criteria. In order to maintain an equal size of the population, some chromosomes are selected more then ones. Then the selected chromosomes undergo genetic operations of crossover and mutation. Thus a new generation of the chromosomes appears. We repeat the steps above for the new generation. After some number of iterations the total fitness of the population is within some prescribed range and the best

chromosome (highest fitness value) in the generation hopefully represents the optimum solution. These steps are outlined in Figure 5.12.
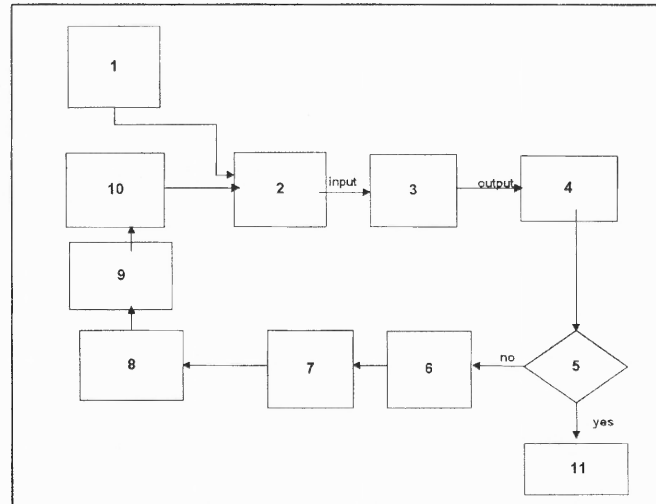
Figure 5.12 GA Based Optimization. Sequence of Operations

1. Initial random population of k chromosomes is generated. 2. The conversion of input from binary to decimal format and scaling. 3. The process model. 4. Determination of the fitness values. 5. The decision is made on whether the fitness values are acceptable. 6. The genetic reproduction. 7. Conversion from decimal to binary format. 8. Genetic crossover. 9. Genetic mutation. 10. New population of chromosomes. 11 The solution population.

CHAPTER 6

INVESTIGATION OF THE FLOW INSIDE WATERJET CLEANING HEAD

6.1 Previous Research on Waterjet Formation

The efficient application of waterjets to industrial surface decontamination requires a thorough understanding of the influence of different parameters involved in the process. The independent parameters involved in abrasive waterjet surface decontamination can be devided in two several groups (Hashish, 1991). The first group of parameters is process related and it includes nozzle traverse rate, standoff distance, number of passes, degree of overlap and the desired degree of surface cleanliness. The second group of parameters is jet-related and can be subdevided into hydraulic, abrasive and mixing (internal) parameters. The hydraulic parameters include water pressure, water flow rate, abrasive parameters include abrasive type, abrasive particle size and flow rate. A special attention needs to be paid to the internal parameters of the waterjet nozzle. These parameters consist of the internal diameters of a waterjet nozzle such as mixing tube diameter, mixing tube length and air flow rate through the abrasive inlet port. The reason a special attention should be paid to this group of parameters is because it is the least studied group and is the most difficult to control and optimize.

The importance of studying the flow charachteristics inside a waterjet flow have resulted in quite a few experimental and numerical studies of this phenomena. But the difficulties in numerical simulations of this complex flow and a lack of non-intrusive experimental techniques have resulted in sometimes controversial data.

A fair number of experimental studies was concerned with velocity measurements of the waterjet. The techniques most often used for non invasive measurements were limited to high-speed digital photography (Sawamura et al, 1999), Laser Transit Anemometry (LTA) (Chen and Geskin, 1990), Laser Doppler Velocimetry (LDV) (Neusen et al, 1992), etc. Neusen et al (1992) have shown that with the cutting head in place but with abrasive flow rate 0.0 kg/min, the exit mean velocity reduces substantially compared to pure waterjet velocities after primary nozzle.(Figure 6.1). Then they have suggested that the reason for the velocity drop is the momentum exhange between the liquid and gas phases in the mixing process. Next they show that after abrasive particles were mixed in the stream the mean exit velocity remained relatively constant, at approximately 260 m/sec, even though the abrasive mass flow rate was varied by 150% , and pressure was varied by 67%. (Figure 6.2).
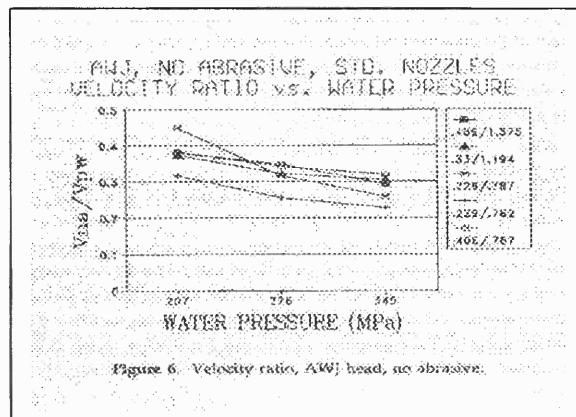
Figure 6.1 Velocity Ratio for AWJ with no Abrasive (Neusen et al, 1992)

Figure 7. Abrasive water jet velocities.
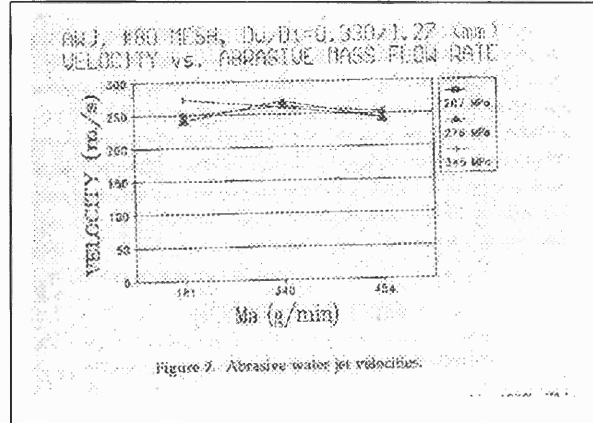
Figure 6.2 Abrasive Waterjet Velocities (Neusen et al, 1992)

Sawamura *et al* (1999) has shown that, on the contrary, approximately 9% velocity loss is found when the media flow rate is 0.0 kg/min. The velocity loss increases with the increase in the abrasive flow rate and it could reach up to 60% of theoretical value when the flow rate reaches 0.2 kg/min (Figure 6.3).
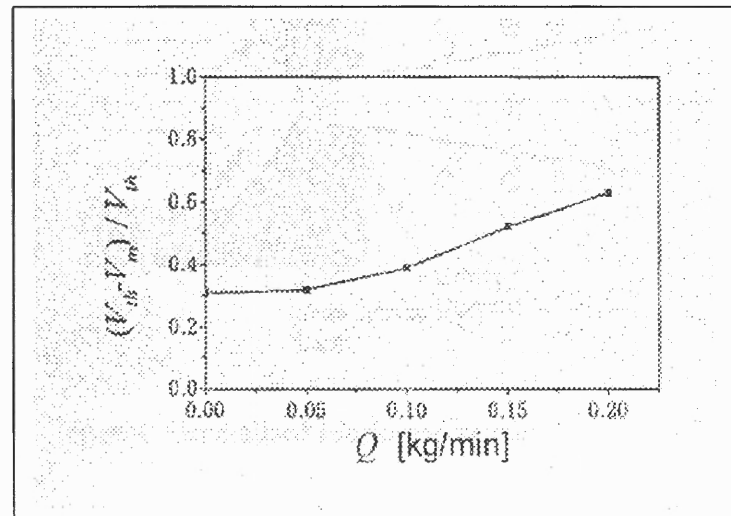
Figure 6.3 The Relation Between the Velocity Loss and the Abrasive Flow Rate
(Sawamura et al, 1999)

Our own experimental studies of the velocities of the abrasive waterjets have shown, that the pure waterjet velocity closely follows the velocity predicted by the Bernoulli equation, as was corroborated by Neusen et al, (1992), (Figure 6. 4).
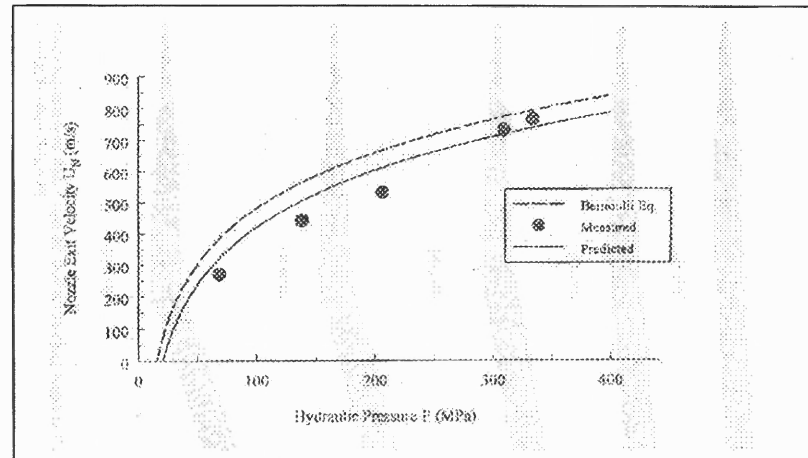
Figure 6.4 Calculated and Measures Nozzle Velocities as Function of Hydraulic Pressure (Li, 1996).

The carbide waterjet velocity is found to be approximately 82% - 99% of the pure waterjet velocity (Chen, 1990), (Figure 6.5).
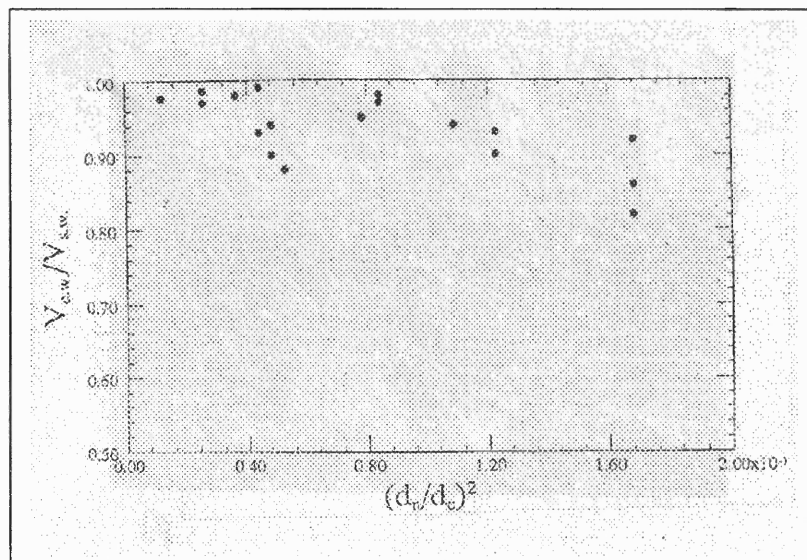
Figure 6.5 Velocity Ratios of Carbide and Sapphire Waterjets Versus the Diameter Ratio of Carbide and Sapphire Nozzles. Vcw – Velocity of Carbide Waterjet

It was also found that the velocity difference between abrasive particles and the carbide waterjet is somewhere in the range of 80 to 500 m/s (Figure 6.6).
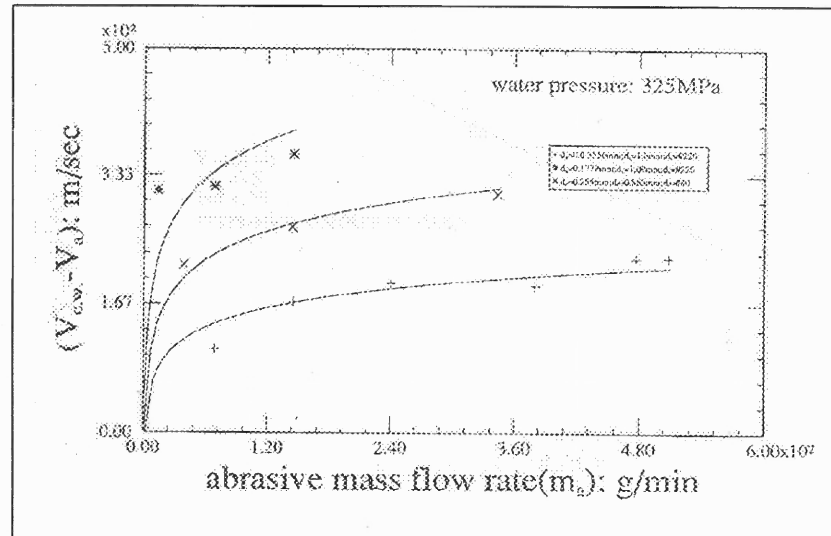
Figure 6.6 Effects of Abrasive Mass Flow Rates on Difference between Velocity of Carbide Water Jets and Velocity of Abrasive Particles.

Contrary to the results of (Neusen et al, 1992) and in support of the results of (Sawamura et al, 1999) Chen (1990) has shown that the is a significant difference in exit velocities of AWJ at 0.0 kg/min flow rate of abrasives and an increased flow rate. Which shows that not only the momentum transfer between the air and water is responsible for the velocity drop, but also and to a greate extent the presence of the third phase- abrasive particles and their mass flow rates. In his work, Chen (Chen, 1990) has developed the regression equation to determine the valocity of a particle entrained in waterjet from given values of diameters of supphire and carbide nozzles and abrasive mass flow rate.

These experimental studies of the pure and abrasive water jets give a lot of insight on the jet structure and the effect of internal nozzle parameters on the mixing inside the nozzle. But it was shown that although some consensus was reached among the

experimental results of some researches, still there are some controversial results. The numerical simulation of the flow inside a nozzle is an economical and efficient way to predict such flow charachteristics as velocity and pressure fields, turbulent charachteristics and to suggest an optimized nozzle design.

There have been limited stidies in jet analysis, and very few works on the jet behaviour inside a waterjet nozzle. Flow characteristics of waterjet in air was investigated by Yanaida and Ohasi (1978). The authors have characterized the waterjet into three regions: continuous flow region, droplet region and diffused region based on axial velocity and breake up leangth. Eddingfield et al (1981) proposed a two-dimensional axisymmetric multicomponent mathematical model which coupled the three flow fields such as continuous water, entrained air, and droplets. Amano et al (1982) carried out theoretical and experimental investigation of the turbulent axisimmetric jets impinging on a flat plate. He has employed the two equation (k-E) turbulence model in his computations. He has solved the standard Navier-Stokes equations together with two-equation turbulence by the hybrid scheme of central and backward finite difference scheme. Vijay et al. (1993) investigated the application and dynamics of cavitating jets. The authors have investigated different nozzle configurations in their numerical investigations and found that the performance of of artificially submerged cavitating jets operating at identical conditions surpassed that of fully sybmerged or noncavitating jets. Several numerical studies were undertaken to investigate flow characteristics inside a waterjet nozzle. A numerical approach was suggested by Lai et al. (1991) to predict the flow characteristics inside three nozzles. The authors have shown numerically that a center body insert into a conical nozzle results in superior performance due to the

increased cavitation. Khan (1994) have investigated the flow characteristics inside waterjet nozzle. He has used the finite element method to solve the turbulent flow fields. His numerical results were validated through the experimental study of the waterjet charachteristics by using velocity measurements with Laser Transit Anemometer, and force measurements with piezoelectric force transducer. He has used the high speed filming to reveal the dynamics and behaviour of the jets. Thus it was shown that at the micro level the high speed jet is a sequence of disintegrated slugs, but at the macro level the jet is the normal turbulent flow.

Most of the numerical studies of the turbulent flow patterns inside a waterjet nozzle carried out up-to-date neglect the presence of the air phase inside the nozzle, although the later takes up to 90-95% of the three-phase mixture volume (air + water + abrasive) according to (Neusen et al, 1990, Osman et al, 1996). Moreover the effect of air flow rate is shown to both affect the jet coherence ultimately causing the jet break up, and reduce the exit velocity of particles by up to 40% (Tazib et al, 1994). The velocity loss is also connected with the flow rate of abrasive media.

Raissi et al (1996) has investigated in detail the influence of internal nozzle parameters on three-phase waterjet flow in a nozzle. In his work he takes into account the presence of air in the cutting head (90% of volume occupation), flow turbulence (eddy viscosity model) and abrasive particle interactions. As the outcome of the study, authors suggest that the numerical tools extremely helpful in nozzle design optimization.

6.2 Numerical Study of the Turbulent Flow Inside a Pure Waterjet Nozzle

6.2.1 Modeling of the Turbulent Flow

The numerical simulation of a turbulent flow involves modification of governing equations for case of laminar flow. For the flow involved in this study being steady, incompressible, isothermal, chemically homogeneous and without body forces the following equations apply:

Continuity:

$$\frac{dU_i}{dx_i} = 0$$ (6.1)

Navier-Stokes:

$$\rho \frac{\partial U_i}{\partial x_j} = -\frac{\partial p}{\partial x_i} + \frac{\partial}{\partial x_j}\left[\mu\left(\frac{\partial U_i}{\partial x_j} + \frac{\partial U_j}{\partial x_i}\right)\right]$$ (6.2)

where U_i is velocity, p is pressure, μ is the dynamic viscosity and ρ is density.

These equations are valid for the case of a turbulent flow, although there is no practical means of solving these equations for a high Reynolds number flows. Therefore a following approach is usually applied. Following the original idea of Reynolds, we assume that the fluid is in a randomly unsteady turbulent state and work with the time averaged or mean equations of motion.

Any variable can be resolved into a mean value $\bar{Q}$ and a fluctuating value Q':

$$\bar{Q} = \frac{1}{T}\int_{t_0}^{t_0+T} Q\,dt$$ (6.3)

Where t is a reference point in time and T is the averaging time which is large compared to the relevant period of fluctuations. Thus applying the time averaging to the equations of conservation of mass and momentum we obtain:

Conservation of mass:

$$\frac{d\bar{U}_i}{dx_i} = 0$$

(6.4)

Conservation of mean momentum:

$$\rho\bar{U}_j \frac{\partial \bar{U}_i}{\partial x_j} + \rho \frac{\partial}{\partial x_j}\left(\overline{U_i'U_j'}\right) = -\frac{\partial \bar{p}}{\partial x_j} + \frac{\partial}{\partial x_j}\left[\mu\left(\frac{\partial \bar{U}_i}{\partial x_j} + \frac{\partial \bar{U}_j}{\partial x_i}\right)\right]$$

(6.5)

Thus the mean momentum equation is complicated by a new term involving the turbulent inertia tensor U'iU'j. These equations can be solved for the mean values of velocity and pressure only when the turbulence inertia term can be correlated in some way. Therefore turbulent modeling is the task of providing additional equations to describe the temporal and spatial evolution of the turbulent inertia flux.

The most popular turbulence model in practical use is the so-called two equation model, or k-ε model. In the k-ε turbulent model the turbulence field is characterized in terms of two variables, the turbulent kinetic energy k, and the viscous dissipation rate of turbulent kinetic energy ε given by:

$$k = \frac{1}{2}\overline{U_i U_i},$$

(6.6)

$$\varepsilon = \nu \frac{d\bar{U}_i}{dx_j}\frac{d\bar{U}_i}{dx_j}$$

(6.7)

Two transport equations for k and ε can be obtained from the Navier- Stokes equations by a sequence of algebraic manipulations. By simplifying these two equations with application of a number of modeling assumption the well known equations of turbulent kinetic energy and dissipation of the k-ε model can be obtained (Launder and Spalding, 1972).

Thus the governing equations for the problem at hand, which is steady, two-dimensional, incompressible, isothermal, turbulent, can be written as follows:

$$\frac{d\overline{U}_i}{dx_i} = 0 \qquad (6.8)$$

$$\rho \overline{U}_j \frac{\partial \overline{U}_i}{\partial x_j} + \rho \frac{\partial}{\partial x_j}\left(\overline{U_i'U_j'}\right) = -\frac{\partial \overline{p}}{\partial x_j} + \frac{\partial}{\partial x_j}\left[\mu\left(\frac{\partial \overline{U}_i}{\partial x_j} + \frac{\partial \overline{U}_j}{\partial x_i}\right)\right] \qquad (6.9)$$

$$\rho U_j \frac{\partial K}{\partial x_j} = \frac{\partial}{\partial x_j}\left(\frac{\mu_t}{\sigma_k}\frac{\partial K}{\partial x_j}\right) + \mu_t \frac{\partial \overline{U}_i}{\partial x_j}\left(\frac{\partial \overline{U}_i}{\partial x_j} + \frac{\partial \overline{U}_j}{\partial x_i}\right) - \rho\varepsilon \qquad (6.10)$$

$$\rho U_j \frac{\partial \varepsilon}{\partial x_j} = \frac{\partial}{\partial x_j}\left(\frac{\mu_t}{\sigma_k}\frac{\partial \varepsilon}{\partial x_j}\right) + C_1\mu_t \frac{\varepsilon}{K}\frac{\partial \overline{U}_i}{\partial x_j}\left(\frac{\partial \overline{U}_i}{\partial x_j} + \frac{\partial \overline{U}_j}{\partial x_i}\right) - C_2\rho\frac{\varepsilon^2}{k} \qquad (6.11)$$

where i,j = 1,2, $\mu = \mu 0 + \mu t$, and $\mu t = \rho C\mu k2 / \varepsilon$, as proposed by Kolmogorov- Prandtl. The above equations contain empirical constants C1, C2, σk, σε and Cμ. Over the years the k-ε model has been tested and optimized against the wide range of flow problems. For the turbulent flow inside the nozzle the following values of these empirical constants was selected: C1=1.44, C2=1.92, σk=1.00, σε =1.30 and Cμ=0.09.

6.2.2 Near-Wall Modeling

The standard k-ε turbulence model is valid mostly for the flows with high Reynolds number. In a problem involving a solid boundary, there is always a special viscocity-affected near wall region, which contains the viscous sub-layers. Therefore a problem arises when we try to apply the standard k-ε turbulence model to a near-wall regions. Thus a special modeling approach is needed to simulate a turbulent flow in a near-wall region. Another reason a special considerationshould be given to the near-wall region is that in order to resolve the sharp variations of flow variables in near-wall regions, a prohibitively large number of grid points must be used, which leads to expensive computation. There are two approaches to modeling of the near wall region. In the so-called wall function approach the special semi-empirical formulas are used to bridge the viscosity-affected region between the wall and the fully turbulent region. Another approach, the "near wall modeling"technique uses the modified turbulence models in the viscocity-affected region to be resolved with a meash all the way to the wall. In this study the Wall Function approach was used to overcome the viscosity affected regions of the flow.

6.2.3 Solution Procedures

The application of Galerkin finite-element procedure to the stationary Navier-Stokes equations results in a set of nonlinear algebraic equations that may be represented in matrix form as:

$$K(u)u=F \qquad (6.12)$$

Where K is the global system matrix, u is the global vector of unknowns (velocities, pressures, etc.) and F is a vector that includes the effects of body forces and boundary conditions.

Presently there are mainly two solution methodologies for solving the systems of equations described above. These two approaches are known as fully coupled approach and the segregated approach. The first approach solves all the equations in a simultaneous coupled manner, while the other approach solves each equation separately in a sequential, segregated manner. In this work the second approach has been chosen to solve the turbulent flow equations resulted after application the Galerkin finite-element scheme to the governing flow equations. In this approach the global matrix system is never directly constructed. Instead, it is decomposed directly into the set of the decoupled sub-matrix systems for the primary flow variables.The segregated solver was used in conjunction with simple pressure-velocity coupling.

The density of computantional domain was varied to make the solution grid independent.

6.2.4 Problem Description

The computational domain for this problem was limited to the pure waterjet nozzle geometry. There are many variations of the sapphire nozzle geometry, but for this study we have limited ourselves to the standard convergant nozzle. The nozzle geometry is presented in Figure 6.7. Two variations of the conventional nozzle geometry was used for numerical simulations. The geometrical parameters of nozzles used in this study is presented in Table 6.1.
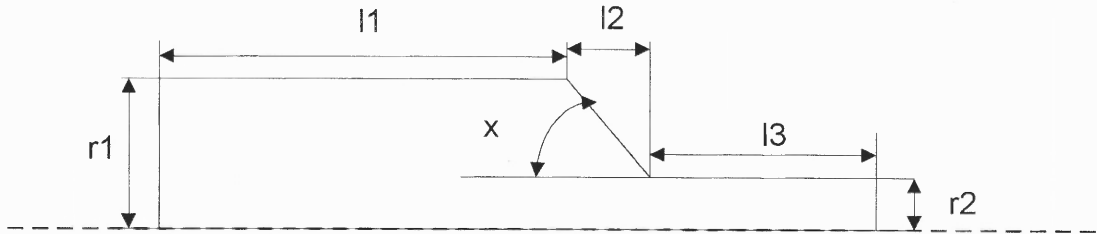
Figure 6.7 Computational Geometry

Table 6.1 Geometrical Parameters of Pure Waterjet Nozzles

Nozzle #	Angle x	R1(cm)	R2 (cm)	L1 (cm)	L2 (cm)	L3 (cm)
1	60°	0.1598	0.0178	1.598	1.68	1.935
2	90°	0.1598	0.0178	1.68	0	1.935

6.2.5 Mesh Development and Boundary Conditions

The computational domain was descritized into 12300 elements using the GAMBIT software. The four node, quadratic elements have been employed. The numerical grid is shown on Fig. 6.8.
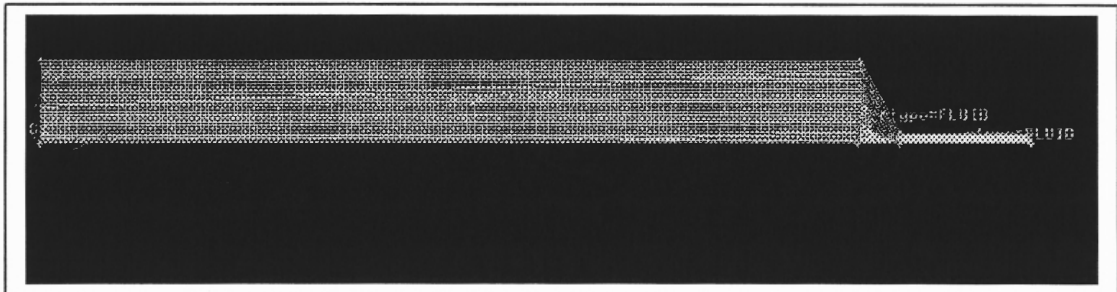
Figure 6.8 Computational Domain

The domain (Figure 6.8) over which the problem is to be solved is comprised of the inlet section, outlet, the axis of symmetry and the wall.

It is required to provide appropriate boundary conditions for k, and ε on the boundaries of the computational domain. The inlet plane is positioned upstream of the regions of interest. At the inlet section the water is prescribed a uniform velocity which was calculated from the constant volume flow rate. The turbulence quantities at the inlet section are determined using the following empirical relations:

$$k = 0.1U^2 \qquad\qquad (6.13)$$

$$\varepsilon = \frac{k^{3/2}}{0.05r} \qquad\qquad (6.14)$$

where r is the radius of the sapphire nozzle.

At the outlet boundary, the Neumann i.e., the zero gradient boundary condition in the axial direction is applied for U, k, ε. At the wall, the near-wall modeling approach is applied for those regions of the computational domain, which coincide with the solid boundary. On the solid wall u, k, ε are set to zero.

The finite element package FLUENT was used for the numerical solution of discretized equations.

6.2.6 Initial Condition

Non-zero initial guess for primary flow variable such as U, k, ε, improves the convergence of the problem. Therefore the constant values for the turbulence quantities were obtained from the above equations and used for further computations. For profiles, the intermediate values are used as the initial guess.

6.2.7 Results and Discussion

The numerical solutions of the turbulent flow representing the jet flow in the pure waterjet nozzle were obtained in terms of velocity fields, pressure, the turbulent kinematic energy k and dissipation ε. The velocity field on the outlet section of the nozzle is of the most interest here, because it directly translates into the exiting energy of the jet, it's primary characteristics. Also the validity of the computational scheme and the obtained results could be checked, by comparing the outlet velocity profile and its magnitude with the available experimental results of other researches. Table 6.2 summarizes the results of velocity computations for nozzle #1 and different pressures.

Table 6.2 Predicted Velocity and Bernoulli Velocity

Mass Flow Rate (g/s)	Water Pressure (MPa)	Outlet Velocity (m/s)	Velocity from Bernoulli (m/s)	LTA Measured Velocity (m/s)
36.45	138	441	504	460
44.6	207	500	617	550
51.6	276	585	712	N/A
57.6	345	674	796	730

The velocity in column four was calculated using the Bernoulli equation:

$$V_{bern} = k*(2p/\rho)^{1/2}$$

(6.15)

where k was taken to be equal 0.96. The experimental values of velocity at different intensifier pressures were measured by Li (1996) with the help of Laser Transit

Anemometer. Here we can see that the predicted values of velocities indeed follow the ones predicted by Bernoulli equation pretty closely. The maximum relative error for the tested ranges does not exceed 20%. The relative error of prediction is even less in case we compare our prediction results with LTA measurements done by Li, (1996). Thus we could agree, based on this numerical results that the jet in the primary nozzle could be closely approximated by the conventional two-equation turbulence model and the exit velocity can be approximated with pretty good accuracy by the Bernoulli equation. Figures 6.10 through 6.15 show the results of the numerical simulations for the waterjet nozzle 0.354 mm and intensifier pressure 276 MPa. Contours of velocity magnitude (Figure 6.10) and turbulent kinetic energy (Figure 6.11) give us an accurate idea regarding the velocity flow field in the nozzle. Thus it could be inferred that the highest velocity occurs exactly after the primary nozzle entrance. And exactly this velocity is best approximated by Bernoulli equation. Immediately after the entrance a not significant velocity loss occurs. The highest pressure (Figures 6.18, 6.19) is achieved at the orifice entry. The spatial velocity distribution (Figures 6.20, 6.21) is similar for both nozzles used in the study and it is uniform and there is no flow separation in the nozzle. Again it suggests that the flow can be represented as the conventional turbulent jet. Thus the results show that the convergent nozzle produces concentrated high-energy jet.

6.3 Modeling of Two Phase Flow in the Waterjet Cutting Head

As it was pointed out earlier, the flow in a waterjet-cutting head is not a simple one-phase turbulent flow. Instead this flow can at best be approximated as a three-phase flow, where the primary phase is the jet, the second phase is the entrained air, and the third phase is

the abrasive particles mixed in the flow. In order to approach this problem, the volume of the fluid (VOF) model was used. The VOF model is a technique designed for two or more immiscible fluids, where the position of the interface between the fluids is of interest. In the VOF model, a single set of momentum equations is shared by the fluids, and the volume fraction of each of the fluids is tracked throughout the domain. The tracking of the interface(s) between the phases is accomplished by the solution of a continuity equation for the volume fraction of the phases. For the qth phase, this equation takes the following form:

$$\frac{\partial \alpha_q}{\partial t} + u_i \frac{\partial \alpha_q}{\partial x_i} = 0 \qquad (6.16)$$

The volume fraction equation will not be solved for the primary phase, instead the primary phase volume fraction will be computed based on the following constraint:

$$\sum_{q=1}^{n} \alpha_q = 1 \qquad (6.17)$$

The properties appearing in the transport equations are determined by the presence of the component phases in each control volume. In general, for an N-phase system, the volume fraction averaged property would take a form:

$$p = \sum \alpha_q p_q \qquad (6.18)$$

where p is some volume fraction averaged property (e.g. density, viscosity, etc).

A single momentum equation is solved throughout the domain, and the resulting velocity field is shared among the phases. The momentum equation depends on the volume fractions of all the phases through the properties ρ and μ. In the case of turbulence

quantities, a single set of transport equations is solved, and the variables κ and ε are shared by the phases throughout the field.

6.3.1 Dispersed Phase Modeling

In this study the Lagrangian approach for two-phase flow modeling is used to model the ice particles mixing process. The underlying concept here is what is usually called dispersed two-phase flow. The idea is to consider one of the phases to be dispersed (abrasive particles) in the other phase (waterjet). At the same time strong coupling occurs between phases. The Lagrangian model represents the dispersed phase as a continuous stream of particles moving through the carrier phase. The governing equations for the carrier phase are given in the standard in fluid dynamics Eulerian frame of reference, while the motion of the particles is described in a Lagrangian coordinate system. The information transfer between phases is accounted for by the momentum along particle paths.

The motion of each particle of the dispersed phase is governed by an equation that balances the mass- acceleration of the particles with the forces acting on it. For a particle of density ρ_p and diameter D_p the governing equation is:

$$\rho_p \frac{dU_i^p}{dt} = \frac{1}{\tau}\left(U_i - U_i^p\right) + \left(\rho_p - \rho\right)g_i + \rho_p f_i^p \tag{6.19}$$

where Up is the particle velocity, U is the velocity of the carrier phase, fp is the combination of forces acting on the particle, and τ is the particle's relaxation time, defined by Equation 6.20.

$$\tau = \frac{4\rho_p D_p^2}{3\mu C_D \operatorname{Re}^p} \tag{6.20}$$

where μ is the viscosity of the fluid, Re^P is the particle Reynolds number defined by:

$$Re^P = \frac{D_p \left| U_i - U_i^p \right| \rho}{\mu}$$

(6.21)

and Cd is the drag coefficient. There exist many models, mostly empirically based for the drag coefficient. Among the most commonly used ones is the polynomial model given by:

$$Cd\ Re^P = 24(a + bRe^P + c(Re^P)2 + d / Re^P)$$

(6.22)

where a, b, c, and d are constants.

The first term on the right hand side of (6.19) is the generalization of the classical Stokes Drag on a particle. The second term is the buoyancy force, important in simulating the sedimentation of solid particles in liquid, and the third term represents different forces that appear in particulate motion in fluid.

A particle trajectory is obtained by the solution of the particle momentum equation (6.19) coupled with kinematic equation:

$$U_i^p = \frac{dx_i}{dt}$$

(6.23)

where x_{pi} is the position coordinate of the particle at time t.

If there is a transfer of momentum from the particulate phase to the continuum phase, then the following computational approach is followed. The computed particle trajectories are combined into source term of momentum, which is then inserted into the right-hand side of the conservation of momentum equation :

$$\rho \overline{U}_j \frac{\partial \overline{U}_i}{\partial x_j} + \rho \frac{\partial}{\partial x_j} \left(\overline{U_i' U_j'} \right) = -\frac{\partial \overline{p}}{\partial x_j} + \frac{\partial}{\partial x_j} \left[\mu \left(\frac{\partial \overline{U}_i}{\partial x_j} + \frac{\partial \overline{U}_j}{\partial x_i} \right) \right] + \Phi_i^M$$

(6.24)

where $\Phi_I{}^M(E)$ is the source term. For each element E it is defined as:

$$\Phi_i^M(E) = \frac{1}{V_E} \sum_{j=1}^{n_B} \eta_j \int_{\delta t_j^E} \frac{3\mu C_D \operatorname{Re}^p V_p}{4D_p^2} (U_i - U_i^p) dt \qquad (6.25)$$

where V_E is the volume of the element, V_p is the volume of the particle, ηj is the number of particles per unit time traversing the j_{th} trajectory and δ_{tj} is the time that a particle on the j_{th} trajectory takes to pass through element E.

The solution procedure used in the Lagrangian two- phase flow model is an iterative one. First a solution to governing equation (6.24) without source term is obtained. The solution Ui of the equation is then substituted into (6.19), which is then solved together with kinematic equation (6.23). From these solutions the source term is constructed according to (6.25) and the obtained values are then substituted back to (6.24). This procedure is repeated until the convergence criteria are met.

6.3.2 Problem Description

The computational domain in this study is limited to the cutting head of a conventional waterjet nozzle. In the cutting head three phases are mixing up to constitute the abrasive-air-water jet flow. The air enters the cutting head through the abrasive port. The cutting head itself consists of mixing chamber and focusing tube. In mixing chamber the mixing of the water stream, air and solid additives occurs, and the three-phase stream is then accelerated in the focusing tube. The computational domain along with process boundary conditions is given in the following chart. To reduce the computer time, the length of the focusing tube was taken smaller then it is in reality, with the assumption that

after this length the flow is fully developed and no significant change of properties occurs.
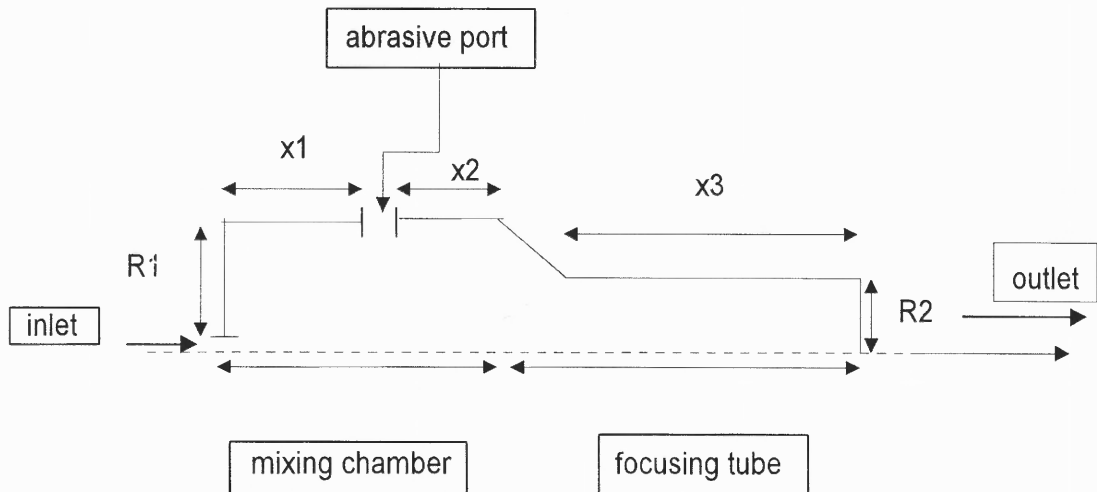
Figure 6.9 Nozzle Geometry

Table 6.3 Nozzle Dimensions

Waterjet Cutting Head Dimensions					
X1	X2	X3	R1	R2	Inlet
0.244 (sm)	0.3556 (sm)	1.5 (sm)	0.203 (sm)	0.116 (sm)	0.017 (mm)

6.3.3 Boundary Conditions

It is required to provide appropriate boundary conditions for k, u, ε on the boundaries of the computational domain. The inlet plane is positioned upstream of the regions of interest. The boundary condition for U is prescribed uniform at the inlet and set to be

equal to 600 m/sec. The volume fraction of air is taken to be equal to zero at inlet, and unity at abrasive port inlet. The turbulence quantities at the inlet section are determined using the empirical relations (6.13 – 6.14).

At the outlet boundary, the Neumann i.e., the zero gradient boundary condition in the axial direction is applied for U, k, ε. At the wall, the near-wall modeling approach is applied for those regions of the computational domain, which coincide with the solid boundary. On the solid wall u, k, ε are set to zero.

The finite element package FLUENT was used for the numerical solution of discretized equations.

6.3.4 Discussion and Presentation of Results

The result of the analysis is presented in Figures 6.20 through 6.30. The contours of velocity magnitude show that after the primary nozzle, centerline velocity dominates the flow. There is a velocity loss along the centerline, not exceeding 10% of the velocity magnitude after the primary nozzle. The average centerline velocity at secondary nozzle exit, for the given operating conditions is 250 m/s. These results are in a good agreement with results available in the literature (Raissi et al 1996, Neusen et al, 1996). The turbulent quantities increase closer to mixing tube and grow even stronger on the jet periphery, further from the jet centerline. This could be explained by the increasing intensity of the jet break up in the secondary nozzle. The volumetric fraction of air in the nozzle can be estimated to be greater then or equal to 85%. This again is in a total agreement with previously reported experimental and numerical results. (Raissi et al, 1996, Osman et al, 1996).
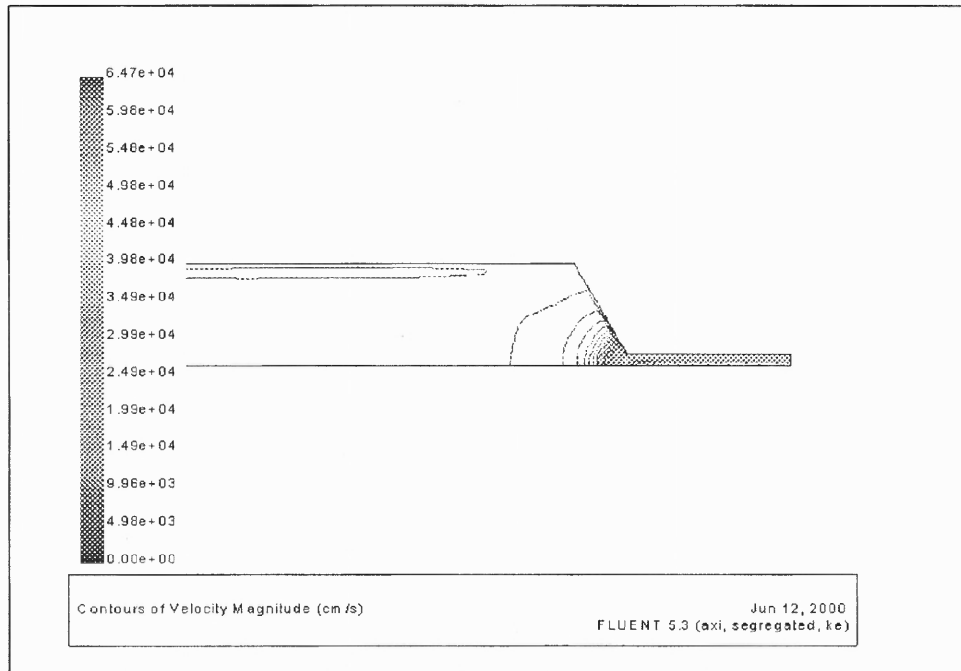
Figure 6.10 Contours of Velocity Magnitude (cm/s) for Nozzle #1 and Mass Flow Rate 52 g/s
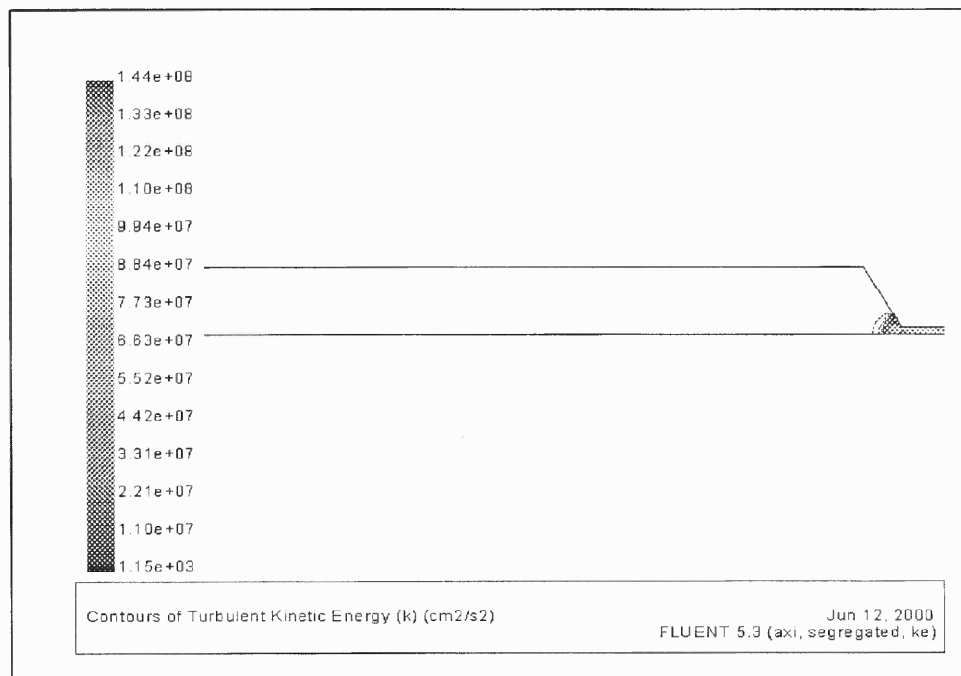
Figure 6.11 Contours of Turbulent Kinetic Enery, Nozzle #1, Mass Flow Rate 52 g/s.

Figure 6.12 Outlet Velocity Magnitude, Nozzle #1, Mass Flow Rate 52 g/s
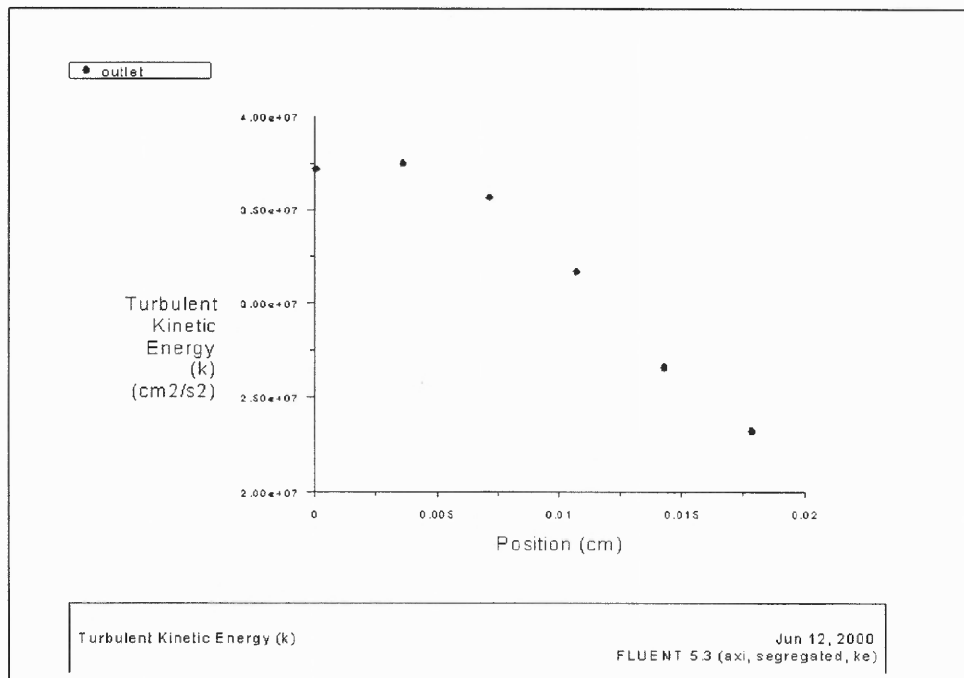
Figure 6.13 Outlet Turbulent Kinetic Energy, Nozzle #1, Mass Flow Rate 52 g/s
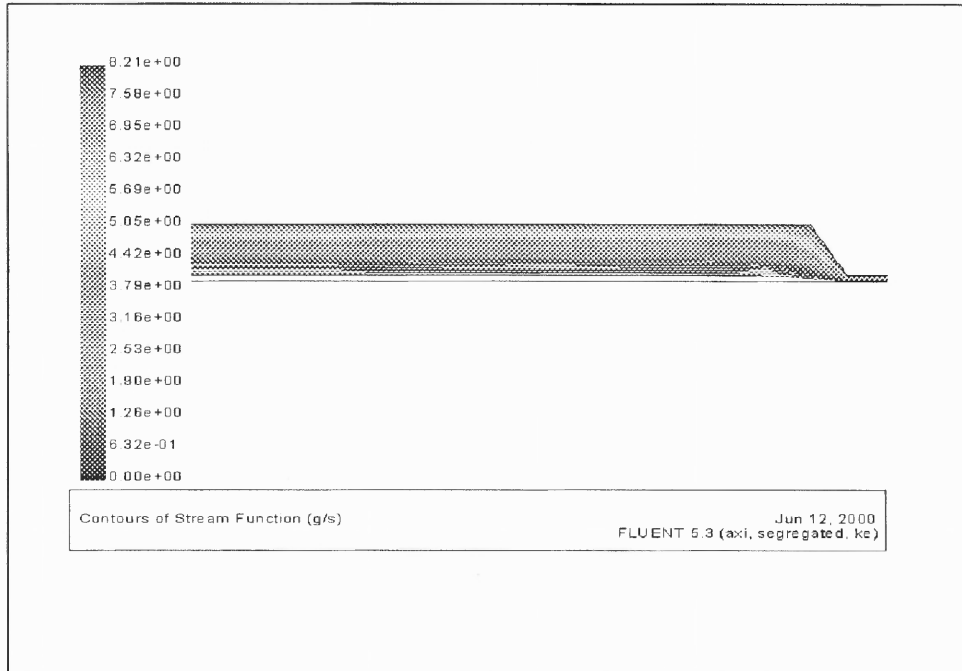
Figure 6.14 Stream Line Contours For Nozzle #1 and Mass Flow Rate 52 g/s
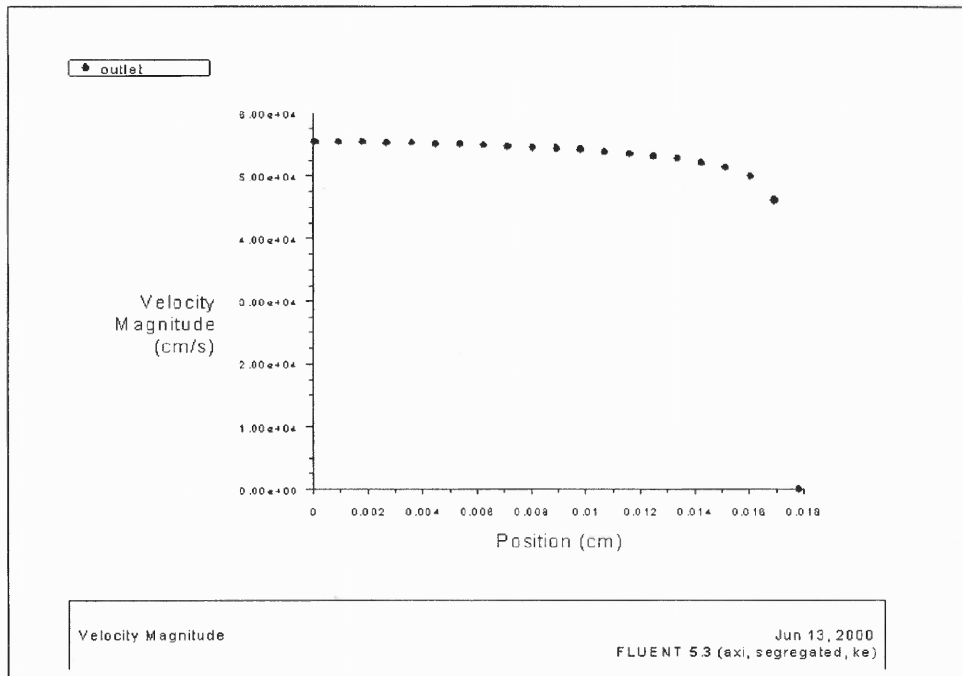
Figure 6.15 Outlet Velocity Magnitude, Nozzle #2, Mass Flow 52 g/m
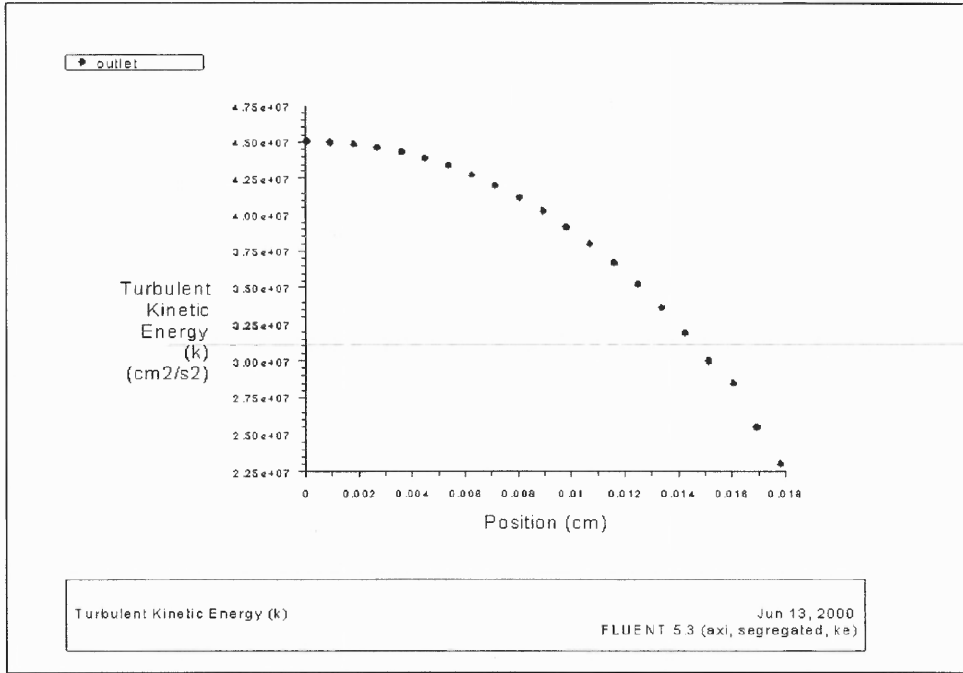
Figure 6.16 Turbulent Kinetic Energy Profile at Exit, Nozzle #2, Mass Flow Rate 52 g/m
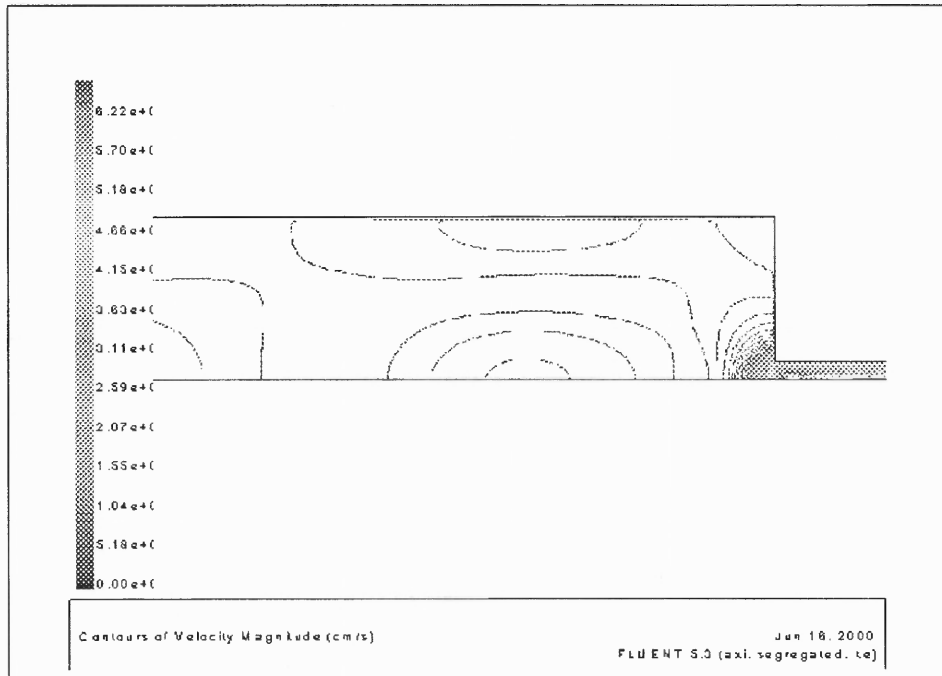
Figure 6.17 Contours of Velocity Magnitude (cm/s)
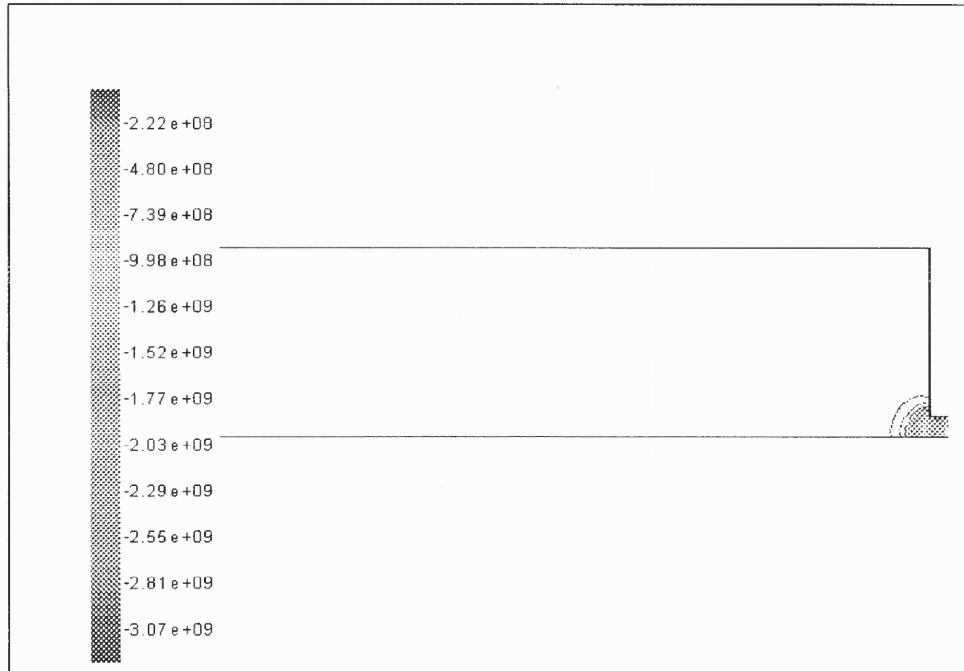
Figure 6.18 Static Pressure Contours, Nozzle # 1
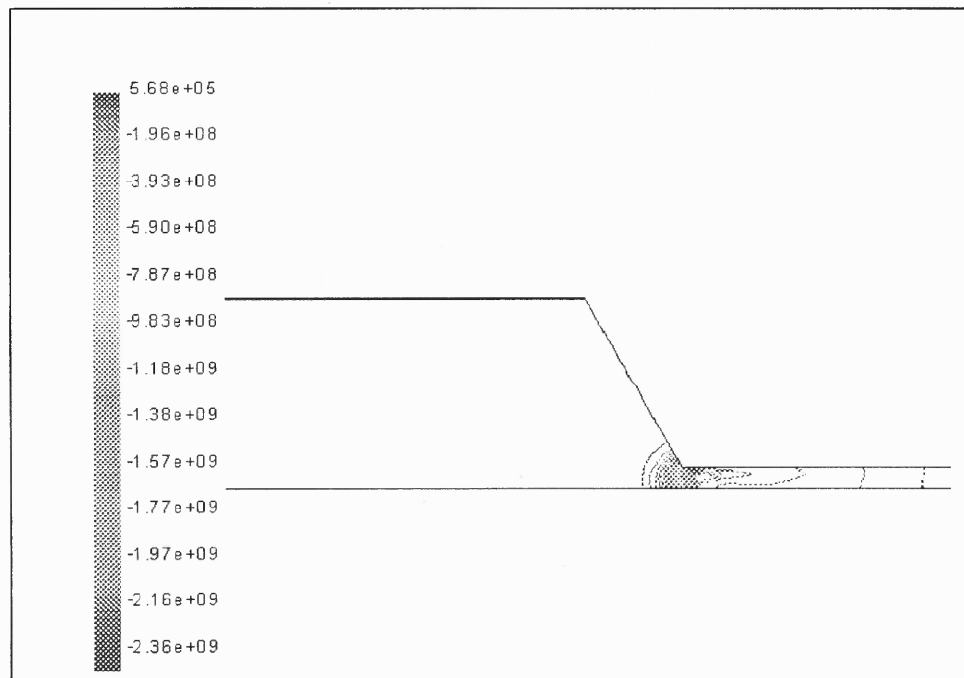
Figure 6.19 Static Pressure Contours, Nozzle #1
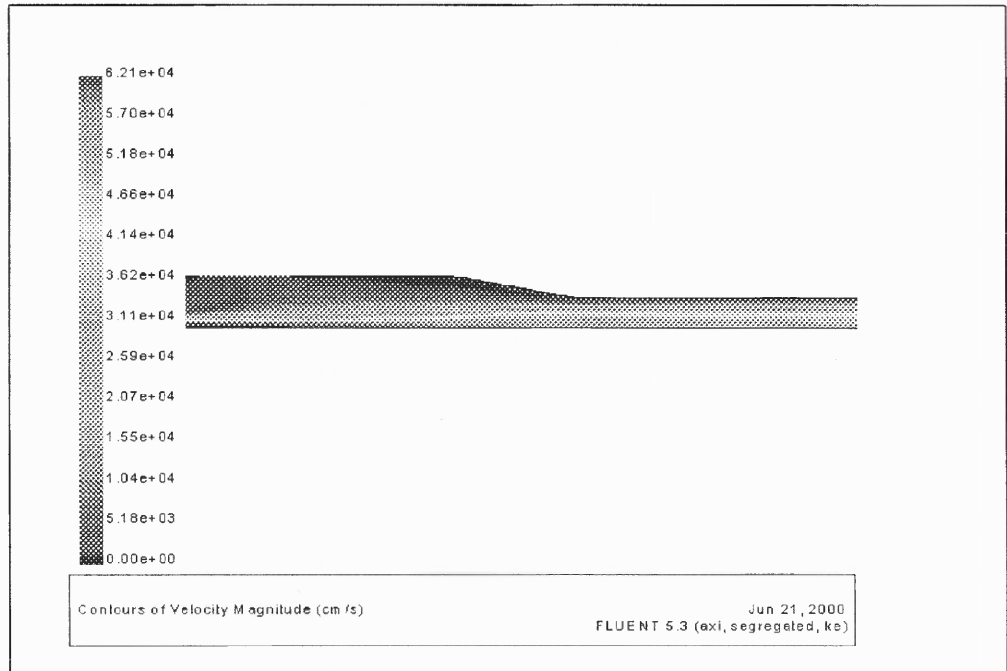
Figure 6.20 Contours of Velocity Magnitude
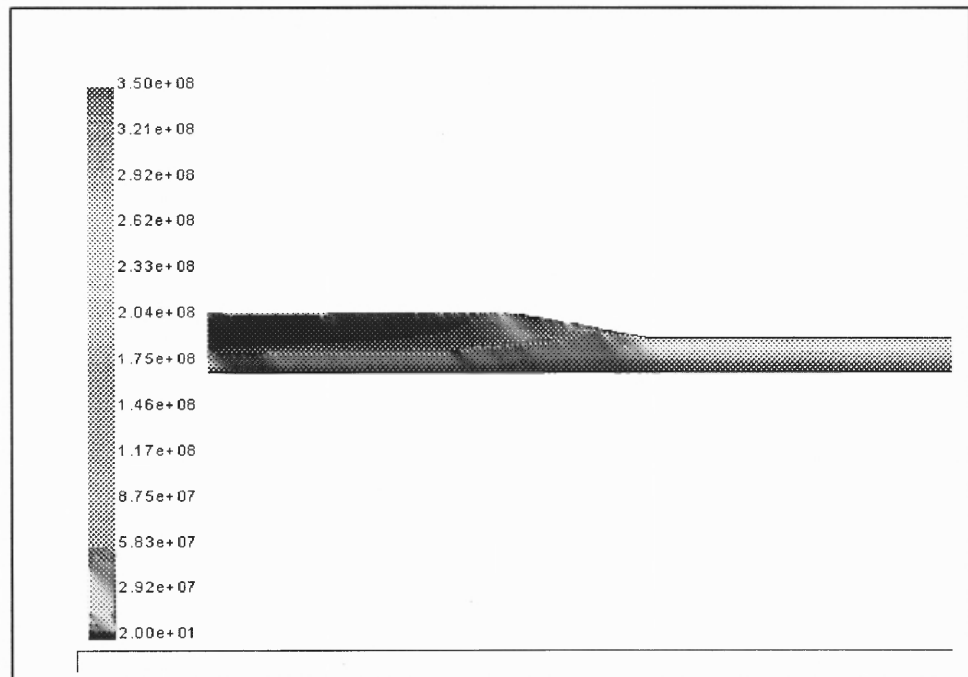
Figure 6.21 Contours of Turbulent Kinetic Energy (k)
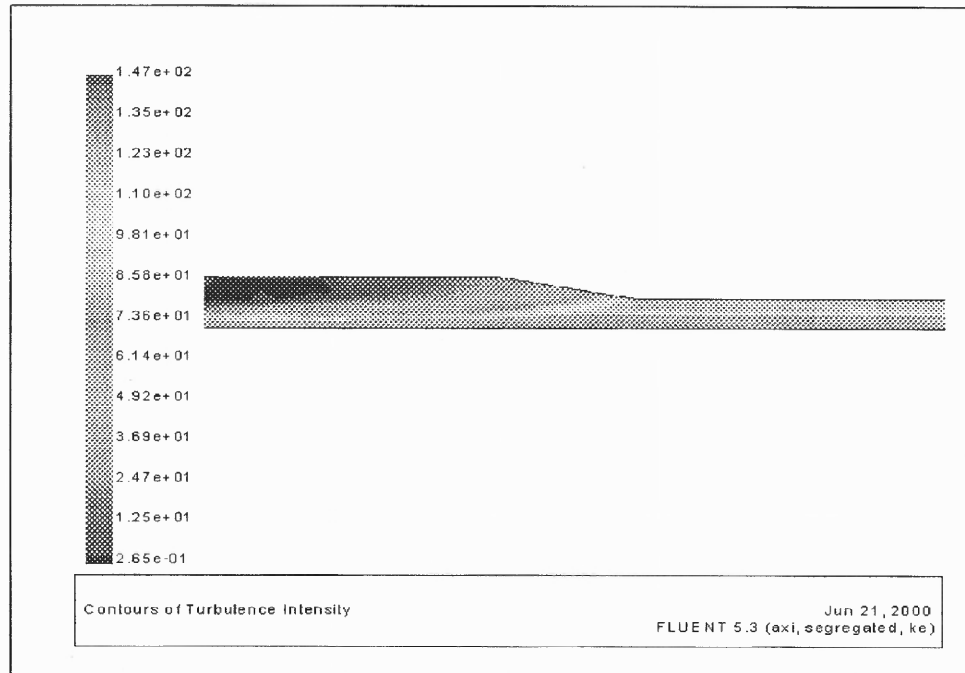
Figure 6.22 Contours of Turbulent Intensity
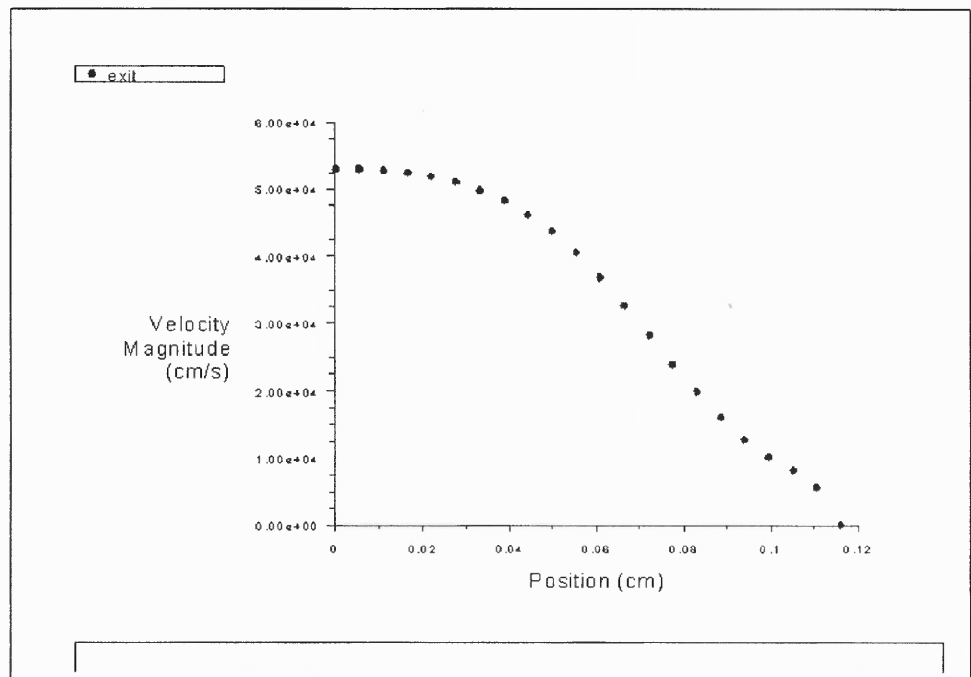
Figure 6.23 Velocity Magnitude at Nozzle Exit
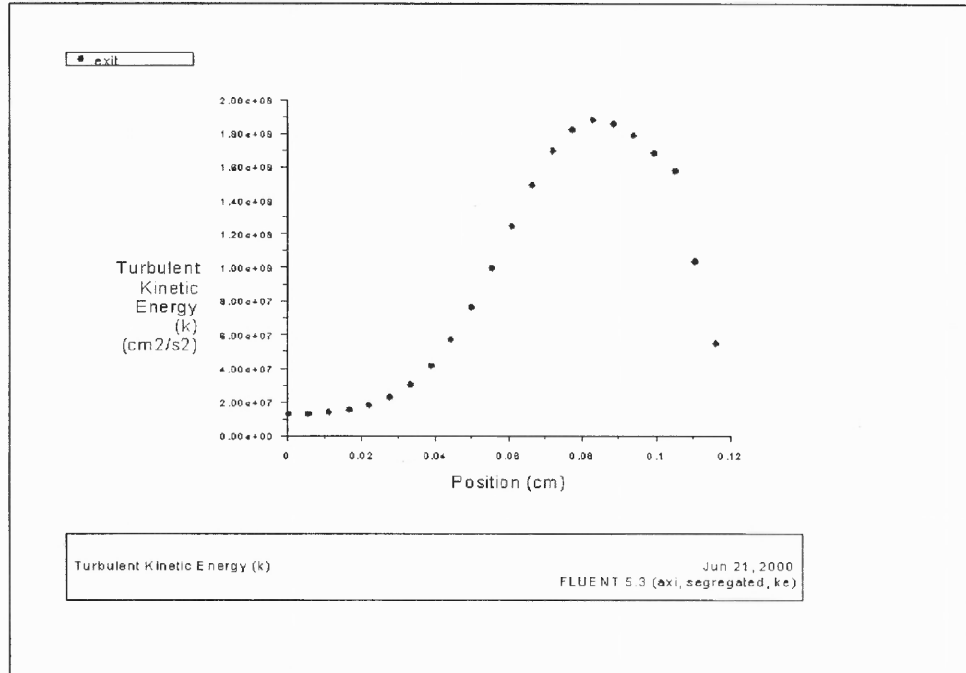
Figure 6.24 Turbulent Kinetic Energy (k)
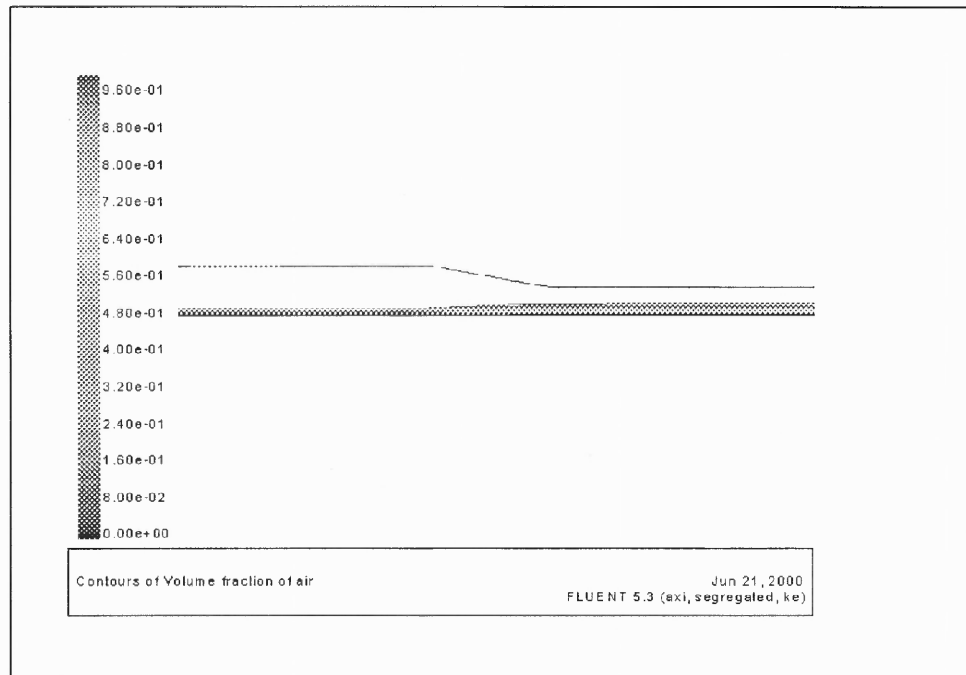
Figure 6.25 Contours of Volume Fraction of Air
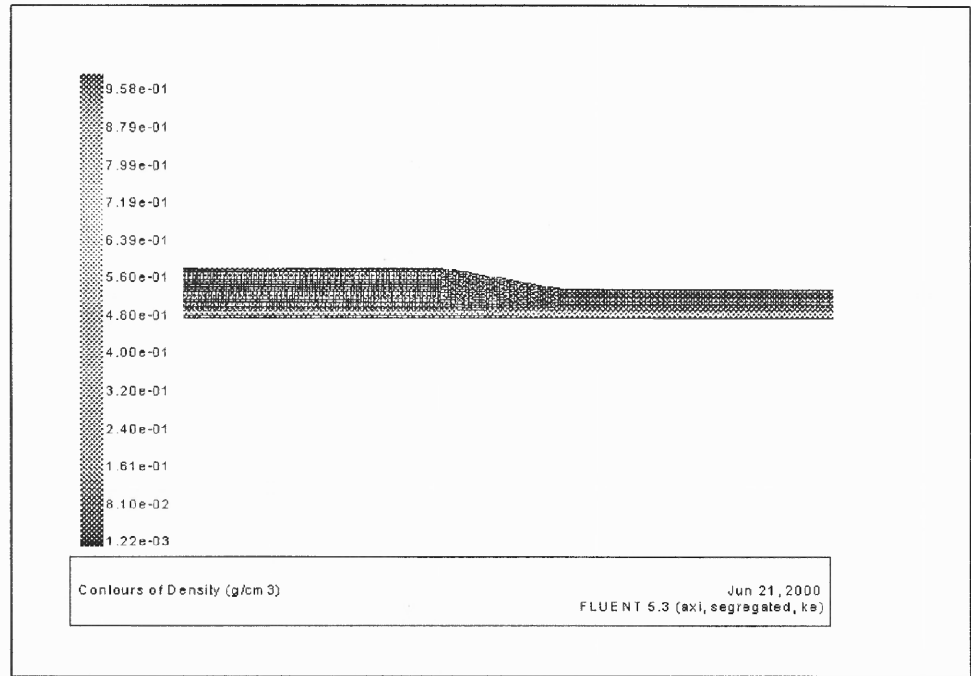
Figure 6. 26. Density Contours (g/sm 3)
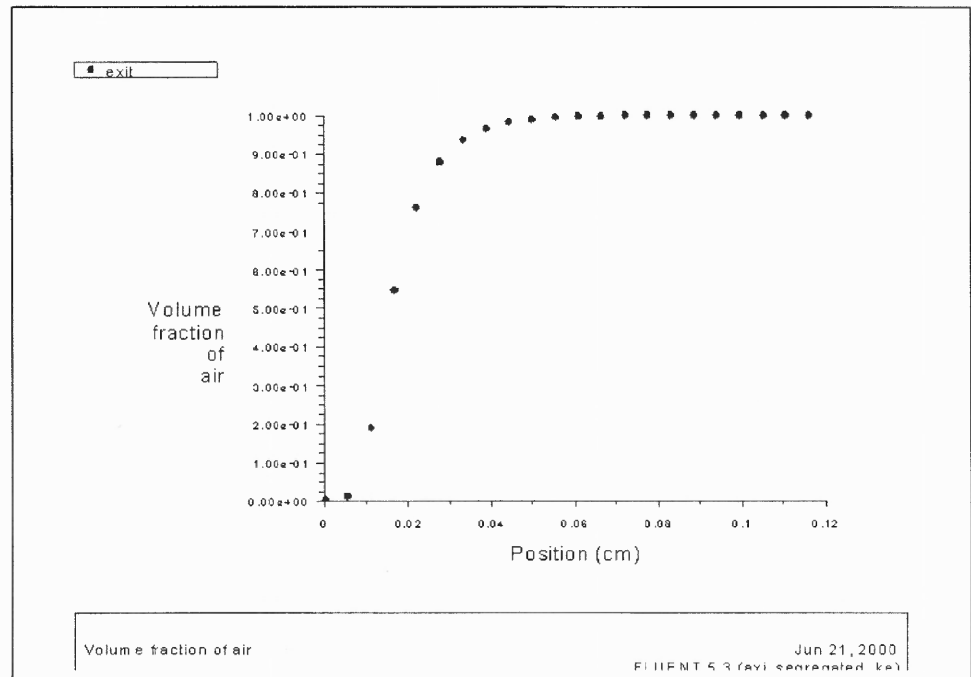
Figure 6. 27 Volumetric Fraction of Air at the Nozzle Exit
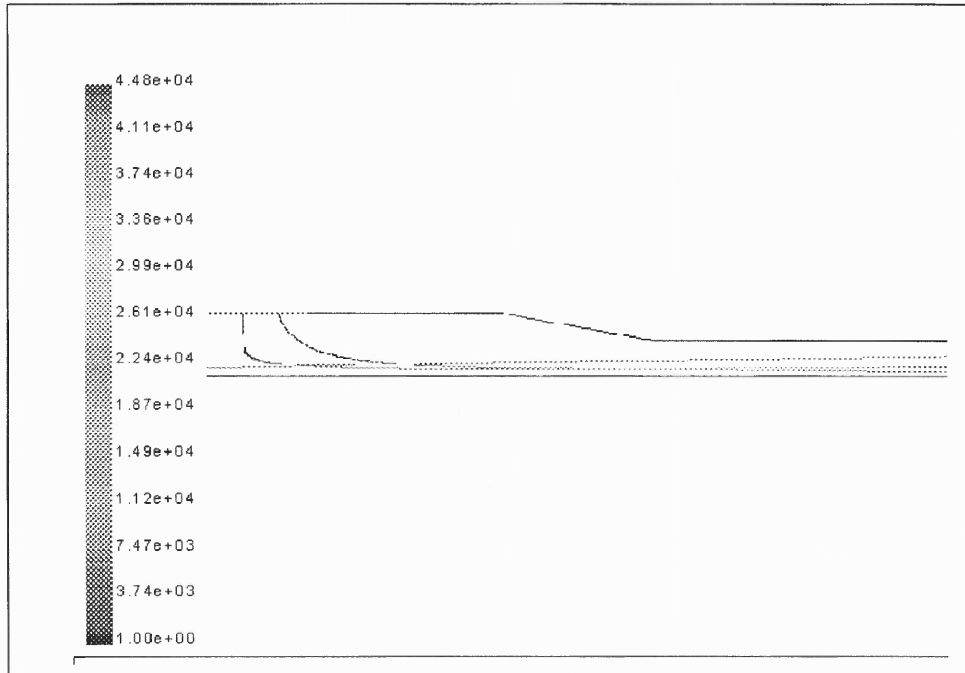
Figure 6. 28 Particle Traces Colored by Particle Velocity Magnitude (sm/s)
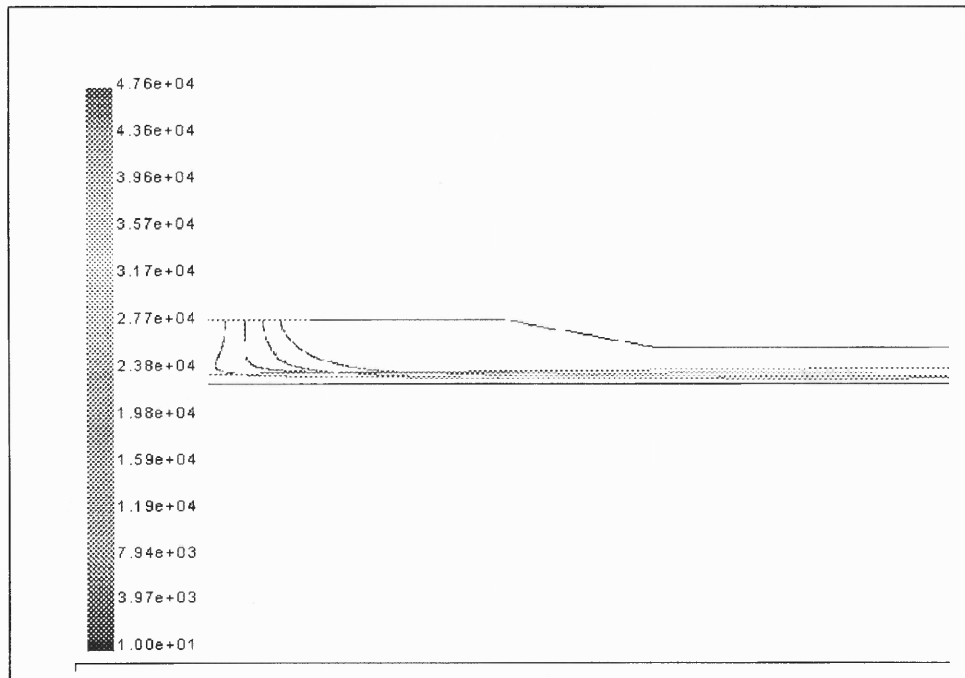
Figure 6. 29 Particle Traces Colored by Particle Velocity Magnitude (sm/s)
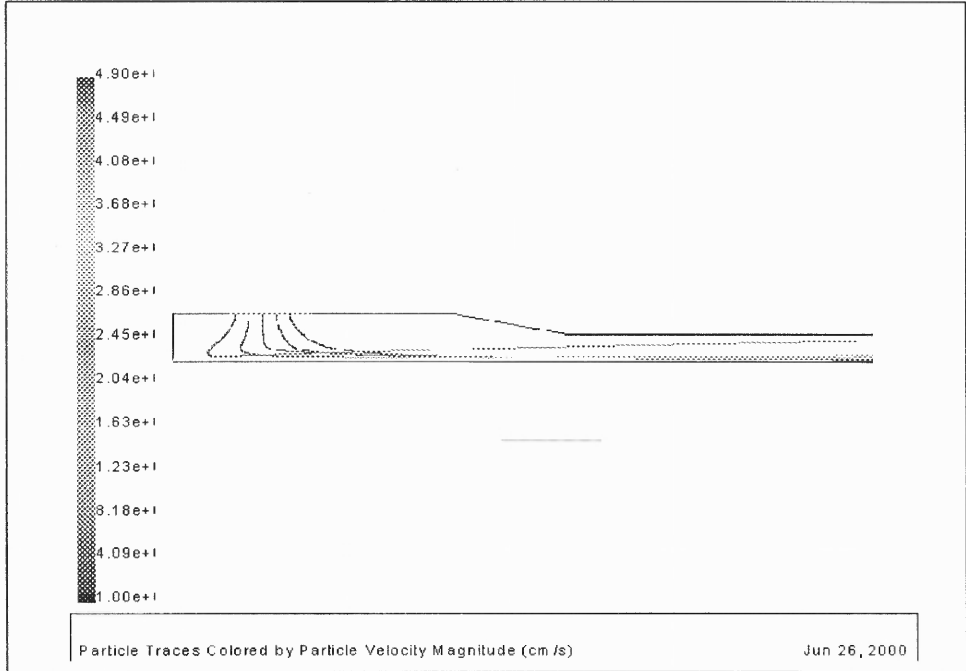
Figure 6. 30 Particle Traces Colored by Particle Velocity Magnitude (sm/s)

CHAPTER 7

EXPERIMENTAL AND NUMERICAL INVESTIGATION OF PURE WATERJET COATING REMOVAL

7.1 Experimental and Numerical Study of Pure Waterjet Paint Removal

7.1.1 Introduction

Paint and other coatings are applied to surfaces to enhance corrosion resistance, improve appearance, or both. Often the coatings need to be removed either as a part of the manufacturing operations or later in the equipment life as the paint becomes soiled, worn, or damaged with use. In many cases, particularly in the aircraft industry, paint must be removed to allow inspection of the underlying parts. In the case of an aircraft and a number of other industries this requirement is paramount.

The most common method of depainting incorporates the use of solvents. Solvent strippers, employed for industrial coating removal for many years, consist mainly of methylene chloride that typically constitutes 60% to 65% of the formulation. Other ingredients such as activators, corrosion inhibitors, thickeners, and evaporation retarders are used to supplement the methylene chloride to improve coating removal performance. However the use of solvent strippers generates organic vapors, and sludge containing solvents and metals. Thus increasing environmental and health concerns call for the reduced use of solvent strippers.

The most effective way to prevent the pollution caused by paint removal is not to paint the part and thus avoid the need to strip it. Some airlines have tried polished

aluminum skins and report that the appearance is acceptable and the life-cycle cost is lower than painting with periodic removal to allow inspections. However, for most applications, the painting improves appearance or performance or both and must still be used.

Cleaner technologies based on physical decoating are commercially available or are being developed to replace solvent strippers. These technologies take advantage of the differences in physical properties between the coating and the substrate to destroy the bonding and/or abrade the coating from the underlying substrate. Among available paint removing techniques the most promising ones appear to be the blasting technologies. These include but not limited to: plastic media blasting, wheat starch blasting, sodium bicarbonate wet blasting, high pressure water blasting and cryogenic blasting. It is clear that the water blasting constitutes the most effective technology. Water is readily available, comparatively inexpensive, and induces no damage to environment. The complete separation of water and debris facilitates material recovery. Therefore complete pollution prevention is feasible.

Water jet depainting includes a sequence of rather complicated phenomena. Jet development and disintegration into an array of droplets, jet impact on the surface, development and superposition of stress waves in the impact zone, material deformation and separation etc. altogether constitute the process in question. A practical model is a necessary for understanding and optimization of this technology.

The experimental study has been carried out to acquire a database representing paint removal by water jet at various operational conditions. The fuzzy logic technique was used to process the obtained data and to construct a correlation between process

variables (water pressure, nozzle traverse rate, and standoff distance) and process results (productivity, water consumption). Additional experiments were carried out to validate the computational results.

7.1.2 Experimental Study of Pure Waterjet Depainting

The experimental study of depainting of steel samples was carried out in order to estimate the effect of the waterjet pressure, the standoff distance and the traverse rate on the rate of paint removal and the specific water consumption. A high-pressure water supply system included a water softener, a booster pump, and an Ingersoll-Rand intensifier. A water softener was used to remove the iron and calcium, and dissolve solids that might cause damage to the sapphire nozzle. Then softened water was fed to the booster pump which would produce the pressure up to 10.4 MPa (1,500 psi), then it was further pressurized by an intensifier using a hydraulically driven plunger pump and carried through a stainless steel pipe to a nozzle head. A sapphire water nozzle with diameter 0.254 mm was installed on the nozzle head, which was kept constant during the experiments. The nozzle head was mounted on a 3-axis Ingersoll-Rand gantry robot whose movements were controlled by GE Fanuc series 18-M CNC controller. Low carbon steel AISI1018, machined to a block with 4x2x1 in3. An oil based paint was sprayed on the steel surface cleaned by a sandpaper, and allowed to dry for 72 hours.

The steel samples are shown on Figure 7.2. The rust seen on the metal surface appeared later, after completion of the study. The samples were depainted by a moving waterjet normal to the specimen surface. Several strips were generated at each steel block at various operational conditions. The ranges of the experimental parameters are shown

in the Table7.1 The maximum values of the operational conditions were determined by the equipment capabilities.

Table 7. 1 Ranges of Experimental Parameters

Process Parameter	Min value	Max Value
Nozzle Traverse Rate	0.635 m/min	8.89 m/min
Standoff distance	100 mm	330 mm
Water Pressure	69 MPa	276 MPa

As a result of the jet impact the paint free strips were generated on the substrate surface. The strips were examined with an optical microscope. Depainting was considered successful if and only if no paint except for several microscopic spots was identified on the metal surface. The existence of these spots was attributed to paint redeposition on the cleaned surface. In two to tree weeks these spots were spontaneously separated from the substrate surface. This demonstrates that the generation of the spots is due to the accidental redeposition of the paint particles. Only successfully depainted strips were further examined. In the course of the following discussion we will term "a strip" the region on the substrate surface, where the paint is considered to be successfully removed. The width of these strips was measured using a Mitutoyo Toolmakers Microscope. Since the width of the clean area was not uniform along the strip, five consecutive measurements of the strip width were taken and the average results were used to determine the rate of the paint removal (RMR m2/min) as well as the specific water consumption (WC m3/m2).

7.1.3 Experimental results

In the present study knowledge pertaining to waterjet depainting was obtained from two hundred experimental data points. The experimental results are depicted in Figures 7.3, 7.4, 7.5. The extremal character of the relationship between the standoff distance and the strip width (Figure 7.3) is due to the increase of the jet diameter and decrease of the water momentum as the standoff distance increases.

As indicated earlier, width of strip is an output variable measured in the course of the experimental study. However, the real process output variables are rate of material removal and specific water consumption. The rate of material removal (Figure 7.4) and water consumption (Figure 7.5) per unit of the cleaned area were determined according to Equations 1 and 2, respectively. These two quantities are the principal indicators of the efficiency and competitiveness of waterjet cleaning. In our further study the combination of these two derived process parameters is used in design of an objective function in optimization problem.

$$RMR \left(m^2 \min^{-1} \right) = T_{raverse\ rate} \cdot W_{idth\ of\ strip} \tag{7.1}$$

$$W_{ater} C_{onsumption} \left(m^3 / m^2 \right) = \frac{C_D \cdot \pi \cdot D^2 \cdot \left(2 \cdot P / \rho_w \right)^{\frac{1}{2}}}{4 \cdot RMR} \tag{7.2}$$

where ρ_w is the water density, C_D is the discharge coefficient of the waterjet orifice, whose diameter is D_n. In present work C_D is taken to be equal 0.7. (Hashish, 1993)

7.1.4 Fuzzy Logic Model of Waterjet Depainting

The data acquired in the course of the performed experiments provides limited information about correlation between process conditions and process results. The

acquired knowledge is sufficient for identification with some accuracy the width of strips generated at a tested set of process conditions. For example, from the experimental data it follows that at P= 207 MPa, SOD=0.177 m, TR=0.635 m/min the value of the strip width is 3.556 mm. Another form of the knowledge inferred from the obtained experimental data base is the generic trends in the change of the strip width. For example, from the acquired data (and from previous experience) it follows that the increase of the water pressure brings about the increase of the strip width.

The information above has a limited scope. However the available data processing techniques enable us to enhance dramatically the knowledge inferred from the acquired experimental database. For example, these techniques enable us to construct the prediction model suitable for process optimization. One of the effective data processing procedures is provided by the fuzzy logic. The fuzzy logic approach integrates the crisp (numerical) information provided by each individual test, and linguistic (generic) information, provided by the whole acquired database. The first step in constructing fuzzy logic model of a process is identification of input and output variables. As an example, in our case, the strip width was chosen as output variable. Although we just as well could have chosen any of the derived quantities (RMR, Water Consumption) as an independent model output. The application of the fuzzy logic involves decomposition of the intervals of the change of input and output variables into several overlapping subintervals. Then, the acquired database is used to infer logical (if...if... if..., then...) relations between these subintervals. As the result, a linguistic (qualitative) process model is constructed. In order to quantify this model we introduce for each subinterval of the change of the process variables a function (membership function) determining the

strength of the belonging (membership) of a variable in question to the different subintervals. The form of the membership functions does not depend on the results of the experiments and is, to a some degree, arbitrary. Finally, the fuzzy logic provides a routine, which enables us to determine the values of the output variable, corresponding to a given set of the input variables, using the constructed fuzzy sets. The construction and the use of the fuzzy sets for prediction of the results of depainting, is presented below. This procedure illustrates the details of the application of the fuzzy logic technique for analysis of waterjet decoating.

7.1.5 The Procedure of Application of Fuzzy Logic

The first stage in the application of fuzzy logic for construction of the process model is an identification of the ranges of input and output variables (determination of universes of discourse). Then the range of the change of each variable is divided into the set of subintervals and each of the subintervals is assigned a membership function, and is given an appropriate linguistic name This combination of a subinterval, its membership function, and its linguistic name constitute a fuzzy set. Fuzzy sets of one particular variable usually overlap. The degree of overlap reflects fuzziness in the definition of fuzzy sets. The number of fuzzy sets for each particular variable is determined by the available database. For example, our experiments were conducted at four different water pressures, and the whole range of the variation of the water pressure was arbitrarily divided into four subintervals (Table 7.2).

The aggregation of all subintervals of one process variable on a single coordinate axis is called the Universe of Discourse of that variable (Figure 7.1). As it follows from

Figure 7.1, the water pressure of 150 MPa has a degree of membership equal to 1 in the fuzzy set Medium (complete representative of this set) and degree of 0 in the fuzzy sets Low and High (not a member of a set). The water pressure of 125 MPa has a degree of membership equal to 0.27 in the fuzzy set Low, and simultaneously a degree of membership 0.58 in the fuzzy set Medium.

Table 7.2 Subdivisions of the Process Variable Water Pressure

Linguistic name	Min Value	Max value
Low	0 MPa	150 MPa
Medium	90 MPa	210 MPa
High	150 MPa	270 MPa
Very High	210 MPa	280 MPa
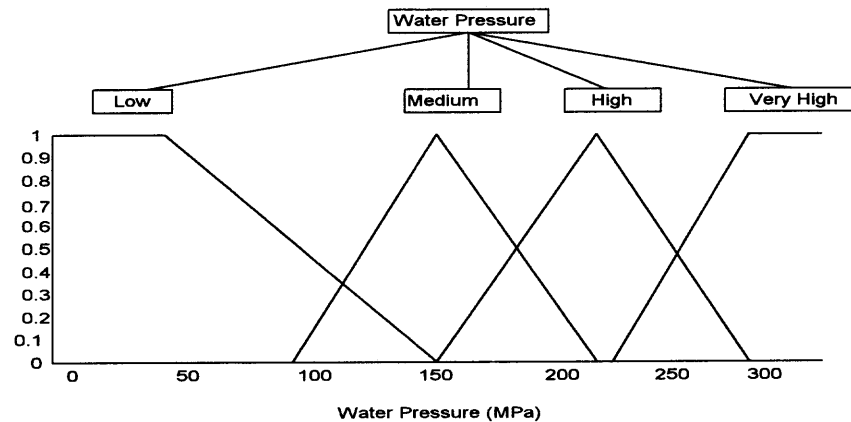
Figure 7.1 Universe of Discourse of the Process Variable "Water Pressure"

$$\mu_{low}(x) = \frac{150-x}{150-60} \text{ for x} \in [60,150] \qquad \mu_{very\ high}(x) = \frac{x-210}{280-210} \text{ for x} \in [210,280]$$

$$(7.3) \qquad\qquad\qquad\qquad (7.4)$$

$$\mu_{high}(x) = \begin{cases} \dfrac{x-150}{210-150} & \text{for } x \in [150,210] \\ \dfrac{270-x}{270-210} & \text{for } x \in (210,270) \end{cases}$$

(7.5)

$$\mu_{medium}(x) = \begin{cases} \dfrac{x-90}{150-90} & \text{for } x \in [90,150] \\ \dfrac{210-x}{210-150} & \text{for } x \in (150,210) \end{cases}$$

(7.6)

Similar charts are constructed for the traverse rate (Figure 7.6), standoff distance (Figure 7.7) and the strip width (Figure 7.8)

Similar equations were constructed for other input variables (standoff distance and traverse rate) and output variable (strip width). In the current model the problem parameter space was discretized into 4 fuzzy sets for water pressure, 8 sets for standoff distance and 5 sets for traverse rate. In general this number of fuzzy sets is excessive and is used for simplicity of developing of Fuzzy Associative Memory.

7.1.6 Representation of the Knowledge of the Depainting Process

In addition to the crisp (numerical) information, the acquired data generated qualitative (linguistic) knowledge about the process of depainting. This knowledge is then formulated in the form of logical (fuzzy) rules. An example of such a rule follows.

IF Waterjet Pressure is Low and Traverse Rate is Slow and Stand-Off Distance is High Then Strip Width is Around Medium

The number of rules in a fuzzy logic model depends on a number of experimental data points. A collection of all fuzzy rules for one particular system (database) is termed - rule

base. For a small number of model variables there is a compact form of representing fuzzy rules. This compact form is commonly referred to as Fuzzy Associative Memory (FAM). The tables representing FAM for the acquired database are given below. In the Tables (7.3)-(7.6) the upper horizontal row represents fuzzy sets of the process variable 'Standoff Distance', while the left vertical column, represents fuzzy sets of the process variable 'Traverse Rate', and the cells of the tables represent fuzzy sets of the output variable,' Strip Width'. Figure 7.8 contains full linguistic names of the above fuzzy sets of 'Strip Width'.

Table 7.3 Fuzzy Associative Memory, Water pressure "Low"

Standoff distance

	EL	VL	L	M	H	VH	VVH	EVVH
VS	VVVL	VL	M	M	AM	AM	L	VL
S	****	VVVL	VL	L	VVL	VVL	VVL	EVVL
M	****	VVVL	VVVL	VVL	EVVL	EVVL	EVVL	EVVL
F	****	****	****	****	****	****	****	****
VF	****	****	****	****	****	****	****	****

Traverse Rate

Table 7.4 Fuzzy Associative Memory, Water pressure "Medium"

Standoff distance

	EL	VL	L	M	H	VH	VVH	EVVH
VS	****	****	L	L	M	M	AM	VVL
S	****	****	L	AM	L	L	VL	VVL
M	****	****	VL	L	AM	L	VL	VVL
F	****	****	****	L	AM	VL	VVVL	EVVL
VF	****	****	****	****	****	****	****	****

Traverse Rate

Table 7.5 Fuzzy Associative Memory, Water pressure "High"

Standoff distance

	EL	VL	L	M	H	VH	VVH	EVVH
VS	****	H	VVH	VVVH	EVVVH	VVVH	VVH	AM
S	****	AM	M	AH	H	AH	L	VL
M	****	VL	L	AM	AM	M	VL	VVL
F	****	VL	L	L	AM	AM	L	VL
VF	****	VL	AM	AM	L	L	VL	VVL

Traverse Rate

Table 7.6 Fuzzy Associative Memory, Water pressure "Very High"

Standoff Distance

	EL	VL	L	M	H	VH	VVH	EVVH
VS	****	****	****	****	****	****	****	****
S	****	L	M	H	VH	VVH	VH	L
M	****	L	AM	M	AH	H	M	VL
F	****	L	AM	AM	M	AH	M	VVL
VF	****	L	AM	H	VH	M	AM	L

Traverse Rate

The way of the knowledge presentation by the above tables is illustrated by the following examples.

Example 1. If we apply Low Water Pressure (Table 3) and **Medium** Standoff Distance (upper horizontal row, fifth cell) and **Slow** Traverse Rate (the leftmost column second cell) then the resulting strip width is **Low**.

Example 2. The combination of **High** Water Pressure (Table 5), **Very Fast** Traverse Rate (VF), and **Medium** SOD (M) will result in Strip Width being **Around Medium** (AM).

Tables 7.3-7.6 represent linguistic correlation between input and output variables. Fuzzy logic provides a simple technique, which enables us to quantify these correlations. A simple example demonstrates the use this technique:

Let us consider the following set of input parameters: Water Pressure 172 MPa, Traverse Rate 5m/min and Standoff Distance 229 mm. From Figure 5, showing the fuzzy input universe of the Water Pressure, follows that the pressure of 172 MPa falls into two fuzzy sets **Medium** and **High** with corresponding degrees of membership of 0.63 and 0.36. Similarly from Figure 6 (fuzzy input universe of Traverse Rate) follows that the traverse rate of 5m/min falls into two fuzzy sets: **Moderate** and **Fast** with corresponding degrees of membership of 0.66 and 0.33. Finally, from the Figure 7 follows that SOD of 229 mm falls into only one fuzzy set, **Very High,** with degree of membership equal to **0.96.**

For a given set of the input variables, and from the Tables 3-6, the following rules were inferred:

1. If Water Pressure is **Medium (0.63)** AND Traverse rate is **Moderate (0.66)** AND Standoff Distance is **Very High (0.96)** Then Strip Width is **Low.**

2. If Water Pressure is **High (0.36)** AND Traverse rate is **Moderate (0.66)** AND Standoff Distance is **Very High (0.96)** Then Strip Width is **Medium.**

3. If Water Pressure is **Medium (0.63)** AND Traverse rate is **Fast (0.3)** AND Standoff Distance is **Very High (0.96)** Then Strip Width is **Very Low.**

4. If Water Pressure is **High (0.36)** AND Traverse rate is **Fast (0.3)** AND Standoff Distance is **Very High(0.96)** Then Strip Width is **Around Medium.**

Here there are two fuzzy sets of Water Pressure, two fuzzy sets of Traverse Rate, and one fuzzy set of Standoff Distance. Therefore the total number of rules is equal to 2x2x1=4.

7.1.7 Inference From Fuzzy Rules.

Fuzzy rules give us only linguistic correlation between sets of the input parameters and the output variable. Instead we would like to estimate to what degree a rule's consequent (part to the right from the **then** statement) is true. In doing so we apply logical **min** operator. For the rule 1 the degree of membership of the fuzzy set **medium** of Water Pressure is found to be (0.63), the degree of membership of the fuzzy set **moderate** of Traverse Rate is found to be (0.66), and the degree of membership of the fuzzy set **Very High** of Standoff Distance is found to be 0.96. We select the minimal out of these three values, which is 0.63. The selected minimal value is assigned to be the degree of the membership of the fuzzy set **Low** of the output variable 'Strip Width'. We repeat these steps for other rules.

Rule 1: min (0.63, 0.66, 0.96) $\rightarrow$ 0.63 (μ of fuzzy set LOW of Strip Width).

Rule 2: min (0.36, 0.66, 0.96) $\rightarrow$ 0.36 (μ of fuzzy set MEDIUM of Strip Width).

Rule 3: min (0.63, 0.3, 0.96) $\rightarrow$ 0.3 (μ of fuzzy set VERY LOW of Strip Width) .

Rule 4:   min (0.36, 0.3, 0.96) $\rightarrow$ 0.3 (μ of fuzzy set AROUND MEDIUM of Strip Width).

The information above states that if the traverse rate is 5m/min, water pressure 172 MPa, and SOD is 229 mm then the resulting strip width can be either Very Low with degree of truth 0.3, or Low with degree of truth 0.63, or Medium with degree of membership 0.36, or Around Medium with degree of truth 0.3. These found degrees of truth of fuzzy sets of the output variable Strip Width are used now to truncate the corresponding triangles of the universe 'Strip Width' (Figure 7.8). The resulting truncating region is called a solution region (Figure 7.9).

7.1.8 Defuzzification

The resultant solution region on Figure 7.9 provides fuzzy information about the resultant strip width. We can infer from this figure that at the water pressure of 172 MPa, traverse rate 5 m/min and standoff distance 229 mm the resulting strip width is somewhere between 1 mm to 2.6 mm. But since the truth function of fuzzy set **LOW** is the biggest one (0.63) it is more likely to expect that the strip width would range from 1.4 to 1.8 mm. Fuzzy logic suggests several routines (defuzzification techniques) which enable us to evaluate the numerical (crisp) value of the output variable using distribution shown on Figure 7.9. The most commonly used defuzzification technique is the centroid method given by the following equation:

$$z = \frac{\sum\limits_{i=0}^{n} d_i \mu_y(d_i)}{\sum\limits_{i=0}^{n} \mu_y(d_i)} \qquad (.7.7)$$

Here d is the value of the width of strip at some point, and $\mu(d)$ is the truth membership value for that point. Applying this defuzzification technique to the solution region under consideration we obtain:

$$Z=1.78 \text{ mm}$$

Comparing this result with the experimental result (1.74 mm) we find that the error is less than 3%, which is regarded acceptable in the current work.

The prediction technique can be improved by the use of the weak λ-cut method. This is defined by the equation:

$$\mu A(x) \geq \lambda$$

In general the λ-cut establishes the minimum truth threshold for a rule. If the truth of a premise (the part of the rule before the **then** statement) evaluation falls below the λ-cut, the rule is not executed. As it is shown by the Table 7.7 the introduction of the λ-cut in some cases improves the model performance, since it eliminates the residual fuzzy spaces (ones that have very small but finite degree of truth) (Cox, 1994).

An additional set of experimental data points, different from those used for the model construction has been acquired. This data set enabled us to test the model performance. The results of the testing are tabulated in the Table 7.7:

Table 7.7 Comparison of Experimental and Predicted Values of Strip Width

Water Pressure (MPa)	Traverse Rate (m/min)	Standoff distance (mm)	Strip width (experiment) (mm)	Strip width (predicted) (mm)	Strip width (mm) (predicted λ-cut= 0.2)	Relative Error (%)
103	3.8	178	1.40	1.64	1.37	2.1
138	3.3	178	1.87	1.75	1.83	2.1
172	5	229	1.74	1.78	1.78	2.3
207	7.6	203	1.83	1.80	1.80	1.6
241	5.8	216	2.54	2.37	2.37	6.7

Here the last column contains the results of calculation of the strip width at the λ-cut = 0.2.

7.1.9 Discussion of Results

Presented results show the feasibility to construct a numerical model of water jet depainting process using fuzzy logic principals. The procedure involved acquisition of the experimental database, fuzzification of the input and output variables, construction of

the fuzzy associated memory representing the acquired database, evaluation of the fuzzy distribution of the output variable for the selected sets of the input variables and evaluation of the crisp value of the output variable. The routines involved in the transformation above are comparatively simple. The results of the prediction for experimental data different from that used for the construction of the model range between 1-7%. At this point it is important to mention that the parametric combination used for verification of the fuzzy model was within the middle of our parametric space where model correlation is the highest. The greater error is expected near the outskirts of the parametric space. This accuracy is acceptable at the first stage of the process investigation and will be improved, as an additional database is generated. The main advantage of the suggested approach is that it can be easily expanded as new process information is acquired, or new process variables are introduced.

In the presented study the process result is characterized by the strip width, which constitutes the only directly measured output variable. Actual process characteristics (productivity and water consumption) can be readily determined using Equations 7.1 and 7.2. The result of the presented analysis provides guidance to the optimization of the waterjet depainting. Particularly, it is shown that the process effectiveness increases if the water pressure is maximum (276 MPa in this study), along with maximal traverse rate (8.89 m/min). The standoff distance should range between 0.15 and 0.25 m. Analysis was carried out at a constant nozzle diameter of 0.254 mm. The procedure of the model construction can be readily modified to account for this and other process variables.

The above presented procedure is designed to predict a process output (strip width) once a set of input parameters (water pressure, nozzle traverse rate and standoff

distance) has been specified. On the contrary most models are used to enhance control of a process. Therefore it may be practical to develop a procedure where we are given a desired width of strip, say 1.5 mm, and need to find the best set of input parameters. One way to address this issue is to use the probabilistic algorithm called Genetic Algorithm. This rather new technology is based on the principles of evolution and hereditary. Such a system maintains a population of potential solutions, it has some selection process, based on the fitness of the individual solution, and some "genetic" operators. For the detailed description of working of the Evolutionary Programs the authors refer you to (Michalewicz, 1996). Thus we could use fuzzy logic model and Genetic Algorithms to obtain any desired strip width along with sets of corresponding input parameters. Then according to some predefined criteria we choose the optimal set of input parameters (for example, those resulting in maximum productivity or minimal water consumption) for the given strip width. The above outlined procedure is the topic of the current work of the authors (Babets et al, 1999).

In the above-presented fuzzy logic model no process parameters resulting in a possible material damage were included. Therefore the model is only concerned with the productivity issues. But it very well may be happening that in an effort to apply this model to a different cleaning environment (different paint thickness for example) the safe combination of process parameters might no longer be safe. And since the rate of material removal (RMR) is meaningful only when there is no substrate damage we need to find the means to account for the possible material damage. One possible solution could be an addition of fuzzy output Universe, say, "Safety" with corresponding fuzzy sets "Not Safe", "Approximately Safe" and " Completely Safe". Then after being

properly correlated, the fuzzy logic model will not only be able to predict the strip width (RMR), but also point to the location on the "Safety" Universe. But this approach was not investigated in our study and is left for the future research.

7.1.10 Concluding Remarks

The approach used in our study is not unique. There are several efficient techniques that enable us to reduce database to a compressed process description. This description, for example, can be obtained using regression analysis. Fuzzy logic technique, however, has a number of advantages. First of all, there is no limitation on the form of the model. Fuzzy logic can account for any form of process nonlinearity. The inaccuracy (fuzziness) of input information effects the final result much less then that in the case of regression analysis. Model improvement using new acquired information is rather simple. Thus, the use of fuzzy logic will improve the planning and control of the waterjet depainting. Although this study is concerned with prediction of the results of paint stripping, with some modifications it can be applied to other surface processing technologies. In our following work we will show how to expend a model constructed for an available data base to a similar system at a limited initial information.

7.1.11 Some Definitions

Fuzzy set –The available range of process variable can be decomposed into several overlapping subintervals (domains). All variables contained in this domain are its members. Each domain is labeled by linguistic term, which clearly represent its main features. The strength of participation (degree of membership) of a member in a given

domain is estimated numerically by a function (membership function), which range from 0 to 1. The domain of members and their membership function constitute a fuzzy set. Thus fuzzy sets relate a value to a linguistic characteristic and shows strength of this relationship. Rigorous definition of a fuzzy set is given below.

Fuzzy sets are actually functions that map (relate) a value that might be a member of a set to a number between zero and one indicating its actual degree of membership. A degree of zero means that a value does not belong to the particular set, while degree of one means that a value is completely representative of the set. And numbers in between [0,1] represent partial degree of membership to a set. This idea of partial membership is the main distinction of fuzzy set theory from the traditional binary set theory, where a value is either a member of a set or not, with no partial degree of membership allowed.

Membership function – is a numerical characteristic which defines the strength of belonging (degree of truth) of given value to selected fuzzy set.

Fuzzification- Fuzzy logic operates with linguistic terms rather then fixed crisp numbers. In order to use fuzzy logic we need to represent the available information in form of fuzzy sets. This representation of the information in form of fuzzy sets is called fuzzification. This includes the decomposition of the universe of discourse into domains, and assigning the membership function and appropriate linguistic name. It should be pointed out that in many practical cases the use of fuzzy sets for description of process information represent existing practice of representation of such information.

Defuzzification- at the same time the output of the model should constitute the numerical (crisp) value, rather then a fuzzy one. On of the available technique for obtaining a crisp number out of a fuzzy one is given by Equation 7.

Fuzzy Propositions- A fuzzy logic proposition, P, is some linguistic statement, which defines a state of a variable, i.e., 'Pressure is High'. The information embedded in a fuzzy proposition could be interpreted slightly differently by various individuals, i.e. water pressure 279 MPa can be considered both HIGH and MODERATE by different individuals.

Fuzzy Logic - Unlike the conventional logic, which deals with precise propositions, fuzzy logic deals with imprecise propositions thus establishing a theoretical foundation for approximate reasoning.

Fuzzy Rule Base- Fuzzy information of system behavior is usually represented in a form of fuzzy rule base. Fuzzy rules are expressed in a conventional antecedent- consequent format:

If x is A and y is B then z is C

where x, y and z are model variables and antecedents A,B,C are fuzzy regions (propositions). This form is commonly referred to as IF-THEN rule- based form. It represents the inference such that if we know the antecedent then the consequent can be inferred or derived.

Fuzzy Associative Memory- Compact form of fuzzy rule base representation. See tables 3-6.

Fuzzy min-max composition- the method for inference from fuzzy rules where the consequent fuzzy region is restricted to the minimum of the predicate truth. The output fuzzy region is updated by taking the maximum of these minimized fuzzy sets. These steps are outlined in the following equations:

$$\mu cfs[xi] \leftarrow \min (\mu pt(1), \mu pt(2), \mu pt (n)]) \qquad (1)$$

which indicates that the consequent fuzzy (cfs) set is modified by taking the minimum of predicate propositions.

And
$$\mu sfs [xi] \leftarrow \max (\mu sfs [xi], \mu cfs [xn]) \quad (2)$$

Which shows that the solution fuzzy set (sfs) is updated by taking the maximum of either the truth value of a solution fuzzy set or that the fuzzy set modified in equation (1).

λ-cut- the λ-cut establishes the minimum truth threshold for a rule. If the truth of a premise evaluation falls below the λ-cut, the rule is not executed.

7.2 Experimental and Numerical Investigation of Waterjet Derusting Technology

7.2.1 Introduction

The corrosion of the metal structures a serious technological and economical problem. It shortens the life span of the steel parts, deteriorates dramatically their performance. Corrosion is a chemical or electrochemical process in which surface atoms of a solid metal either react with or dissolve in a substance that contacts an exposed surface. Corroding mediums are generally classified as aqueous or non-aqueous. The rate of steel corrosion in atmosphere depending on geographical location, and can reach 1070 μm/yr. When rust corrosion depth reaches 1% of the thickness of the still, the strength of the steel reduces by 5-10%. Throughout the world steel corrosion annually equals to 20-40% of its annual production (Liu et al, 1993). The corrosion of all carbon steels is most devastating when the metal is subjected to alternately wet and dry atmosphere combined with the presence of chloride salts. Typically this environment can be encountered on the underbodies of automobiles and trucks. The most conventional way of rust prevention is

coating of the metal surface. But prior to the coating the complete cleanliness of surface must be assured to ensure that a surface is clear of any rust.

The conventional methods of rust removal involve acid or cleaning and sandblasting. These technologies though proven to be effective, could be environmentally hazardous. Some new derusting technologies, such as Rust Neutralizers convert rust to chemically neutral surface, leaving the surface ready for coating application. However the use of this chemical is limited to oil-based types only, and the chemicals contained in the product can be detrimental to worker's health.

Waterjet surface derusting constitutes rather efficient way to clean steel surfaces. The following experimental study is concerned with optimization or at least improvement of jet based derusting technology.

7.2.2 Experimental Setup

The derusting experiments were carried out at the Ingersoll-Rand waterjet system (Figure 7.10). The nozzle head was mounted on a 3-axes gantry robot whose movements were guided by an Allen Bradley 8200 series CNC controller.

The major obstacle in the experimental study of a derusting technology is the extreme diversity of the rusted surfaces. It is difficult to find several samples with similar degree of rusting. As a result a rather low reproducibility of the experiment follows. In order to at least partially overcome this problem we used the ISO developed standard for classification of the rusted steel surfaces. This standard specifies four rust grades, designated A, B, C and D (ISO, 1999) The rust grades are defined by written descriptions together with representative photographic examples. The selected steel samples were

sorted according to visual similarity and compared to the given photos. Those identified as the class C were used as experimental samples. In the above mentioned ISO publication grade C of the rusted surface is defined as the "steel surface on which the mill scale has rusted away or from which it can be scraped, but with slight pitting visible under normal vision". Still it should be stressed that the existent rust grades classification based on visual comparison does not provide a reliable procedure for rust identification and thus makes it quite difficult to collect uniform experimental data samples.

In our experiments the effects of water pressure, traverse rate and nozzle diameter on cleaning productivity and surface quality were investigated. The tests were run at water pressures of 310, 241, 172, 69 MPa (i.e. 45,000, 35,000, 25,000 and 10,000 psi). The water nozzles with diameters 0.127, 0.1778, 0.254, 0.3556 mm were used. In these experiments the effect of the standoff distance (the distance between a nozzle exit and a sample) as an independent process parameter was not investigated. Instead, the ratio of nozzle diameter to the nozzle standoff distance was kept constant. Thus a number of standoff distances were tested to find a near optimum value for a selected nozzle diameter. Then the obtained ratio was kept constant for the other nozzle diameters. The study was carried out at the traverse rates 635, 2540, 7620 and 12700 mm/min. The upper bound of the nozzle traverse rate (12700 mm/min) was imposed by the equipment limitations.

In order to study the effect of the waterjet parameters on generated surface the full factorial experimental design was applied. In such a design one process variable is tested at its different levels, while the other variables are being held fixed at some level. The experimental procedure involved the following steps. For each cleaning situation (i.e. the

combination of water pressure, nozzle traverse rate and nozzle diameter / standoff) the single nozzle pass width of strip was measured with Mitutoyo Toolmakers Microscope and recorded. This value of strip width (STW) is then used to calculate process productivity (Rate of Material Removal) and specific water consumption according to Equations 7.1 and 7.2. Then several nozzle passes with 25% overlapping were made at the same operational conditions. The resulting derusted area was evaluated visually and photographed with Olympus photo microscope with 12X magnification in order to determine the quality of the cleaning.

7.2.3 Surface Examination

In current study, the X-Ray diffraction was used to evaluate the presence of oxides (rust) on the material surface after rust removal with waterjet. The Siemens D5000 diffractometer with θ-2θ diffractometer geometry at Stevense Institute of Technology was used for this investigation. The experimental samples consisted of rusted – cleaned pairs. The following procedure was used for sample preparation. First the metal samples were machined to a block 0.4 X 0.4 X 0.25 inches. Then the samples with similar rust were grouped in pairs. From each pair one sample was left as it was, and the another one was cleaned of rust using waterjet. The following waterjet parameters were applied: Water Pressure 200 MPa, Nozzle Diameter 0.254 mm. Two cleaning runs were made. At first the rust was removed from the metal surface at a low nozzle traverse rate, and at the second run the flash rusting was removed at the high traverse rate of 3175 mm/min. Then the sample was dried in hot air. Each pair was evaluated for the presence of oxides on the

diffractometer. The resulted diffraction patterns enabled us to compare the oxides content on the samples before and after the waterjet treatment.

7.2.4 Experimental Results

7.2.4.1 Surface Classification. The quality of derusting by waterjet was evaluated in accordance with ISO standards (ISO 8501-1:1988). This standard defines four grades of cleanliness of the surfaces generated by jet derusting. These surfaces are termed Sa 1, Sa 2, Sa 2 ½ and Sa3. The qualitative description of each grade along with the representative photographs of the surface is presented. During this experimental study it was found difficult to follow the ISO classification. Instead, the following "fuzzy" classification was suggested. According to the developed procedure we divided the derusted surfaces into two classes: "well cleaned', and "poorly cleaned". A surface is allowed to have a partial degree of membership in both classes. The class "well cleaned" would roughly correspond to ISO grades Sa3 and Sa 2.5, while the class "poorly cleaned" would correspond to surface grades Sa 2.5, Sa 2 and Sa1. Figure 7.11 depicts a typical well-cleaned surface. Here two shades of green can be distinguished. Light green corresponds to the derusted surface, while dark green corresponds to flush rust, which appears immediately after waterjet pass. It was found that flash rust can be removed easily by an additional application of the waterjet at a high traverse rate, or prevented by immediate drying of the surface in hot air.

Figure 7.12 shows a typical "poorly cleaned" surface. Such a surface is free from lightly adherent mill scale, rust and other contamination, but some firmly adherent rust is remaining on the surface. Thus the most representative surface samples were classified as

either belonging to one of these classes, or, not. The "fuzzy" memberships in the two fuzzy classes for the remaining surfaces were determined using the artificial neural network assisted fuzzy classification method described in the following section.

7.2.4.2 Surface Cleanliness. In order to evaluate qualitatively and quantitatively the waterjet-based derusting technology, several studies were carried out. These examinations included SEM photographing of the surface, SEM chemical analysis, and the x-ray diffraction analysis. Figure 7.13 shows a rusted surface at 500 X magnification level. The main features of the surface are the oxidized metal grains of different sizes. Figure 7.14 represents a surface derusted with waterjet. No oxidized metal grains are observed, the surface is smoothed over and visually clean of rust.

In order to estimate qualitatively the effectiveness of the derusting the chemical analysis of the surface prior and after treatment were determined. The SEM was used for this study. The typical results of the analysis are presented in Figures 7.15-7.16. These Figures show that the oxygen content of the surface was significantly reduced after the water jet treatment. In order to evaluate the degree of the derusting more accurately chemical analysis was supplemented by the x-ray diffraction. The corresponding diffraction patterns of the metal surfaces before and after waterjet cleaning are presented in Figures 7.17 and 7.18 respectively. Roughly speaking each peak on these figures corresponds to a chemical compound. The intensity of a peak represents a relative amount of this chemical compound. The atomic spacing values shown just above each peak allow us to determine the type of a chemical compound present on the surface. From Figure 7.17 and Table 7.8 it is clear that a rusted surface in addition to Fe contains

significant amounts of **Fe$_2$ O$_3$, and Fe$_3$O$_4$**. After waterjet cleaning (Figure 7.18) the three still remaining peaks represent Fe, with significantly increased intensity levels. Most of the oxides are no longer present on the diagram, and intensity level of those still present is much lower than that of Fe content. Moreover due to low intensity levels these peaks most probably should be attributed to the noise. The wide base peak at angles 10 –25 degrees on Figures 7.17 and 7.18 is due to the presence of the holder clay used to attach a sample in the holder. Thus, Fig. 7.18 constitutes a compelling proof of the efficiency of the waterjet rust removal.

7.2.5 Model of the Process

7.2.5.1 Choice of a Modeling Technique. In data /information processing the objective is to gain the understanding of a complex phenomena through "modeling" of the system either experimentally or analytically. Then after a model of a system has been obtained, various procedures (e.g. sensitivity analysis, statistical regression, etc.) can be used to gain a better understanding of the system.

There are, however situations in which the phenomena involved are very complex and not well understood and for which the first principle models are not effective. Even more often, experimental measurements are difficult and/or expensive. These difficulties lead us to explore the application of Soft Computing (A.I.) techniques as a way of obtaining models based on experimental measurements. Our problem at hand is a good example of a system with highly nonlinear relationship between process inputs and outputs. The problem of defining the cleaning quality is one of the classification type. Therefore it was found reasonable to apply an advance artificial intelligence modeling

technique based on the combination of fuzzy logic and artificial neural networks. The method used is known as NN-Driven Fuzzy Reasoning (Takagi and Hayashi, 1991), and was used with only slight modifications.

7.2.5.2 Model of the Process. The fuzzy classification of derusted surfaces contained two classes, "well cleaned', and "poorly cleaned". Some of the cleaned samples were prescribed to class "well cleaned" with degree of membership 1, correspondingly they had degree of membership 0 in the class "poorly cleaned". Some samples were identified as "poorly cleaned" and correspondingly were given the degree of membership 1 in this class and zero degree of membership in the class "well cleaned". The rest of the samples had a non-zero degree of membership in both classes. We use a special neural network to determine these degrees. The procedure involved training of the neural network (NNmem), using only well defined samples, that is samples having the degree of membership 1 in either class. Then, after being properly trained, such a network will not only be able to predict the binary degree of membership (either 0 or 1) for some input data, but also the dual degree of membership (fuzzy membership) for the input data points in that neighborhood. As the result of training we obtain neural network, which is able to determine the degree of membership in each of the two classes using input conditions, such as water pressure, rate of traverse, etc. This procedure is described in details in Takagi, et al, (1991) and by Ross (1995). Our actual goal, however, was to determine the process productivity and the resultant degree of cleanliness. In order to reach this goal we divide the available database into two data sets. The first data set contained only the data earlier identified to crisply (i.e. with degree of membership 1) belong to the class "well cleaned", and, similarly the second data set contained the data

belonging only to the class "poorly cleaned". We then train two separate networks, on these two data sets, and as the result each network was able to determine productivity for the class it was responsible for.

Table 7.8 Determination of chemical compound. To accompany Figures 7.17, 7.18

Experimental atomic planes spacing values d (A)	ICDD Tables atomic planes spacing values d (A)	Chemical Compound		
		Fe	Fe_2O_3	Fe_3O_4
3.281	3.24		X	
3.009	2.967			X
2.795	2.728		X	
2.546	2.532			X
2.174	2.176		X	
2.106	2.099			X
2.027	2.03	X		
1.723	1.715			X
1.624	1.616			X
1.49	1.485			X
1.437	1.43	X		
1.289	1.281			X
1.211	1.212			X
1.168	1.17	X		

As the result, we obtained the model of the process in terms of the three trained neural networks that were connected according to Figure 7.19. According to this figure, given some input data set, the network NN_{mem} identifies the degree of membership of a

sample in each of the two classes. Network NN_1 predicts productivity for class "well cleaned", and NN_2 for class "poorly cleaned". Input information is fed to all three networks. The outputs of all three networks are then fed into the special elements which process the networks outputs to determine the weighted sum and as the result predicts final process productivity and the degree of cleanliness.

As the result, we were able to obtain an accurate prediction of the process productivity (the average error of prediction was within 8 %). Also we were able to estimate the quality of derusted surface, based on the fuzzy degrees of membership in "well cleaned' and "poorly cleaned" classes inferred by the NN_{mem} neural network. The results of the prediction are presented in Figures 7.10-7.13. These figures show the process productivity as a function of different process parameters, without regard to the quality of resultant surface. The quality (degree of belonging to the two classes) for any data point in these figures is obtained with the help of the neural network NN_{mem}.

7.2.6 Concluding Remarks

We demonstrate the feasibility and, in fact, effectiveness of waterjet steel derusting. The effect of the operational conditions on the process economy was evaluated and a set of the operational conditions was suggested. This set can be used an initial state in the search of the operational conditions by a practitioners. Because of wide variations of the states of the rusted surfaces and insufficiency of the available identification technique, an advance soft computing procedure (neural network driven fuzzy identification) has been suggested for surface identification.

Analysis of the results of derusting conditions demonstrates the effectiveness of the use of several nozzles rather a single nozzle of the same surface area.

7.3 Experimental Investigation of Waterjet Based Cleaning of Sensitive Surfaces

One of the main advantages of application of waterjet technology for surface decontamination lies in the specifics of the tool itself. Waterjet can be described as a universal tool for material processing. High-speed stream of water (with some modification, such as solid particulate addition, etc.) can be powerful enough to cut through very hard to machine materials, such as titanium, or remove very hard rust. At the same time by changing the process parameters the waterjet can be used as a tool of precision machining of extremely sensitive surface. The following case studies were aimed at investigation of the feasibility of application of high pressure waterjet for cleaning highly sensitive surfaces.

The specific goal of the experiments was to estimate the feasibility of cleaning of the sensitive surfaces with water jets. The following samples were used for these experiments:

A foam coffee cup.

A soda can.

A boiled egg.

7.3.1 Paint removal from a Foam Coffee Cup.

This example of a high pressure waterjet cleaning of sensitive surface represents a challenging cleaning task. The reason is that the substratum in this case is softer then the

deposit itself. In this experiments the working water pressure was 69 MPa (10,000 Psi), nozzle diameter 0.254 mm (10 mils). A specially designed hand-held nozzle body was used with no solid particle addition.

The results of the experiments was the definite conclusion that the paint can be removed with no soft substratum damage observed. This result is represented in Fig. 7.24

7.3.2 Paint removal from an Aluminum Can.

Although the pure waterjet is capable of removal of paint from a substratum, the addition of solid particles to a water stream allowed us to decrease the working pressure and to increase dramatically the process productivity and precision. As a solid additive the backing soda was used in the case of paint removal from the aluminum soda can. As a result of the cleaning operation a surface was successfully cleaned with no induced damage.

7.3.3 Paint removal from a Boiled Egg

As a last sample of sensitive surface an extremely brittle surface of a boiled egg was chosen. For this experiments an oil-based paint was applied on the egg's surface. The working pressure was 130 MPa, nozzle diameter 0.254 mm. A specially designed nozzle holder with two inlet ports for abrasive and air to soften the jet was used for this experiment. As a result we have proved that an extremely brittle surface can be cleaned with high speed waterjets with no surface damage induced (Fig. 7.3.3)

7.3.4 Conclusion

The main conclusion of these series of experiments is that the success of the experiments described above demonstrates the feasibility of the damage free decontamination of the extremely sensitive surfaces using waterjets. And thus demonstrates the universality of the application of waterjetting technology.

7.4 Figures
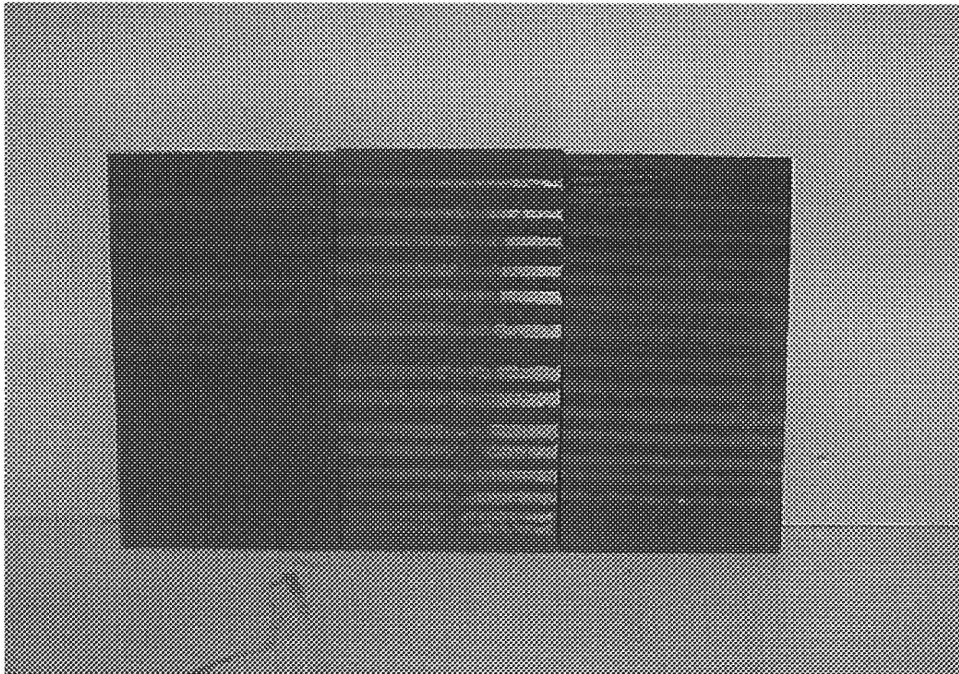
Figure 7.2 Experimental Steel Samples

Strip Width vs. Stand-off Distance
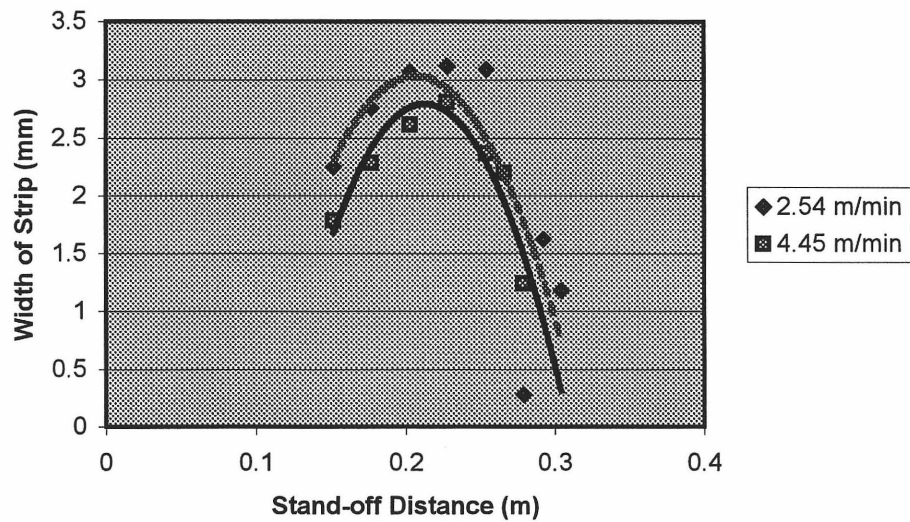
Figure 7.3 Width of Strip vs. Standoff Distance for Water Pressure 276 MPa.

Cleaning Rate vs. Travel Speed
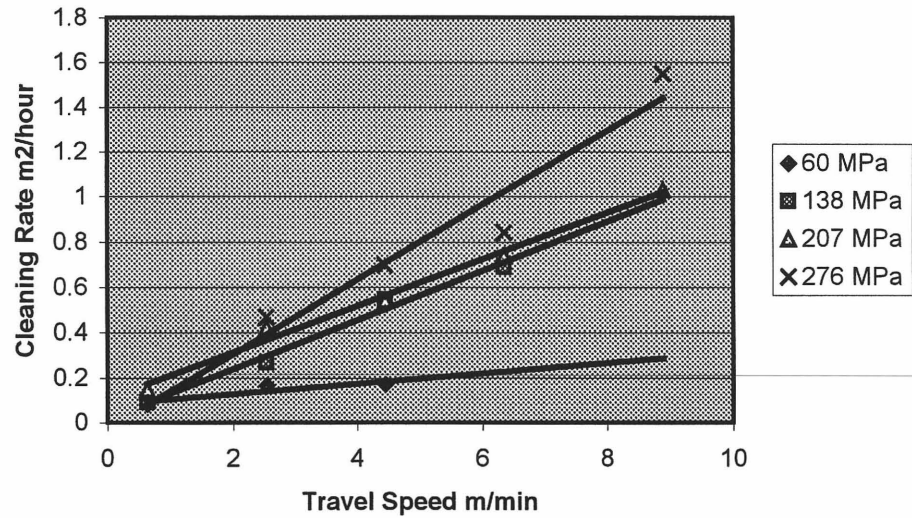
Figure 7.4 Cleaning Rate vs. Travel Speed

Water Consumption
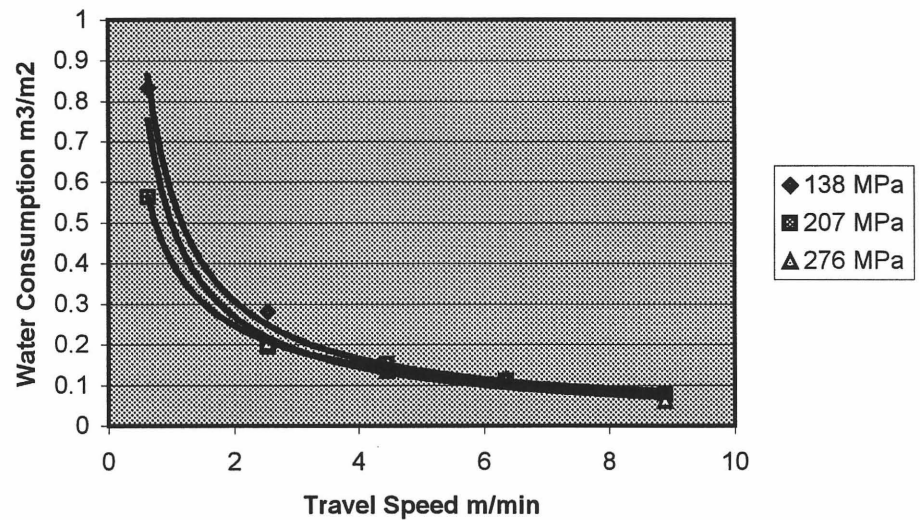
Figure 7.5 Water Consumption vs. Travel Speed
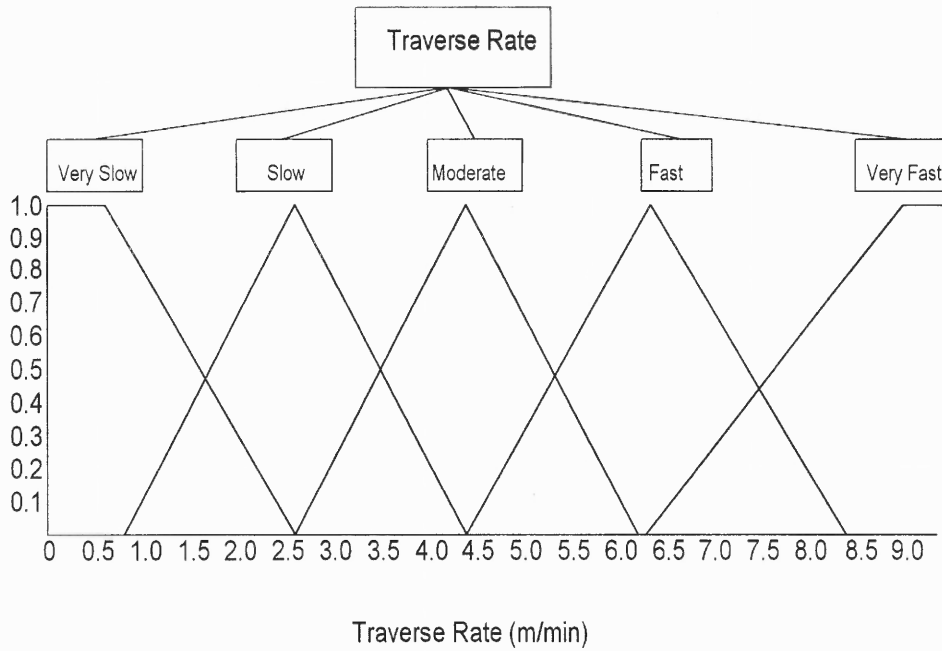
Figure 7.6 Universe of Discourse of the Process Variable 'Traverse Rate'
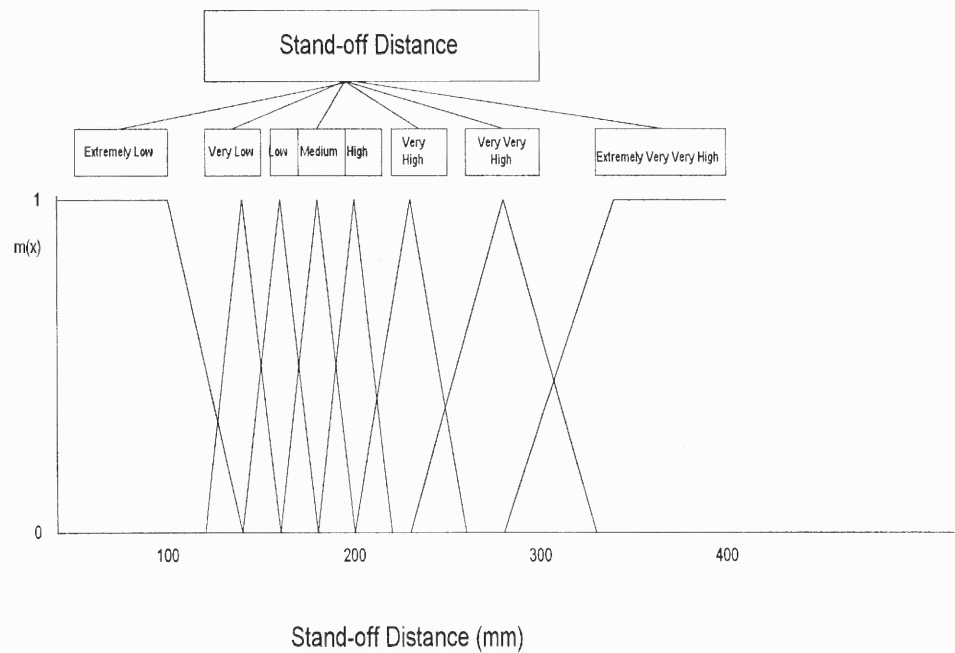
Figure 7.7 Universe of Discourse of the Process Variable "Standoff Distance"
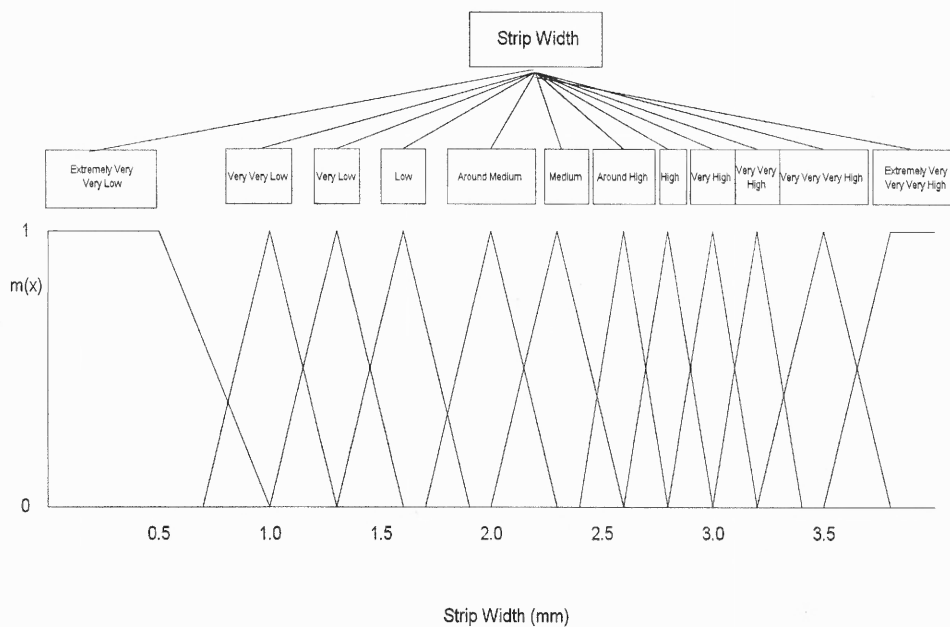
Figure 7.8 Universe of Discourse of the Process Variable "Strip Width"
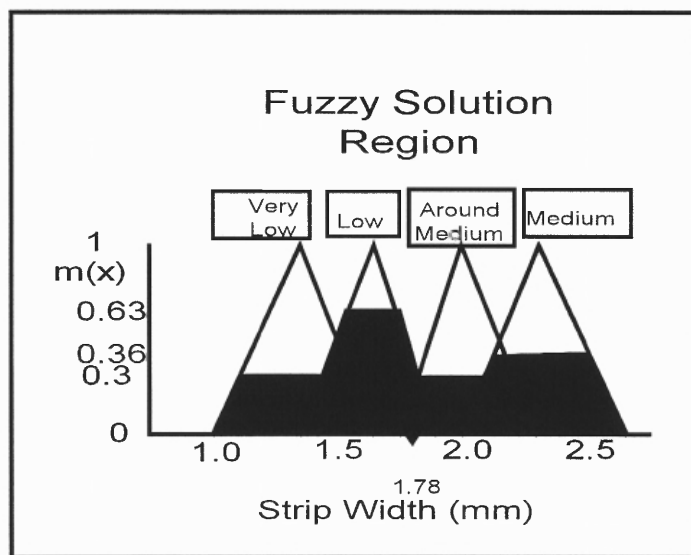
Figure 7.9 Fuzzy Solution Region.
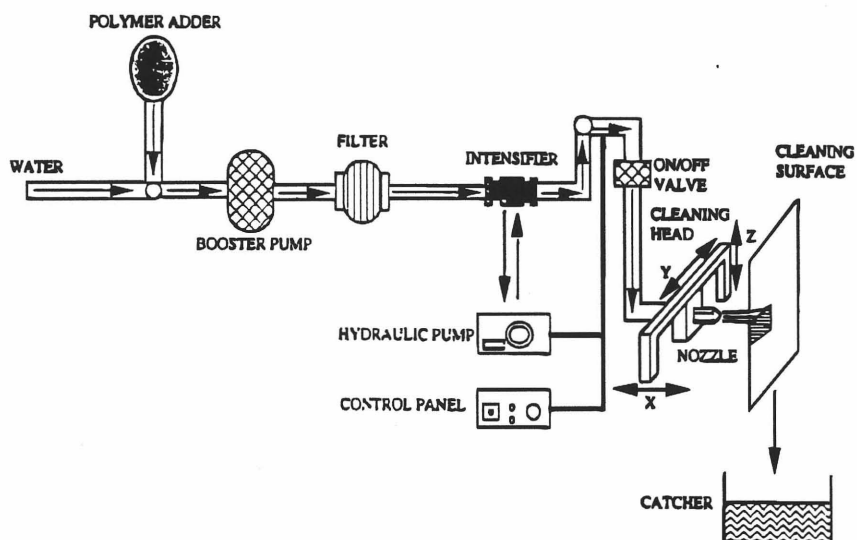
Figure 7.10. Waterjet Setup
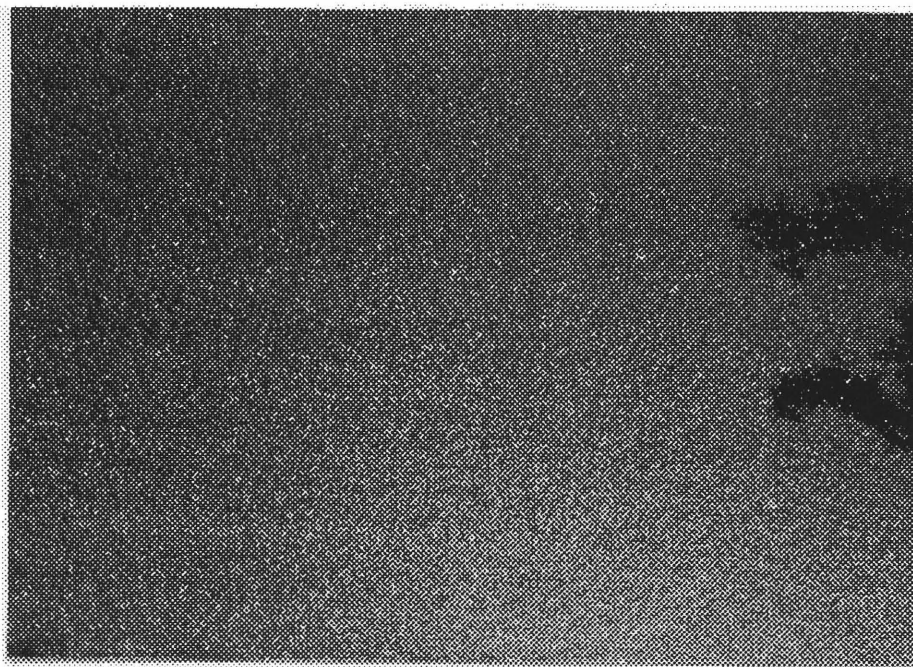
Figure 7.11 "Well Cleaned" Metal Surface. (12X Magnification)
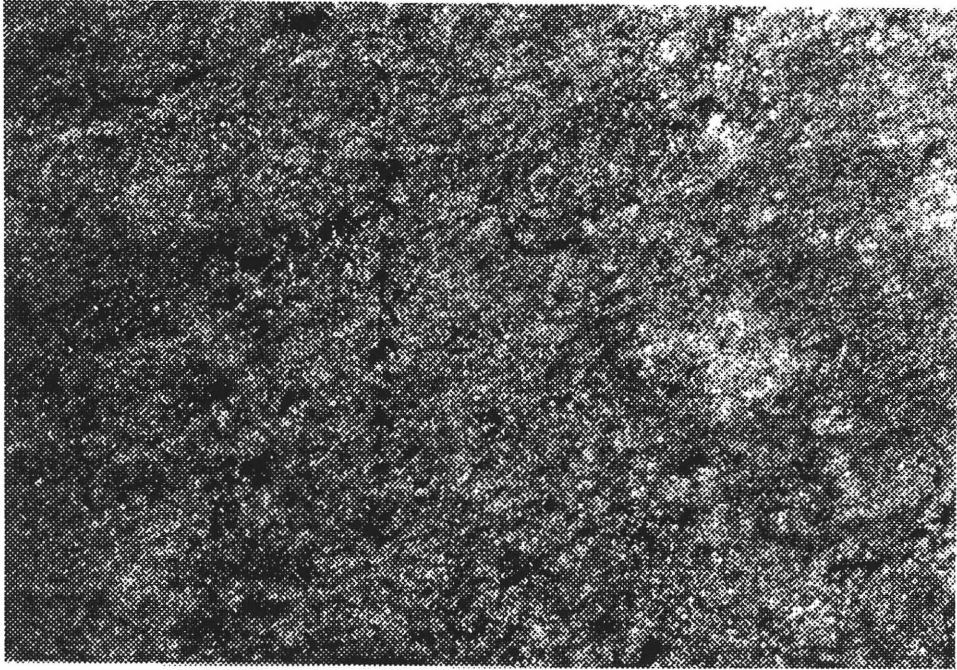
Figure 7.12 Poorly Cleaned" Surface.(12 X Magnification
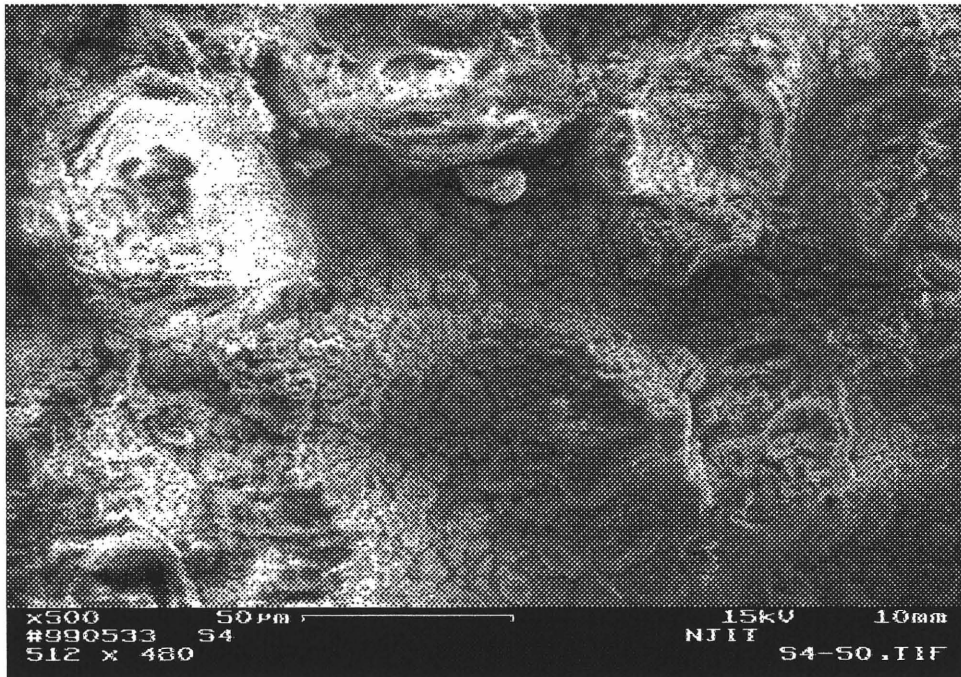
Figure 7.13 SEM Photograph of Rust Covered Metal Surface
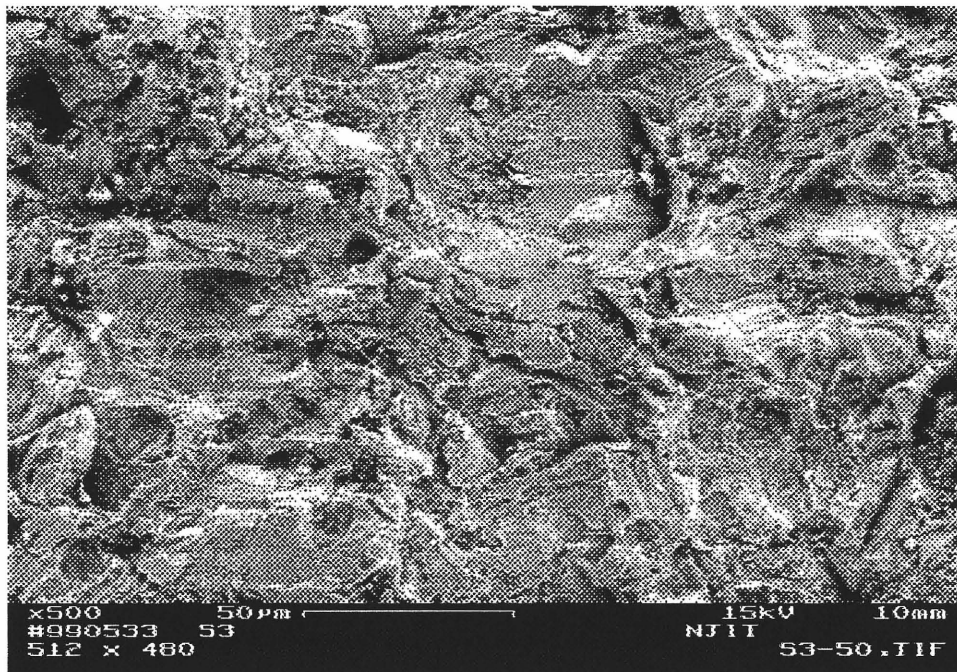
Figure 7.14 SEM Photograph of Waterjet- Derusted Metal Surface
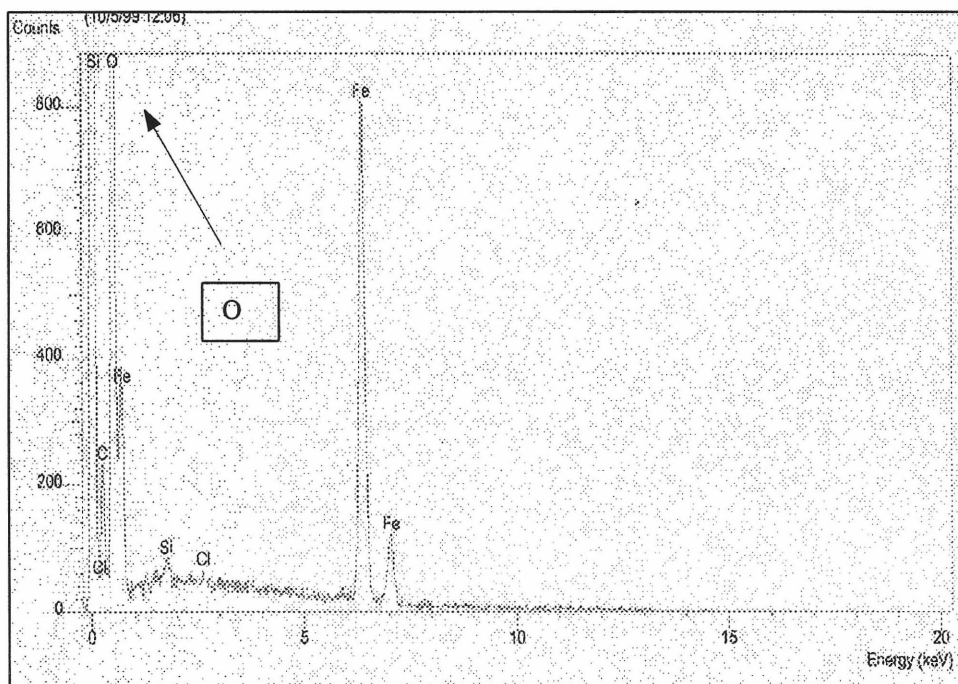
Figure 7.15 SEM Chemical Surface Analysis. Metal Surface Prior to Waterjet Rust Removal. Oxygen Content is at 900 Count.
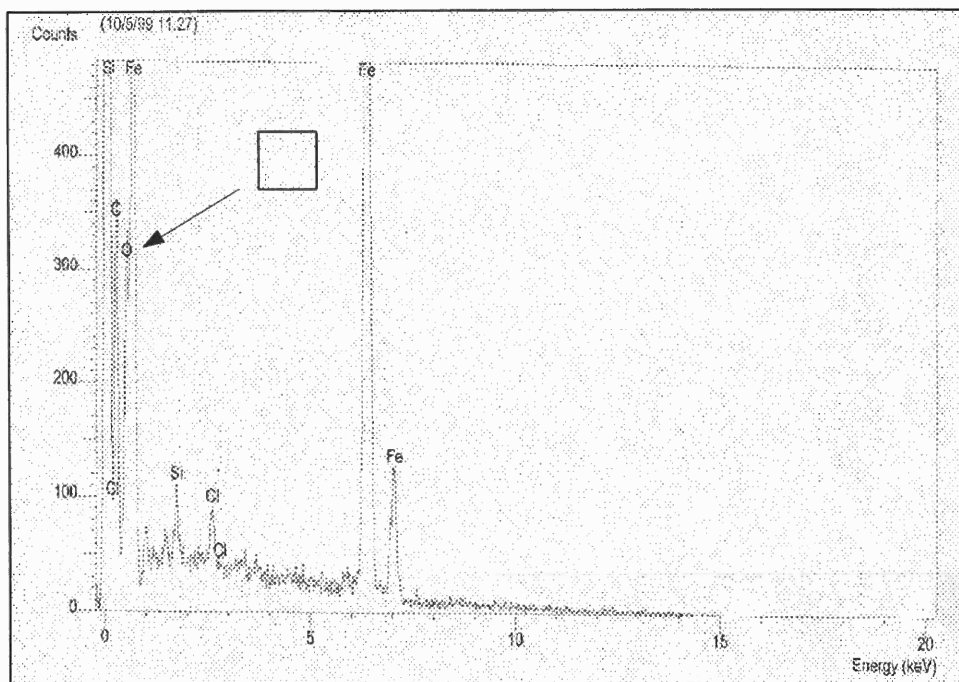
Figure 7.16 SEM Chemical Surface Analysis. Metal Surface After Waterjet Rust Removal. Oxygen Content is at 320 Count
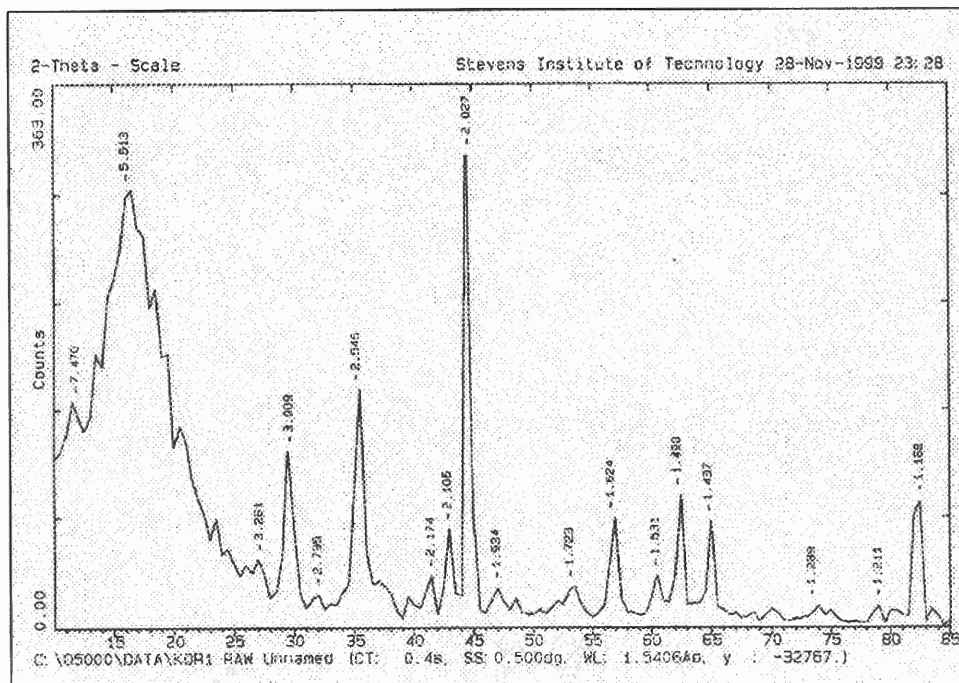
Figure 7.17 X-Ray Diffraction Analysis. Diffraction Pattern of Rusted Metal Surface Prior to Waterjet Treatment
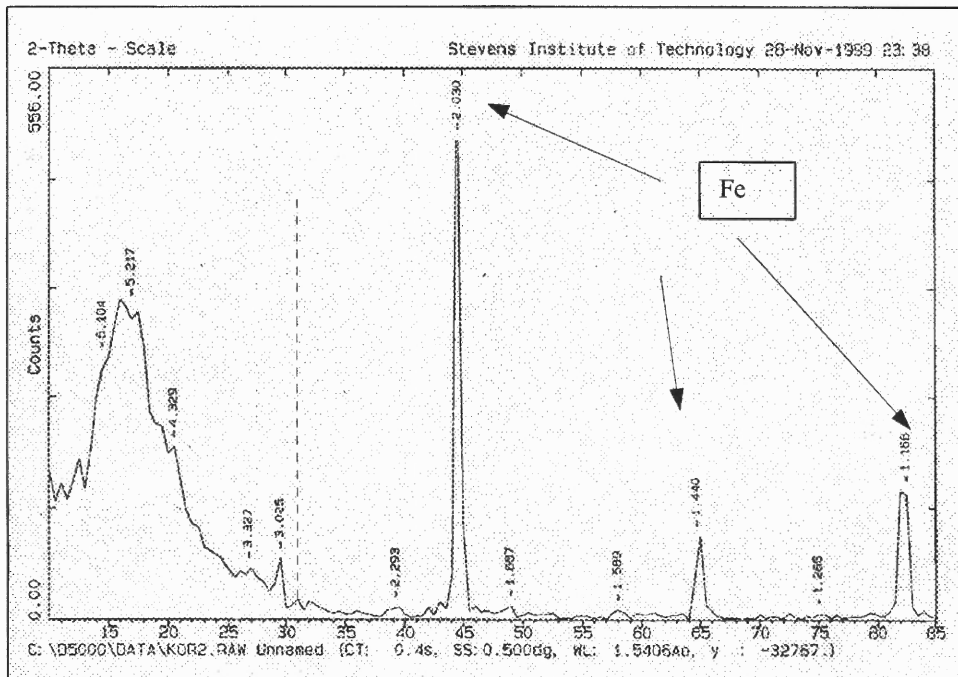
Figure 7.18 X-Ray Diffraction Analysis. Diffraction Pattern of the Surface After Waterjet Rust Removal
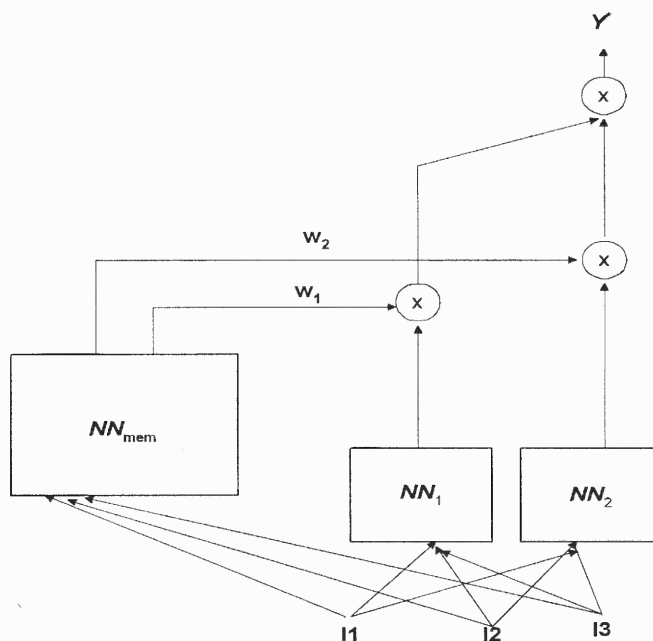
Figure 7.19 Computational Approach.

(I_1, I_2, and I_3 are the input parameters (water pressure, traverse rate, and nozzle diameter). NN_{mem} is the neural network that decides the membership values (w_1, w_2) in each class, of the above input parameters. NN_1 and NN_2 determine the outputs (productivity) y_i for each class.)
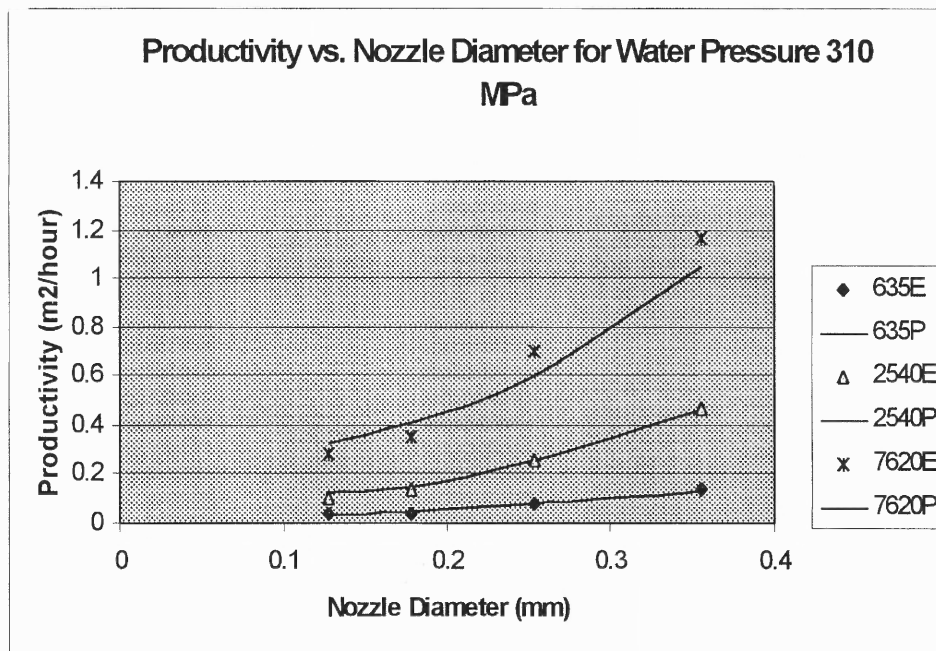
Figure 7.20 Model Prediction Results for Water Pressure 310 MPa. E- Experimental, P-Prediction
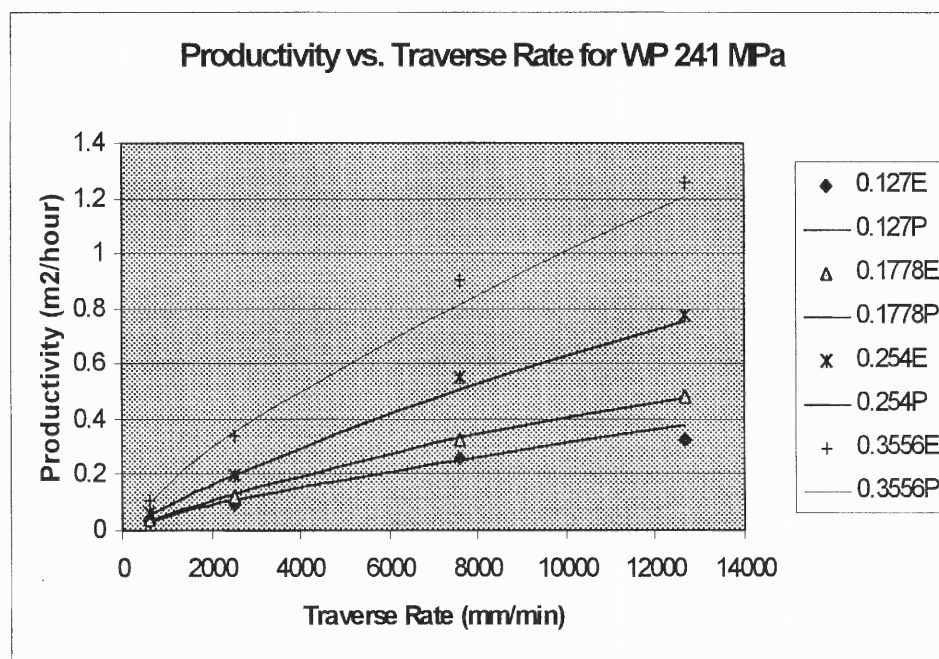
Figure 7.21 Model Prediction Results for Water Pressure 241 MPa. E- Experimental, P-Prediction
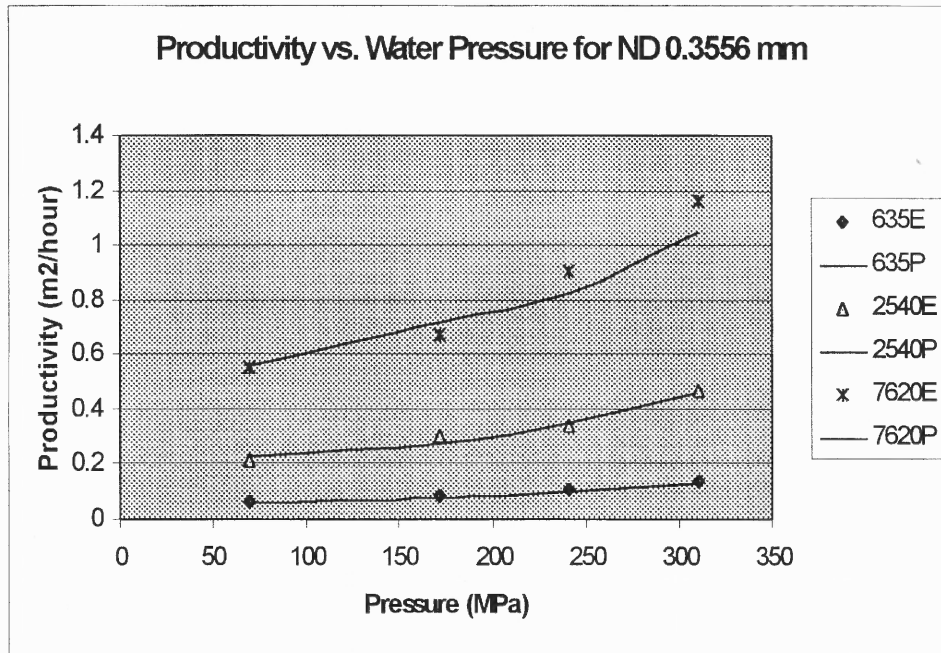
Figure 7.22 Model Prediction Results. E- Experimental, P- Predicted
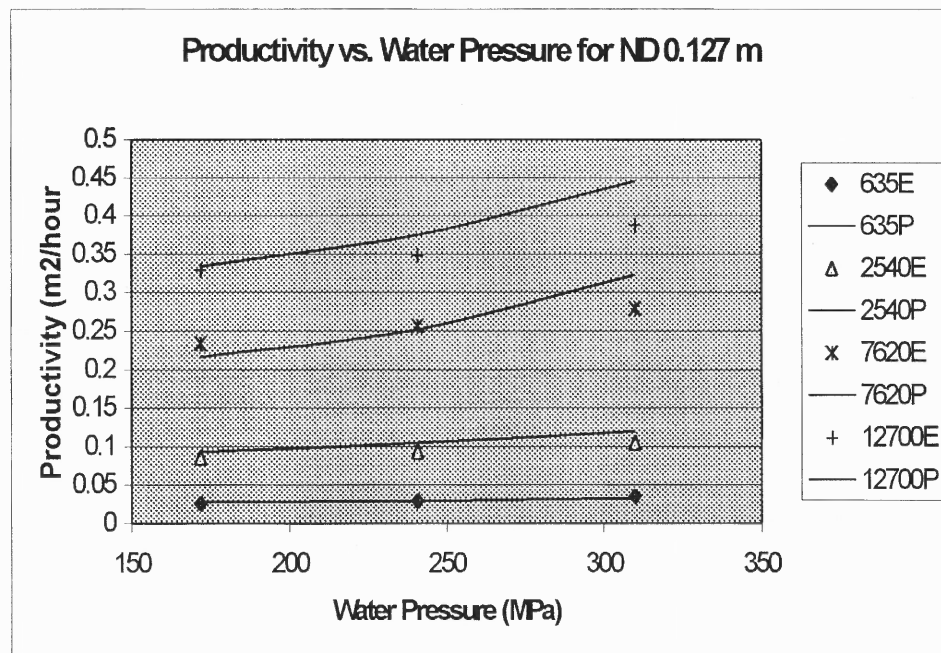
Figure 7.23 Model Prediction Results. E- Experimental, P- Predicted

Figure 7.24 Waterjet Paint Removal From a Foam Cup.
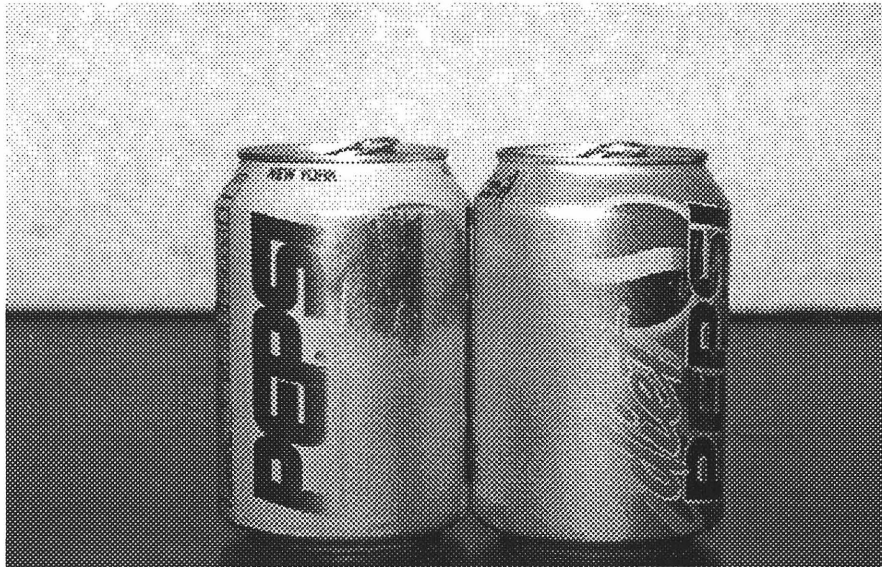
Figure 7.25. Waterjet Paint Removal From a Soda Can.
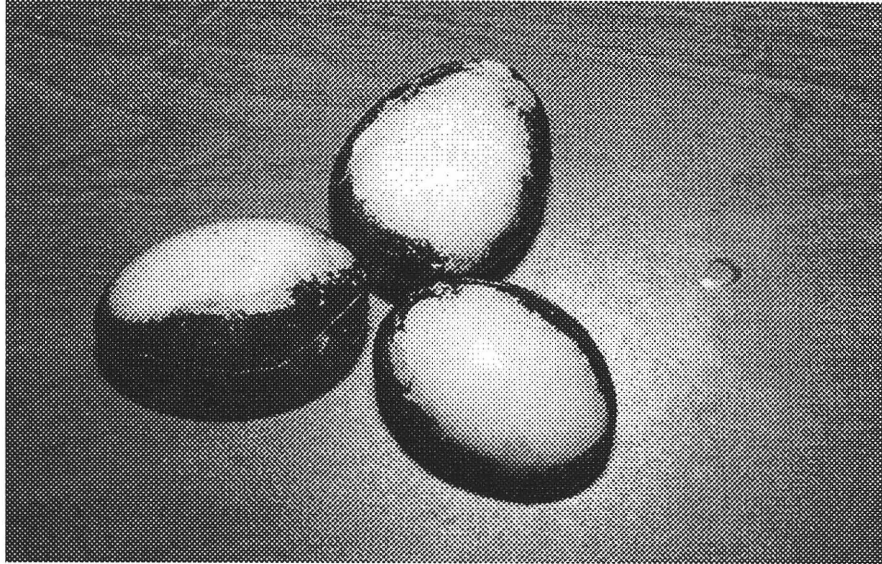
Figure 7.26 Water Jet Paint Removal From a Sensitive Surface.

CHAPTER 8

EXPERIMENTAL STUDY OF WATERJET CLEANING WITH BLASTING SODA ADDITION

8.1 Introduction

Today's rapidly developing and changing technologies and industrial products and practices frequently carry with them the increased generation of materials that, if improperly dealt with, can threaten both public health and the environment. Solvent strippers have been widely used for industrial coating removal for many years. Solvent strippers consist mainly of methylene chloride which typically constitutes 60% to 65% of the formulation. Other ingredients such as activators, corrosion inhibitors, thickeners, and evaporation retarders are used to supplement the methylene chloride to improve coating removal performance. However the use of solvent strippers generates organic vapors, and sludge containing solvents and metals. Thus increasing environmental and health concerns call for the reduced use of solvent strippers.

ARMEX® Blast Media is an abrasive blast media designed for the removal of paints, oils, grease, and process residues from a variety of substrates including steel, aluminum, composite plastics and architectural stone. It represents a significant technological breakthrough from the use of more traditional paint stripping materials (such as methylene chloride which has substantial environmental and human health and safety issues) or blasting materials (such as those that are silica-derived).

Abrasive blasting is the pressurized air containing a suspended particulate that is projected at a surface for the purpose of removing a coating or contaminant. An abrasive

blasting system would usually be composed of the following four components: Pressure Vessel Source of Compressed Air, Abrasive, Nozzle. Some common applications of the sodium bicarbonate blasting include but not limited to the following.

1. **Architectural**

- Fire Restoration (removing smoke damage, restoring what is salvageable to pre-fire condition)

- Brick Cleaning (depainting and pollution soil removal)

- Stone Cleaning (includes limestone, granite, marble, sandstone, not as porous as brick)

- Metal Cleaning (two types - structural & decorative. Structural is usually steel, iron or aluminum, and it includes depainting and cleaning. Decorative can be copper, bronze, brass, aluminum, and it usually involves removing pollution and corrosion).

- Wood

- Graffiti

- Glass

2. **Remanufacturing/Rebuild**

- Aerospace (aluminum, titanium, steel, magnesium, composite materials, precision parts that require preservation, removing paint, oil, grease, dirt, and carbon.)

- Automotive (steel, iron, aluminum, copper, brass, composites, best where substrate preservation is required, removing paint, grease, oil, dirt, and carbon).

- Marine (composites, engine components (steel, aluminum and brass), removing from composites; barnacles, sea residues, failed gelcoat, engines (grease, oil, paint, carbon)

- Turbines (removing residues from blades).

3. General Facility Maintenance

- Petrochemical (removing paint, grease, oil, dirt, pollution residues from structural steel, concrete, aluminum, painted surfaces)

- Pulp & Paper (paint and dirt, wood pulp residues and creosol build up)

- Food & Beverage (animal fats, greases; vegetable oils)

4. Mold Cleaning

- Removing mold release build up and casting residues

5. Military Applications (same types of applications)

- General Maintenance

- Auto and Aerospace Remanufacture

- Architectural Cleaning

8.1.1 Description of Experiments

Series of experiments have been conducted to investigate the abrasive waterjet cleaning with Arm & Hammer blasting soda used as abrasive. Experimental study was mainly concerned with examination of the effect of different waterjet parameters on cleaning efficiency for different types of deposits and substrates. The parameters investigated included types of coatings and substrate materials, water pressure, nozzle traverse rate, nozzle diameter, standoff distance, and modification of jet structure through improvement of nozzle body design. The waterjet parameters in question and their corresponding ranges are presented in Table 8.1

Table 8.1 Description of Experiments

Parameter	Unit	Description
Type of Coating		Epoxy-based paint (thickness ~ 3-4 mils) Epoxy-based paint (thickness ~ 12 mils) Roofing Tar (4-5 mm) Viton Rubber (2-3 mm)
Type of Substrata		Aluminum Low Carbon Steel (AISI 1018)
Type of Nozzle Body		Conventional Abrasive, Water Nozzle
Nozzle Diameter	mm/inch	0.254 / 0.01 0.305 / 0.012 0.356 / 0.014
Pressure	MPa psi	69 ~ 276 10,000 ~ 40,000
Traverse Rate	m/min in/min	0.635 ~ 17.78 25 ~ 700
Stand-off Distance	Sm Inch	1.3 ~ 26 0.5 ~ 10.4
Abrasive Size	Mesh	
Abrasive Flow Rate	gr/min lb/min	0 ~ 44 0 ~ 1

8.1.2 Evaluation of Abrasive Waterjet Cleaning Performance

Three criteria cleaning width, cleaning rate and coefficient of relative performance have been used for the evaluation of waterjet cleaning performance. Cleaning width and maximum cleaning width are closely related to operational parameters as well as properties of coatings and substrates. Cleaning rate is the direct measure of the process productivity and is a linear function of the cleaning width. This work introduces the term *"coefficient of relative performance"* as a criterion for the evaluation of cleaning performance.

Cleaning Width

The direct experimental output, which can be easily measured and used in further calculations, is the cleaning width. This is the output parameter, which is obtained as a result of a single nozzle pass. In all cleaning experiments cleaning width was used as the basis for all further efficiency calculations.

Cleaning Rate

The rate of cleaning, or productivity of a process, is the major criterion for evaluation of the effectiveness of waterjet decoating. Cleaning rate for a single nozzle (single jet) is defined as following:

Cleaning Rate(m2/hour) = STW (mm) * TR (mm/min)*(60/1000000)   **(8.1)**

where STW is the cleaning width (strip width), and TR is the traverse rate.

8.1.3 Experimental Setup and Procedures

The cleaning experiments with abrasive addition were carried out with an Ingersoll-Rand waterjet system. Two waterjet Ingersoll-Rand -manufactured robots were used in experiments. The robots are 3 and 5-axis Ingersoll-Rand gantry robots, which movements were controlled by GE Fanuc series 18-M CNC and Allen Bradley 8200 series CNC controllers respectively.

A high-pressure water supply system included a water softener, a booster pump, and an Ingersoll-Rand intensifier (Figure 8.1). A water softener was used to remove the iron and calcium, and dissolve solids that might cause damage to the sapphire nozzle. Then softened water was fed to the booster pump which would produce the pressure up to 10.4 MPa (1,500 psi), then it was further pressurized by an intensifier using a

hydraulically driven plunger pump and carried through a stainless steel pipe to a nozzle head. Sapphire nozzles with the range of diameters can be installed on the nozzle head.
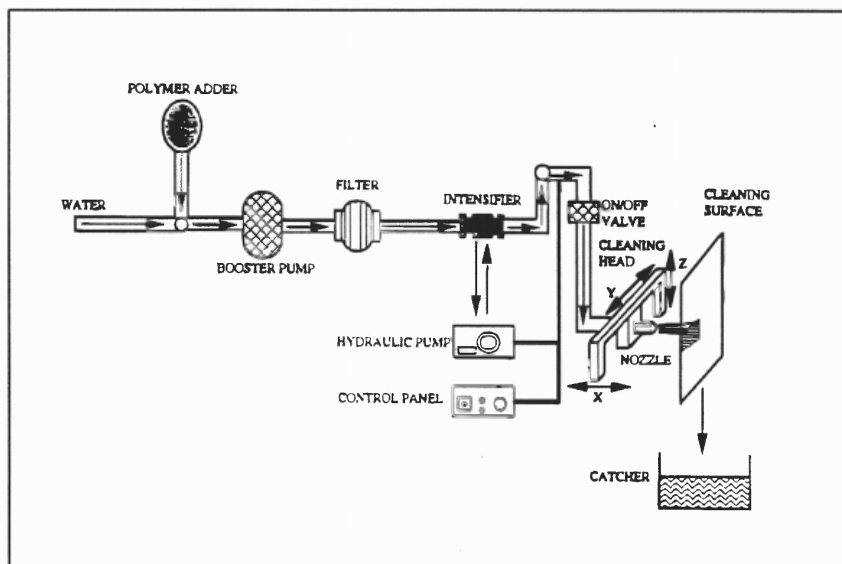
Figure 8.1 Schematic of Waterjet Setup.

8.1.4 Abrasive media

In all cleaning experiments of this section the only type of abrasive media used ARMEX® Blast. The media is based on sodium bicarbonate (baking soda) which is a natural, water soluble, inorganic compound with a soft crystalline structure that makes it an ideal, mild abrasive. The media can be used to clean and remove virtually any coating from any substrate. It also is USDA-approved as an A-1 cleaner and suitable for use in FDA-regulated facilities.

Key Features and Benefits

- Free flowing qualities reduce flow problems associated with other baking soda-based blast medias.

- Water Soluble - eliminates media residue concerns; simplifies clean-up & disposal; less solid waste generated

- Safe to use on virtually any substrate, including delicate surfaces, rotating equipment & moving parts

- Ideal for NDT/NDI preparation - does not remove metal

- Nontoxic & nonhazardous as defined by EPA & OSHA

- Contains no free silica, is nonflammable and is nonsparking resulting in significant worker safety advantages

- Contains no solvents or caustic chemicals - reduced air pollution

- USDA-approved as an A-1 cleaner and suitable for use in FDA-regulated facilities

Particle Size

- The media has an optimized particle size distribution as follows:

- Retained on 60 mesh sieve (250 microns):   8% max.

- Retained on 100 mesh sieve (150 microns): 55% min.

- Retained on 170 mesh sieve (90 microns): 93% min.

General Properties

Appearance...................White crystalline powder

Bulk Density................. 60 lbs/ft^2 (1 g/cc)

Figure 8.2 Solubility in

Taste.............................Slightly alkaline

Specific Gravity............2.2

Solubility in Water........See Figure 1

Solubility in Alcohol.....Insoluble

pH (8% solution)........... 8.2

Mohs Hardness.............2.5

Figure 8 Solubility in Water
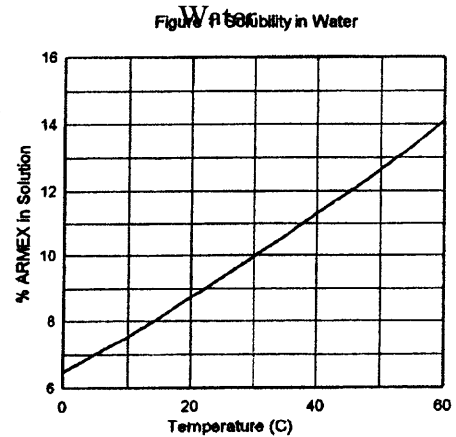
Corrosion Data

Aluminum and carbon steel coupons were immersion tested in saturated solutions at 120 F for 14 days. Corrosion rates of the media were found to be significantly lower than those of distilled water.

Table 8.2 Corrosion Properties

	Immersion Corrosion Rate (mils/yr.)		
Product	AL-7075	AL-5050	CS-1020
Distilled Water	1.15	1.11	9.0
ARMEX® Blast Media	0.25	0.20	0.17

Therefor this media was found to be an ideal candidate for waterjet-based surface decoating, where slight rusting could appear after surface is cleaned.

8.1.5 Media Supply Setup

The following setup was used to supply the media into the waterjet stream (Figure 8.2).
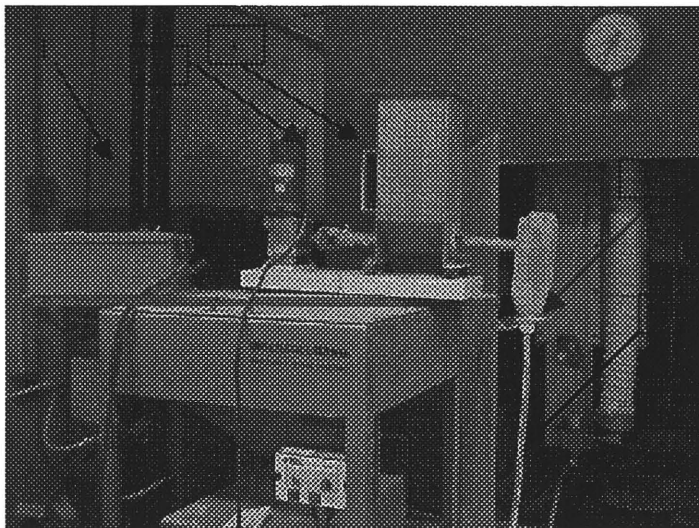
Figure 8.3 Media Supply Setup
1) Calibrated controller of the media supply. 2) Media supply screw. 3) Media storage bunker. 4) Intermediate media storage bunker. 5) Media supply line. 6) Abrasive waterjet nozzle.

Cleaning media is stored in the media storage bunker (3) with media supply screw (2) on the bottom. The media supply screw is controlled by controller with calibrated dial (1), so that the rate of media supply could be varied. With the help of the supply screw, media is delivered to the waterjet nozzle (6) via the intermediate supply bunker (4) through the media supply line (5).

8.1.6 Sample Preparation

Coatings and Substrates

The choice of experimental coatings was dictated by the diversity of the possible coatings, which might be encountered by practitioners. Therefore, for a systematic investigation of the abrasive waterjet cleaning, we need to cover all types of material to

be encountered. All the possible coatings can be roughly categorized into two groups (1, 2).

1. hard, brittle layers (inorganic layers, scale, ceramics, enamel)

2. ductile layers (most plastic materials, kinds of rubber and metals, viscoelastic to viscous layers will also be placed in this group)

The following coatings were used in this study.

1. Paint

2. Viton Rubber

3. Roofing Tar

The epoxy-based paint represents very cohesive, thick and hard to remove coating. It is believed that exactly this type of coating will accentuate the differences between abrasive waterjet and pure water coating removal, if any.
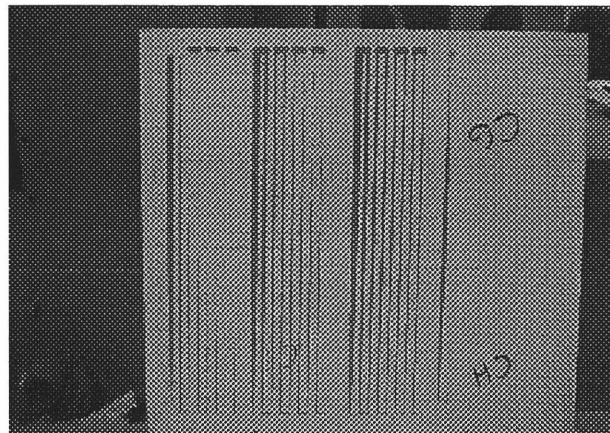
Figure 8.4 Experimental Steel Panel with Two Layers of Epoxy Paint

Two layers of epoxy paint with thickness 0.1524mm (0.006 inch) each were applied on a low carbon steel plate with dimensions 61 x 61 x 0.3 sm (24 x 24 x 0.12) inches. Both layers of coatings were industrially (robotically) applied, which assures an

even layer of coating. A typical experimental sample is shown in Figure 8.4. This type of coating could be placed into the first class according to classification above. The properties of these coatings are listed in Table 8.3.

As an example of a coating from the second group (ductile layers) a fuser roll used in copy machines (Xerox type) was tested. A fuser roll is 40.6 sm- long (16 inch), 20.3 sm (8) inch in diameter aluminum cylinder covered with a layer of Viton rubber, approximately 0.2 mm thick (Figure 8.5). The fuser rolls with worn layer of coating are usually stripped of rubber, which is reapplied later. This process is repeated until the roll's roughness after stripping exceeds admissible levels. Unfortunately not all the samples tested had the same wear level and surface roughness. Therefore experimental results are not general in all aspects, but somewhat specific to the given rolls.
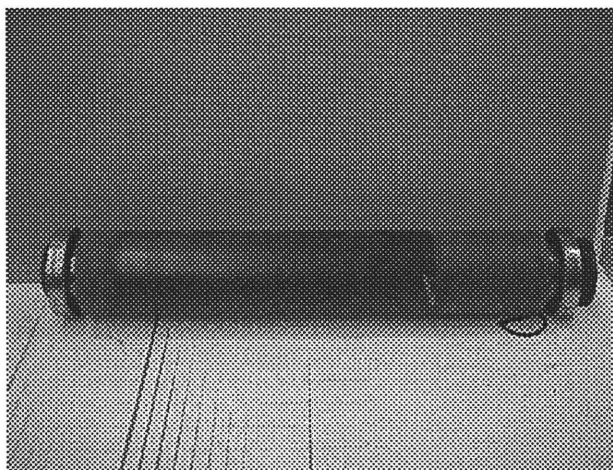
Figure 8.5 Worn Fuser Roll

Another coating used in experimental study was represented by a layer of roofing tar (Gardner fibered roof coating) on aluminum plate (Figure 8.6). This type of coating could also be related to the second group in coating classification, but this coating is more viscous. The coating was applied with accordance to the instructions on packaging.
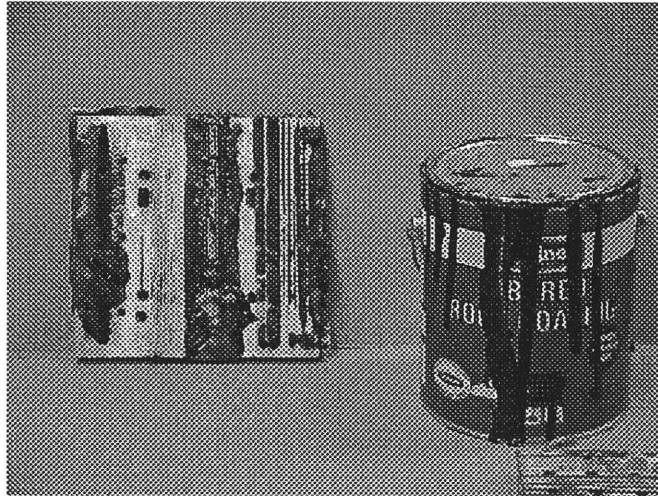
Figure 8.6 Roofing Tar Removal Experimental Samples

Table 8.3 Properties of Coatings and Substrata

Coating	Substrate	Application Method	Thickness of Coating (one layer)	Number of layers
Epoxy Paint	Low carbon steel	Industrially applied	0.1524 mm (0.006 inch)	2
Epoxy Paint	Low carbon steel	Industrially applied	0.08 mm (0.003-0.004 inch)	1
Viton rubber	Aluminum	Industrially Applied	0.2 mm (0.007 inch)	1
Roofing Tar	Aluminum	Hand brushing Time to dry: 1 year	3-4 mm 0.11 inch	1

8.2 Experimental Study of Abrasive Waterjet Paint Removal

8.2.1 Experimental Procedure

In this experiment the effect of the several waterjet parameters on cleaning efficiency was investigated. The parameters of interest were water pressure, water flow rate (nozzle diameter), abrasive flow rate, and nozzle traverse speed. In order to get a thorough

understanding of the influence of the above parameters on media assisted waterjet cleaning, the full factorial experimental design was applied. In such a design each variable (called a factor), although continuous in nature, was discretized into several levels, according to criteria specific to this variable. In order to reveal all the nonlinearities of the process we need at least three levels for each factor. One particular combination of levels of all factors is referred to as a treatment combination. Number of experimental replications at a fixed treatment combination is an observation (replication). Since the number of factors is fairly large, only one observation for each treatment combination was made. Experimental design of the tests on media assisted waterjet paint removal is shown in Table 8.4.

Table 8.4 Experimental Design

Factor	Number of levels	Levels*
Water Pressure	4	69,103, 152, 221 MPa 10,000 , 15,000, 22,000, 32,000 Psi
Traverse Rate	7	635, 3175, 5175, 8255, 13335, 15875, 18415 mm/min 25, 125, 225, 325, 525, 625, 725 inch/min
Nozzle Diameter	3	0.254, 0.305 ,0.3556 mm 0.01, 0.012, 0.014 inch
Media Flow Rate	3	100, 268, 415 gr /min 0.23, 0.6, 0.92 lb/min

•Not all levels are actually used for every treatment combination.

A special attention was paid to the experimental parameter –standoff distance. Standoff distance is not actually a cleaning parameter of interest, but it plays an important role in every jet-cleaning experimental setup. As was shown in earlier studies (Meng, 1996) there are two critical standoff distances- *"critical cleaning standoff distance (CCSD)"*

and *"critical damage standoff distance (CDSD)"*. Cleaning in excess of CCSD will result in ineffective cleaning, while working at CDSD will bring about substrate damage. Both CCSD and CDSD were shown to be related to the properties of coating and substrate and also to be the function of waterjet parameters (Meng et al, 1996 a). It was also shown in (Meng, 1996 b, Babets et al, 1999), that in the effective working space bounded by CDSD and CCSD there exists an optimum standoff distance (OSD). Cleaning at OSD brings about maximum width of cleaning and consequently the maximum cleaning rate, for a given treatment combination. Therefore, it should be clear that all experimental runs for every treatment combination must be done at some optimum (or near optimum) value of the standoff distance, to assure the fair comparison between different treatment combinations.

The addition of a new factor into an experimental design will increase the number of experimental runs dramatically, and a fair number of levels for this new factor is required, since optimal standoff distance occurs at different distances for each treatment combination. To avoid tedious experimentation the technique of dynamic test was applied. For each treatment combination, the standoff distance was dynamically varied over the whole range, which was limited by the equipment capabilities only. As a result the trace of the waterjet was left on the surface (Figure 8.4). After the horizontal distance on a panel was related to the elevation of the nozzle it became possible to measure the resulting strip width at any standoff distance. Also this approach allowed easily estimating an OSD for every treatment combination.

For each level of the following experimental factors (Water pressure, Nozzle diameter, Media flow rate), the Traverse rate factor was varied through all levels, with

dynamically changing Standoff distance for each level. In all of the tests on paint removal, waterjet stream was perpendicular to the surface of coating material.

8.2.2 Experimental Results

Intuitively and from our experience we know that productivity increases with the increase in traverse rate. But after it reaches some critical point, the further increase in traverse rate leads to decrease of productivity. This point, or rather a range, where the derivative of the function changes its sign is called an optimal point. This point or a range is unique for any given set of process conditions. For example the increase in working water pressure results not only in different optimal ranges but also in different optimal range values. It could be noted that as the water pressure increases the optimal range becomes wider and the optimal values of productivity increase.

The process productivity increases with the increase in standoff distance until some point is reached, after which the further increase in standoff distance results in lower process productivity. It is very important to locate and work within the vicinity of this optimal point, or rather optimal range, because it directly translates into efficiency gain with no additional input into the process. This optimal range is unique for different sets of operational conditions. Higher media flow rates (Figures 8.7, 8.8, 8.9) result in wider ranges of optimal standoff distance and in higher values of productivity. The increase in media flow rates makes the process more stable, but this increase has limits, and after these limits have been reached the further increase in media flow rate would actually deteriorate the performance. Although the absolute magnitude of the productivity

may stay the same, the optimal working range will drastically decrease (Figures 8.10, 8.11).

The increase in the working nozzle diameter with all the other variables kept fixed will bring about the increase in process productivity (Figure 8.13). By analogy with the discussed properties of other process variables it could be suggested that the further increase in nozzle diameter nozzle diameter should locate an optimal range of nozzle diameters for a given set of operating conditions. But in our study this optimal range was not located, most probably because our experimental ranges of nozzle diameters were too narrow.

The benefits of the addition of media into the waterjet can be evaluated best if we compare the performance of abrasive jet with the performance of pure waterjet at the same process parameters. Figures 8.14, 8.16) show that at low values of water pressures the media assisted flow outperforms pure water jet in terms of productivity at least 12 times. As the working water pressure increases, the difference in productivity is less significant but still quite noticeable, at 2.6 times. At the same tome the specific water consumption is drastically lower for the case of media assisted jet (Figures 8. 15, 8.17).

8.2.3 Conclusions

The basic conclusions that can be drawn from this experimental study can be summarized as following:

1. Addition of media significantly enhances the rate of deposit removal and reduces specific water consumption.

2. Absolute effect of media addition increases with increasing water pressure.

3. Productivity grows with increasing media supply.

4. Effects of media supply are stronger for stronger deposits.

5. The maximum process stability is attained at the rate of media supply of 0.5 Lb/min.

6. The optimal flow rate increases for higher nozzle diameters.

7. Optimal process results are attained at the narrow range of process conditions.

8. Specific water consumption is reduced by at least 8 times for strong deposits and 3 times for less stronger deposits.

9. Media addition increases productivity 2.5 ~ 3 times at high pressure and 10- 12 times at low pressure.

10. Addition of media enables the removal of strong deposits at lower water pressure

11. Monotonous increase in productivity and decrease in specific water consumption demonstrates the feasibility of improvement of obtained results.

8.2.4 Model of the Process

The modeling of the experimental database was done with the help of Artificial Neural Networks (Chapter 5). In our problem several feed forward artificial neural networks have been constructed and trained, one for media assisted waterjet depainting, one for pure waterjet depainting. The network architecture used in modeling of media assisted waterjet removal of paint had the 7 x 15 x 15 x 1 structure. The input layer contained seven neurons (one for each process variable i.e. paint layer thickness, water pressure, nozzle diameter, media flow rate, traverse rate of nozzle, standoff distance, plus one special neuron called a bias), two hidden layers contained 15 neurons each, including

bias, and the output layer contained one neuron, which corresponded to the process output – the width of strip.

To train the network (find optimal weights that minimize the error) the standard backpropagation of error algorithm was employed. The only modification of the standard training algorithm involved the inclusion of the so-called momentum term. In backpropagation with momentum, the weight change is in direction that follows the direction of the current gradient and the previous gradient. This is a modification of the gradient descent whose advantage arises when some training data is significantly different from the majority of data, or even incorrect.

The experimental data contained 577 data points organized into input-output pairs. This database was then scaled between 0.15 to 0.85 to override large fluctuations in magnitudes within experimental data. Then the experimental data was divided into the two subsets, the training data set (TDS, contained 446 input-output pairs), and the testing data set (TDS, 131 input-output pairs). The training data was used to train the network, while the testing data set was used to check the model performance. During the training the root mean square error was monitored for each training. Every 100's iteration the network's performance was checked on the testing data. The training was stopped when the training data error decreased less then 1 % in 1000 iterations but the testing data set error had started to grow more then 1% in 1000 iterations. The network was trained for 21289 Epochs, while at this point the TDS error reached 1.46%, and the CDS error reached 3.47%. At this point network is considered trained and can be used for process prediction or for the process optimization. The average relative error of prediction in this

study was 12%, tested on 577 data points. The error was considered acceptable for this study. The results of the prediction are presented on Figures 8.20 8.23.

8.3 Experimental Study of Removal of Elastic Deposit with Abrasive Waterjet

8.3.1 Experimental Procedure on Fuser Roll Rubber Removal

The objective of the experiment on removal of rubber from a fuser roll was twofold. Firstly, the feasibility of the process was to be investigated and the ranges of the optimal process parameters were to be found. Secondly, the level of the damage to aluminum substrata (if any) after abrasive waterjet was to be evaluated and the magnitude of the damage was to be estimated in terms of the change of a roll's roughness in one cycle.

The optimal parameters in question should account for the acceptable process productivity (roll should be completely clean in under 4 min) and subject to the following constraints: blasting soda flow rate should be less then 2 lb/min, driving pressure should be within 10 to 40 thousand psi (69 – 276 MPa), quality of the generated surface must 1-2 (see the discussion section for classification of the surface).

Fuser roll was fixed on two cone-like protrusions, connected to a variable speed motor. The experimental sample was rotated, while waterjet stream was impinging normally and moving along horisontal axis. A controller was used to vary the rotational speed of a motor.

8.3.2 Experimental Results

This study was concerned mainly with finding a working range for the rubber layer removal from a fuser roll with only limited number of experimental samples available.

Therefore there was no real possibility for the planned experiment and systematic study of the effect of different process variables on the deposit removal. Further contribution to the complexity of this study was the necessity of dealing with a comparatively large number of independent variables. These were water pressure, diameter of the nozzle, nozzle traverse rate, rotation of the motor and the media flow rate. The output variable is the degree of cleanliness of the surface defined in terms of visual cleanliness and measured surface roughness. The experiment was run by intuitively varying the input variables and recording the generated surface in terms of visual cleanliness. The cleanliness of the generated surface was defined in terms of the two classes "first degree and "second degree". These two classes is further let to be "fuzzy" in nature, thus a surface can belong to both classes with different degree of belonging to each. At first some of the samples were classified "crisply" as belonging to either class. The representative photographs of the generated surfaces for the both classes are given in Figures (8.24 – 8.25). The rest of the surfaces could not be identified "crisply" and were left for futher determination. The randomly selected surfaces, visually classified to belong to only one class were used to measure the surface roughness. The Hommel Tester T 1000 was used to make totally sixteen surface roughness measurements, eight for each class. The data is presented in Table 8.5. Observing the results of the tests one could infer that classes I and II must overlap, since the roughness measurements produces results identical (in some points) to both classes.

The general result of these series of tests is possibility of producing a surface acceptably clean, with acceptable productivity (under four minitues) with low media consumtion (around 200 g/min). These results constitute a significant progress as

compared to the productivity of the currently used setup by the roll's manufacturer which involved water pressures in excess of 300 MPa but with a per roll cleaning time in the vicinity of sixteen minutes.

8.3.3 Determination of the Surface Damage Level

One of the most important factors in waterjet based surface cleaning is assessing the level of the damaged on the surface produced by the jet. Therefore the following experimental test was designed.

Table 8.5 Surface Roughness Results

Degree of Cleanliness	Surface Roughness Measurements (μinch)	Average Surface Roughness (μinch)
First Degree	120.1, 129.1, 135.4, 136.6 145.2, 160.2 165.7, 139.7	141
Second Degree	195.2, 161.0 188.5, 143.3 190.9, 209.8 193.3, 191.3	185

Aluminum fuser roll with rubber coating layer was subjected to abrasive waterjet treatment. After the rubber layer was removed the aluminum surface's roughness was measured. Then the same surface was subjected to abrasive waterjet at the same working conditions. After the treatment, the surface roughness tests was repeated. The experimental conditions used in these tests involved the following set of parameters.

Experimental Conditions:

Water Pressure: 138 MPa

Stand_Off Distance: 10 mm

Traverse Rate: 102 mm/min

Rotational Speed: 160 Rpm.

Nozzle Diameter: 0.356 mm.

Media: ArmaKleen Blasting Media (Sodium Bicarbonate)

Media Flow Rate: 360 g/min.

The results of the damage tests is presented in Table 8.6. Five different runs have been made and the corresponding surface roughness prior to and after the second impact have been recorded. From the data in Table 8.6 it follows that the damage produced by the impacting jet at the above experimental conditions is insignificant and the surface finish is completely complient with the manufacturer's specifications.

At this point it is important to note that the roughness measurements varies widely from roll to roll. This leads to inconsistency in the surface degree of cleanliness defenitions, if based solely on the surface roughness. The incosistency in surface' roughness measurements is attributed to the different re-manufacturing life cicles of the rolls, where the initial finish of the aluminum surface is different from the beginning.

Table 8.6 Surface Damage Test

Aluminum Surface Roughness (µinch)	
First Impact	**Second Impact**
247.2	222.4
224.8	279.1
248.4	254.3
266.5	262.5
Average Roughness	
246.73	254.575

8.3.4 Model of the Process

The control over any process is enhanced when a model corresponding to the process is constructed. Such a model can be based on any of the available statistical techniques (such as regression analysis, analysis of variance together with the planned experimental design etc.), or can be constructed based on the phisical properties of the system in question. The model is then can be used to further study the process (prediction analysis) and/or for the process optimization. In the case of the current study any of the available statistical modeling technique would, most likely, fail, due to the limited experimental data (too few data points) and noizy and 'fuzzy' results, because of the different re-manufactiring life cycle of the rolls. Furthermore the limited experimental data results in inability to construct the charts of the influence of process parameters on process results. Therefore the techiques of "soft" computing have been used to construct the correlation between process dependent and independent parameters.

The computational technique used for the current purpose consisted of the combination of artificial neural network (NN) and classical fuzzy logic (FL) techiques. The approach is to obtain an artificial neural network, capable of predicting the "fuzzy" or dual membership degree of any combination of the input parameters in the two classes. Thus the I / O relationship of the data is represented in the form :

$$y = NN\ (x) \tag{8.2}$$

After such a network is obtained, the fuzzy sets for the classes class I and class II representing the degree of surface cleanliness must emperically be constructed. Then the modeling procedure follows the conventional fuzzy inference and defuzzification process. Thus in this approach the fuzzy model is expressed by the following two rules:

R1: **IF x** = (x$_1$, x$_2$, x$_3$, ... x$_n$) is Class I, **THEN** d^1 -> μ (Class I)   (8.3)

R2: **IF x** = (x$_1$, x$_2$, x$_3$, ... x$_n$) is Class II, **THEN** d^2 -> μ (Class II)

for n = number of independent variables = 6, d^1 and d^2 are the outputs for rules 1 and 2 expressed in terms of the degree of belonging of the given set of input parameters to the classes I and II respectively. For example, for any given input **x,** if the IF part of the rule 1 evaluates to a membership degree of μ (with the help of the NN), then the output d^1 (roughness) is said to belong to class I with degree of truth (membership) μ. The same scenario is applied for the rule 2. Then the process output z is found using the defuzzification technique given by Equation 3.

$$z = \frac{\sum_{i=0}^{n} d_i \mu_y(d_i)}{\sum_{i=0}^{n} \mu_y(d_i)}$$ (8.4)

where d is the value of the roughness at some point, and μ(d) is the truth membership value for that point.

8.3.5 Development of the Model

8.3.5.1 Development of the Neural Network. In order to obtain the Neural Network (NN) responsible for determination of the degree of belonging of any input set **x** the experimental data in Table 8.7 was devided in two parts, where the first part was used for training the NN and second part was used for testing of the NN. This database was then scaled to fit between 0.15 to 0.85 based on the largest and the smallest magnitude of

a parameter, to override large fluctuations in magnitudes within experimental data. The data which could be classified to either belong to a class I or not was used for training of the NN. To develop the desired NN we have used the following network architecture: 6 x 5 x 3 x 2. Where the first layer contained six neurons (corresponding to each independent process parameter) the second and the third (hidden) layers contained five and three neurons respectively and the output layer contained two neurons, one for every output class (class I and class II). For example if a data set from Table 8.7 (a row) contains output evaluated to belong to the "first" class, then the training example will be represented as 1 and 0, for the output neurons one and two respectively. The network design contained the momentum coefficient $\mathbf{m} = 0.31$ with the learning rate of 0.09. The logistic binary sigmoid function was used as activation function to pass information within the network.

The network with above described architecture was trained for 20,000 iterations (epoches) after which the network root mean square error reached 27%. The network was then tested by substituting some random numbers, but other then those used for training. It was found that the network failed to train at all. Different trials with different network parameters were attempted, but the network has repeatedly failed to converge. This means that either the data is incosistent and noisy or insefficient number of training samples is available, or both. Therefore in order to proceed the technique known as backward elimination was used to identify and eliminate the input variables contributing mostly to the noize. In such a technique a network is first trained with the full number of independent parameters fed as inputs. In this case the network with six inputs was used and trained for 20,000 iterations to obtain the final error of ~ 27. Then one variable from

the input set was eliminated and the network was trained again for 20,000 iterations and the final error was recorded. After all the variables were eliminated (one at a time) the final errors were compared. It was then found that after eliminating variables two and three (one at a time) the final error was well below 27, approximately at 15. While in all other cases the training resulted in much bigger magnitudes of the error, ~35-40. Thus it was decided to eliminate variables two and three (nozzle diameter and standoff distance) from the model. It appears that in this case the ranges of change for these variables were two insignificant to produce an effect on the output. Thus the network with four inputs and the architecture 4 x 5 x 3 x 2 was used for training. The results of the training are given in Table 8.8.

8.3.5.2 Development of Fuzzy Sets. The fuzzy sets representing the degree of cleanliness in terms of the Class I and Class II were constructed empirically, using the data from the Table 1. Close examination of the data may give an insight into the degree of the overlap between the two sets. The fuzzy sets were constructed by using the so-called S-curve, commonly used to represent fuzzy numbers. An S-curve is defined using three parameters: its zero membership value (α), its complete membership value (γ), and the inflection point (β). At the inflection point the domin's value is 50% true. These values were identified from the data in Table 8.5 and plotted in Fig 8.26. The expression for the S-curve is given by Eq. 8.5 (Cox, 1996).

$$S(x;\alpha,\beta,\gamma)= \begin{cases} 0 & \text{for } x<=\alpha \\ 2((x-\alpha)/(\gamma-\alpha))^2 & \text{for } \alpha<=x<=\beta \\ 1- 2((x-\gamma)/(\gamma-\alpha))^2 & \text{for } \beta<=x<=\gamma \\ 1 & \text{for } x>=\gamma \end{cases} \tag{8.5}$$

8.3.6 Prediction Results

The results of the developed model's prediction are presented in Figures 8.27-8.29. These results demonstrate that given a set of waterjet parameters the model is capable of predicing the membership values of the resulting surface in the two fuzzy classes and the corresponding surface roughness can be inferred from this information.

Unfortunately, Figures 8.27-8.29 represent only theoretical values of the process output, since due to the unavailability of the experimental samples these results could not be tested experimentally.

8.4 Experimental Study of Viscous Deposit Removal

8.4.1 Experimental Procedure on Tar Removal

Roffing tar represents viscoelastic-to viscous types of deposits. Therefore the study of waterjet cleaning of this deposit will enhance the understanding of cleaning of broad category of ductile and elastic materials. A roofing tar, available in retail stores was applied on to aluminum surface according the instructions on packaging. Since the deposit is very viscous it was found difficult to obtain an even coating of the same thickness on all aluminum samples. The samples were let to dry for one year. The experimental removal procedure involved two steps. First, the thisk and viscous layer of deposit was removed at high speed (approximately 18 m/sec) and with angle of impact approximately 150 degrees. The remaining thin and hard layer of deposit was then removed at varying process parameters. The parameters in question were water pressure, nozzle traverse rate, standoff distance, media flow rate (sodium bicarabanate), and impact angle. The output of the process was the single strip width, which was measure and then

converted to process productivity. Due to the relatively large number of process parameters and a few experimental samples no experimental planning procedure was employed.

8.4.2 Experimental results

The experimental results are presented in Table 8.7, columns 1 through 7. It is really difficult to speculate on the trends involved given the change of any one process parameter due to the limited experimental database. Only general conclusion regarding the change in water pressure and traverse rate can be made. Thus we can conclude, based on the data in Table 8.7 that the increase in water pressure generally results in higher productivity and that the increase in traverse rate results in narrower width of the strip. As for the other process conditions no concludion can be drawn based on the existing data. Therefor a model of the process must be build and analyzed in order to investigate the change patterns in the experimental process conditions.

8.4.3 Model of the Process

Due to the limited and unorganized experimental database it was found difficult to apply a standard statistical techniques, routinely used for establishing the correlation between the process inputs and outputs. Therefore the modeling techique based on the principles of the artificial neural networks was applied. The experimental database was divided into the training data set (TDS) and checking data set (CDS). TDS was used to train the network and CDS was used to check the network's performance. The TDS contained data sets numbers (Table 8.7) {1, 2, 3, 6, 7, 10, 11, 13, 14, 16, 17, 19, 20, 21, 22, 24, 25, 26,

27, 29, 31, 33, 34, 35, 36}. And CDS involved the following data sets from Table 8.7 {4, 5, 8, 9, 12, 15, 18, 23, 28, 30, 32}. The artificial neural network design to model this problem contained five input neurons (one corresponding to each process input variable), one layer of five hidden neurons and an output layer of one neuron, corresponding to process output – the strip width. The network learning rate was set to 0.2, and the momentum coefficient was set at 0.4. The network was trained for 40,000 – 60,000 iterations, every 100 iteration the checking data set was substituted into network and the checking error was recorded. The iterations were stopped when the training data set have reached an acceptable error tolerance (~ 2%), but the CDS error have started to grow above ~5%. At this point the network was considered trained and was used for studying the influence of process parameters.

8.4.4 Results and Discussion

Model prediction results along with some experimental data points are presented on Figures 8.30-8.34. Thus, analyzing Figures 8.30 8.32 we can conclude that the width of strip, and consequently the productivity, decreases when the angle of attack changes from 90 degrees to 145 degrees. Moreover it follows that for higher traverse rates the single width of strip also decreases, although it does not necessarily mean the increase in productivity. In fact, Figures 8.31 and 8.32 demonstrate that the process productivity increases with increased traverse rates. Figure 8.31 also supports the experimental conclusion that the increase in water pressure brings about the increase in productivity. As was speculated before the increase in traverse rate generally results in higher process productivity.

The neural network based prediction technique performance is shown to accurate and stable when modeling a process under conditions of limited and unorgainized experimental data. Figures 8.30 through 8.32 and Table 8.7, columns 8- 11 demonstrate this conclusion.

Table 8.1 Training Data and Prediction Results

Number	WP Descale (MPa)	TR mm/min	Angle Degrees	SFR (g/min)	SOD (sm)	Strip Wildth (mm) Experim	Predict	Relative Error	Productivity (m2/hour) Experim	Predict
1	138	2540	90	612	0.7	3.7	3.5	0.06	0.56	0.53
2	138	7620	90	612	0.7	2.9	2.9	0.01	1.33	1.31
3	138	10160	90	612	0.7	2.5	2.7	0.09	1.52	1.66
4	138	12700	90	612	0.7	2.2	2.6	0.19	1.68	1.99
5	138	2540	90	612	4.0	3.8	3.7	0.01	0.58	0.57
6	138	7620	90	612	4.0	2.5	2.5	0.01	1.14	1.13
7	138	12700	90	612	4.0	2.8	2.4	0.15	2.13	1.82
8	207	2540	90	612	2.0	5.3	5.2	0.02	0.80	0.79
9	207	7620	90	612	2.0	4.5	4.3	0.05	2.06	1.95
10	207	12700	90	612	2.0	3.5	3.4	0.02	2.67	2.63
11	207	17780	90	612	2.0	3.0	3.0	0.00	3.20	3.20
12	207	5080	90	612	5.0	5.2	4.9	0.07	1.58	1.48
13	207	12700	90	612	5.0	3.0	2.9	0.02	2.29	2.24
14	207	20320	90	612	5.0	2.5	2.4	0.02	3.05	2.98
15	172	2540	90	612	1.0	5.0	4.6	0.07	0.76	0.71
16	172	10160	90	612	1.0	3.3	3.3	0.01	2.01	1.99
17	172	15240	90	612	1.0	2.9	2.8	0.03	2.65	2.59
18	172	2540	125	612	1.0	3.8	3.0	0.20	0.58	0.46
19	172	7620	125	612	1.0	2.8	2.5	0.11	1.28	1.14
20	172	15240	125	612	1.0	1.3	1.3	0.04	1.19	1.15
21	207	5080	90	612	1.0	5.0	4.9	0.01	1.52	1.51
22	207	12700	90	612	1.0	4.0	3.9	0.03	3.05	2.96
23	207	17780	90	612	1.0	3.2	3.6	0.12	3.41	3.81
24	172	2540	145	612	1.0	3.0	2.8	0.06	0.46	0.43
25	172	10160	145	612	1.0	1.8	1.8	0.01	1.07	1.07
26	172	2540	110	612	1.0	3.8	3.8	0.00	0.58	0.58
27	138	2540	90	612	1.0	2.5	3.0	0.21	0.38	0.46
28	138	2540	125	612	1.0	1.7	2.1	0.24	0.26	0.32
29	138	12700	125	612	1.0	1.0	1.0	0.02	0.76	0.74

Figure 8.7 Media Assisted Waterjet Paint Removal. Experimental Results

Figure 8.8 Media Assisted Waterjet Paint Removal. Experimental Results

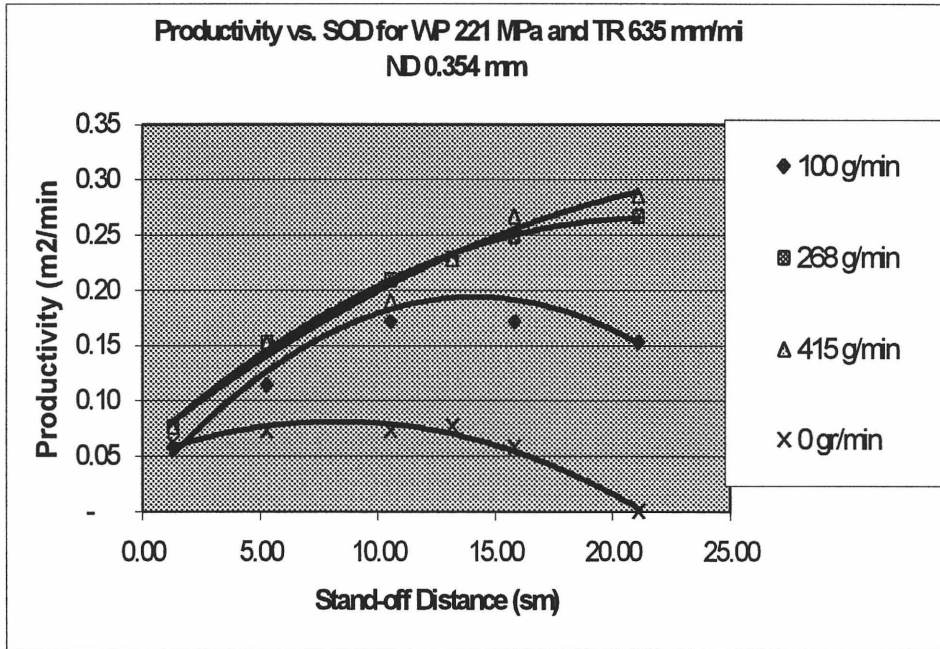**Figure 8.9** Media Assisted Waterjet Paint Removal. Experimental Results

Figure 8.10 Media Assisted Waterjet Paint Removal. Experimental Results

Figure 8.11 Media Assisted Waterjet Paint Removal. Experimental Results

Figure 8.12. Media Assisted Waterjet Paint Removal. Experimental Results. Effects of Traverse Rate and Water Pressure
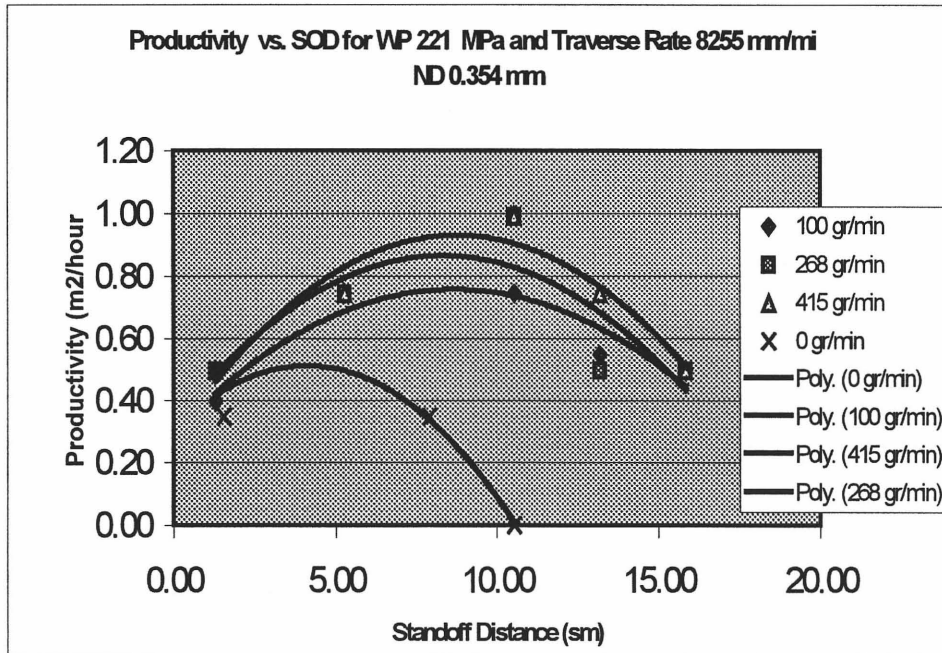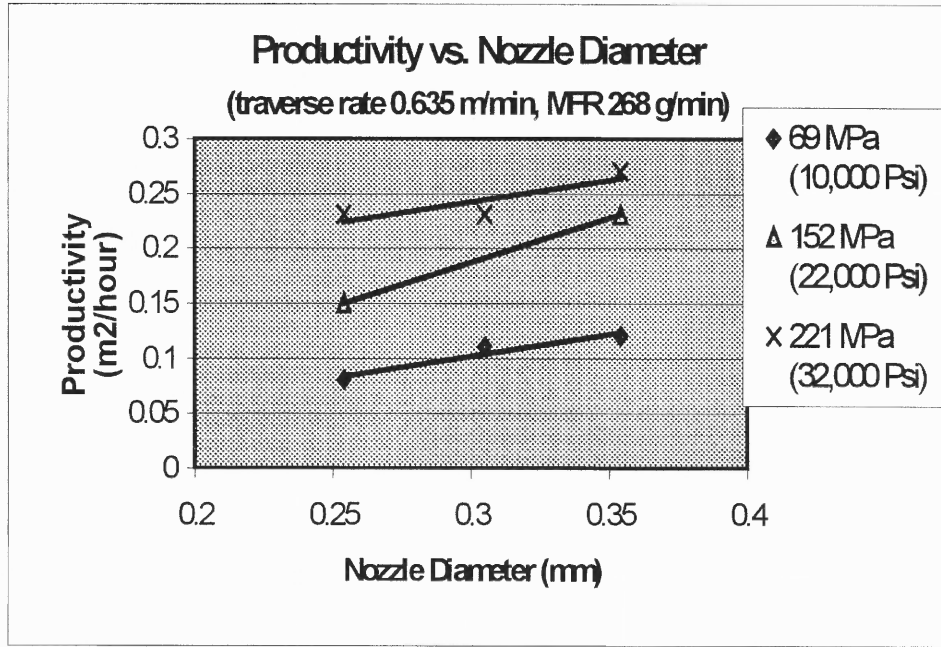
Figure 8.13 Media Assisted Waterjet Paint Removal. Experimental Results
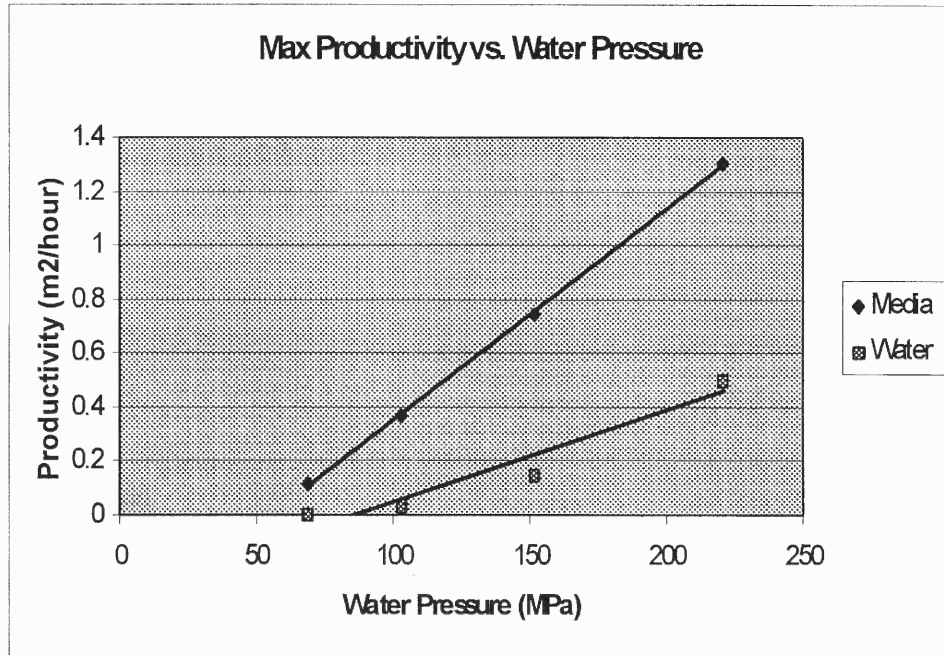
Figure 8.14 Media Assisted Waterjet Paint Removal. Experimental Results
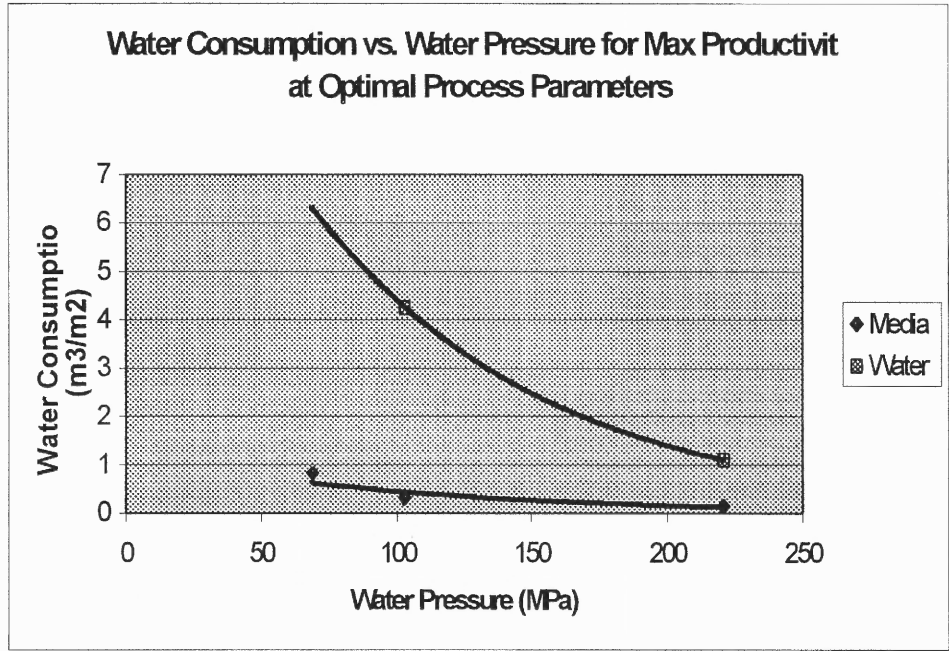
Figure 8.15 Media Assisted Waterjet Paint Removal. Experimental Results
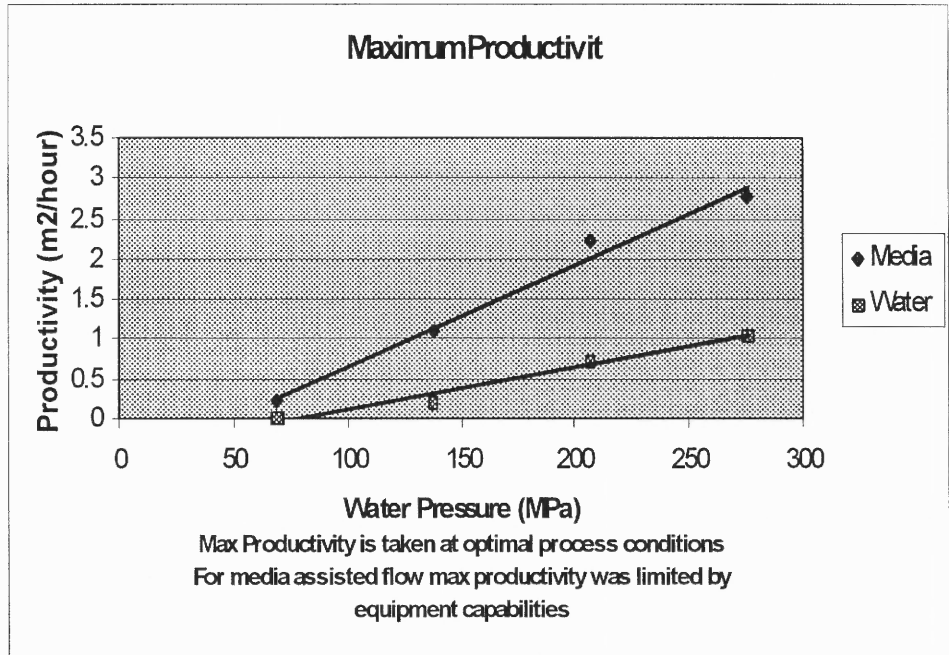
Figure 8.16 Media Assisted Waterjet Paint Removal. Experimental Results
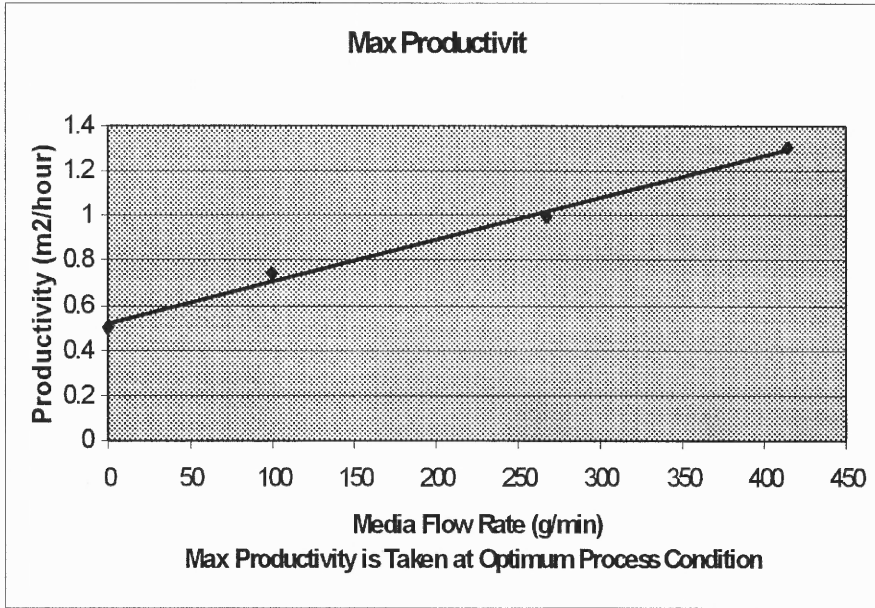
Figure 8.17 Media Assisted Waterjet Paint Removal. Experimental Results
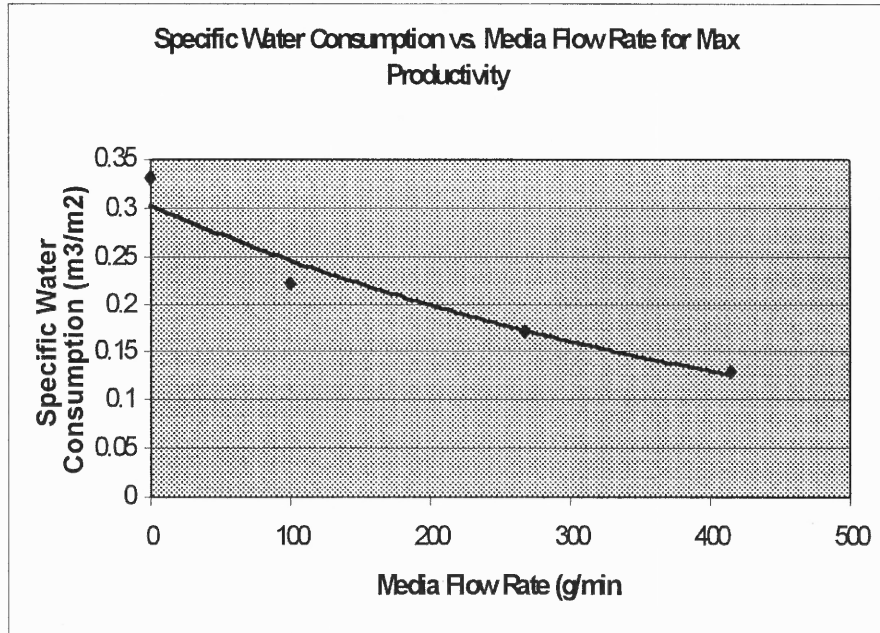
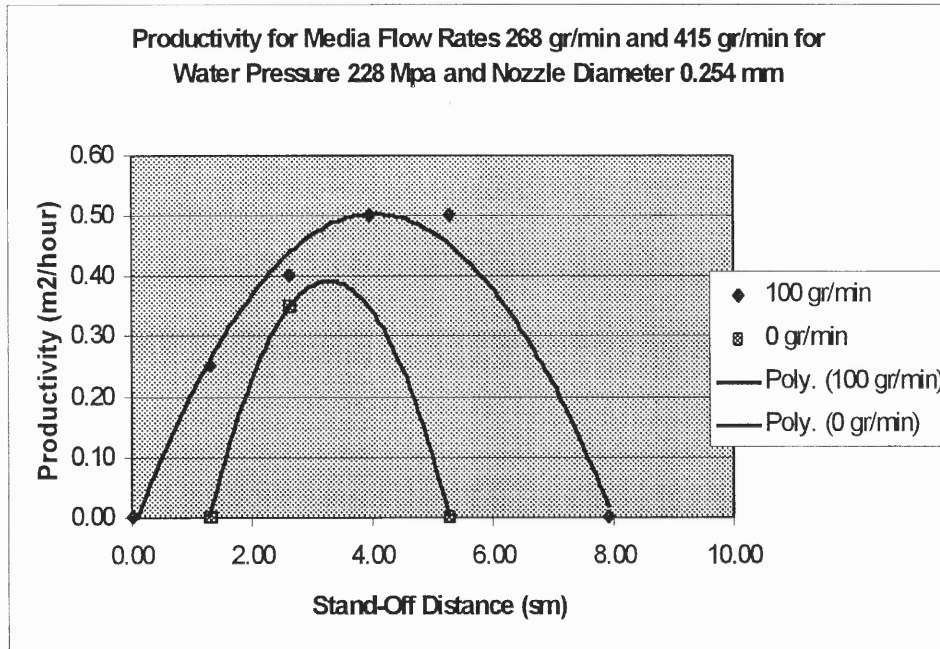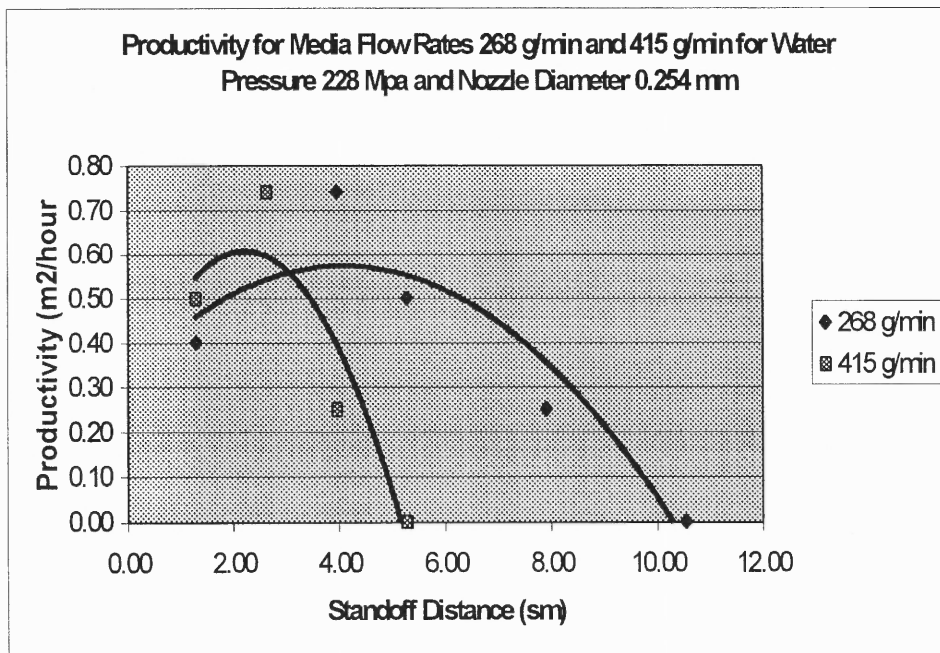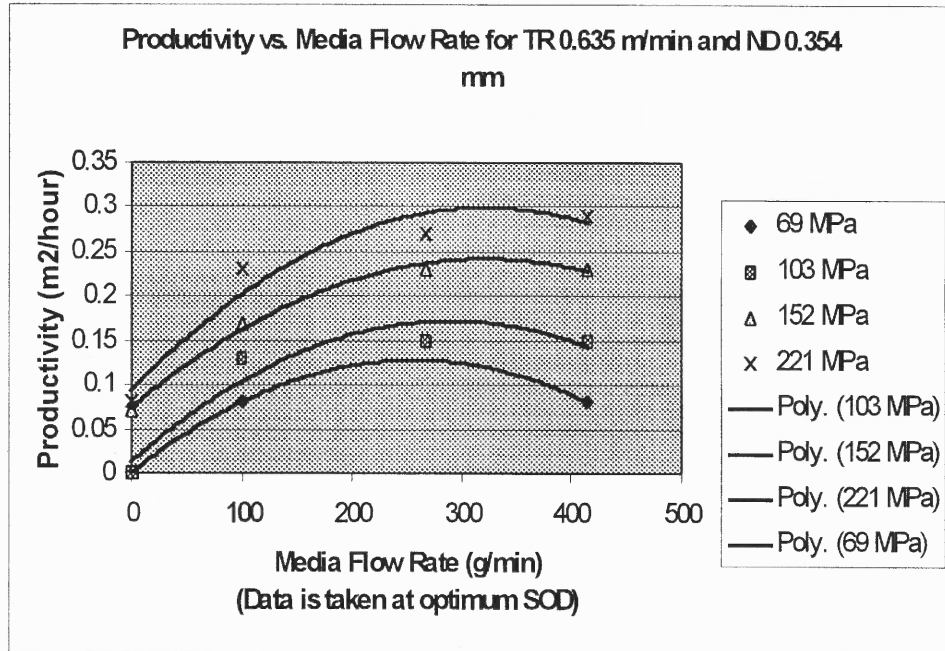**Figure 8.18.** Media Assisted Waterjet Paint Removal. Experimental Results
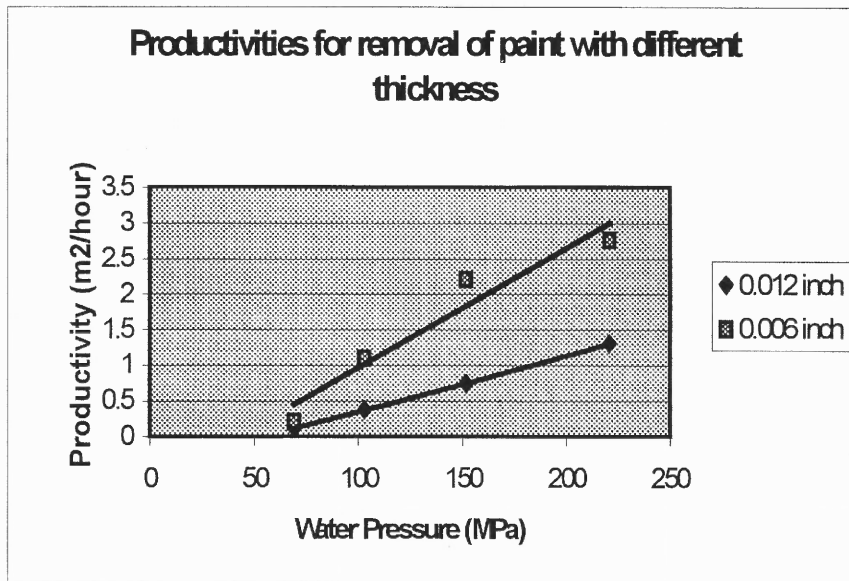
Figure 8.19 Media Assisted Waterjet Paint Removal. Experimental Results
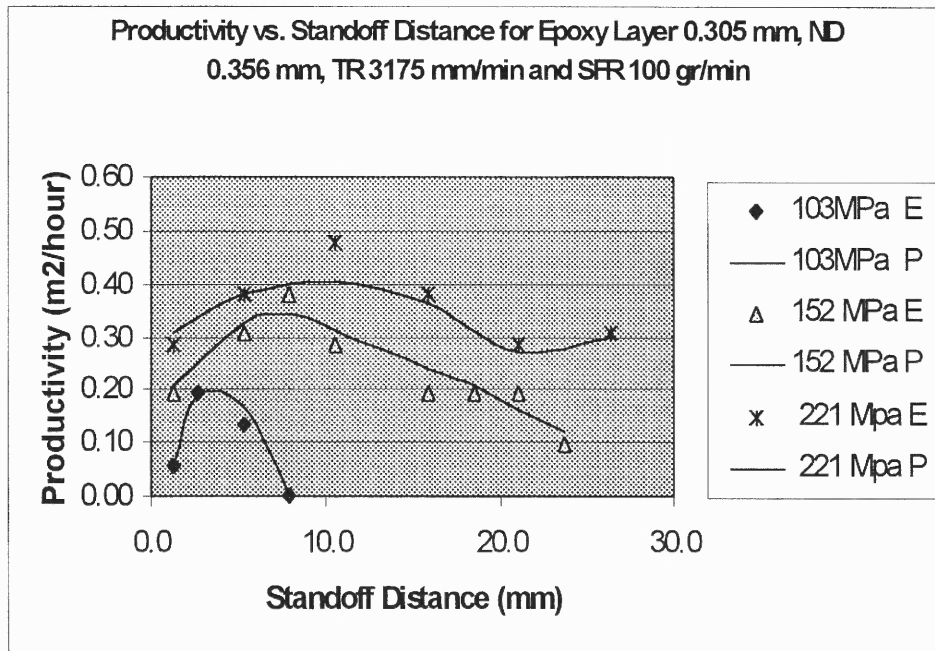
Figure 8.20. Media Assisted Waterjet Paint Removal. E-Experimental, P-Prediction
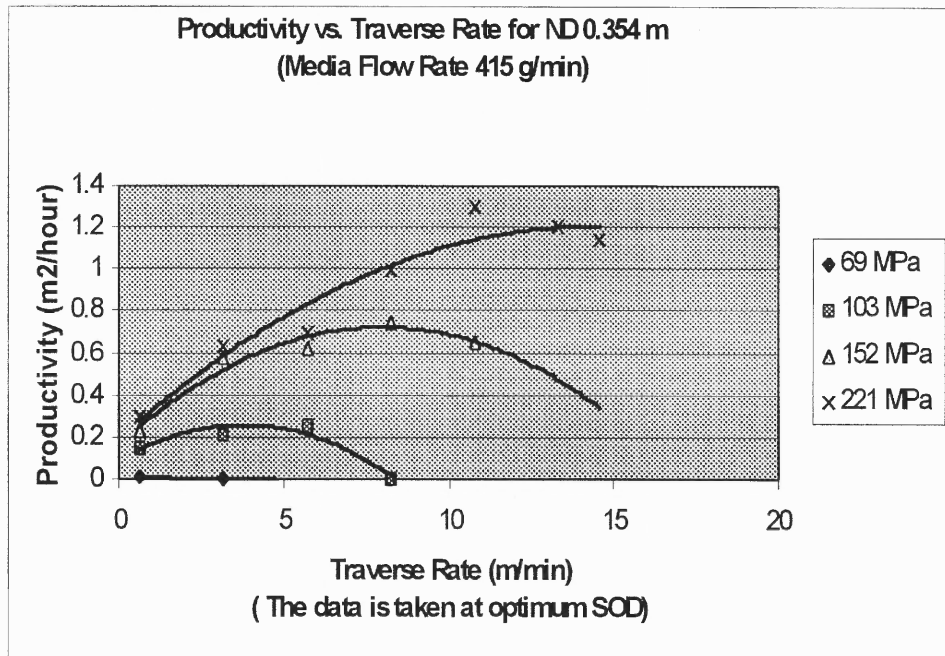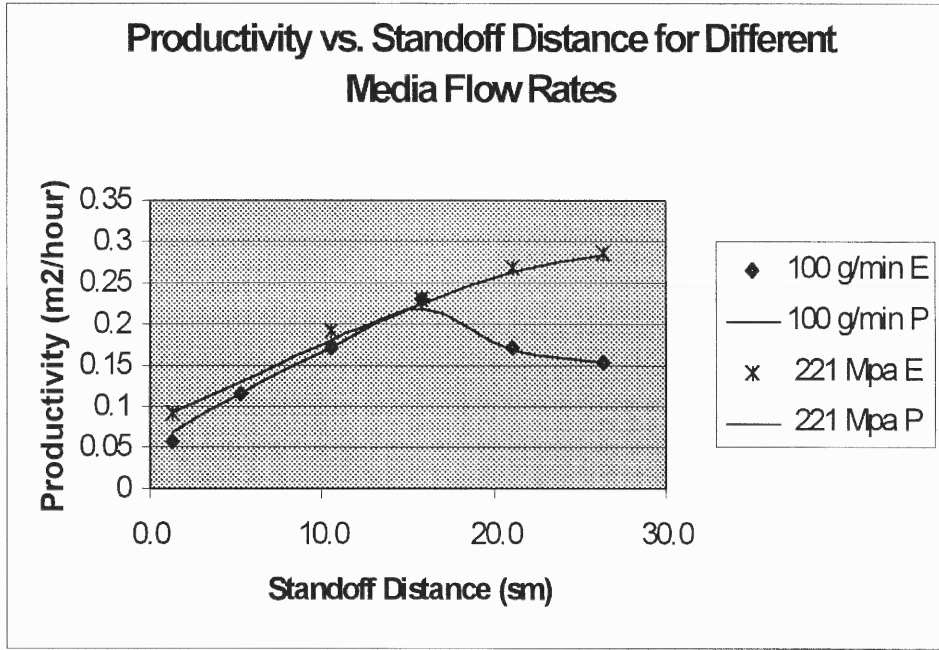
Figure 8.21 Media Assisted Waterjet Paint Removal. E-Experimental, P-Prediction. The data is plotted for Water Pressure 221 MPa, Traverse Rate mm/min, ND 0.3554mm, Layer 0.305 mm.
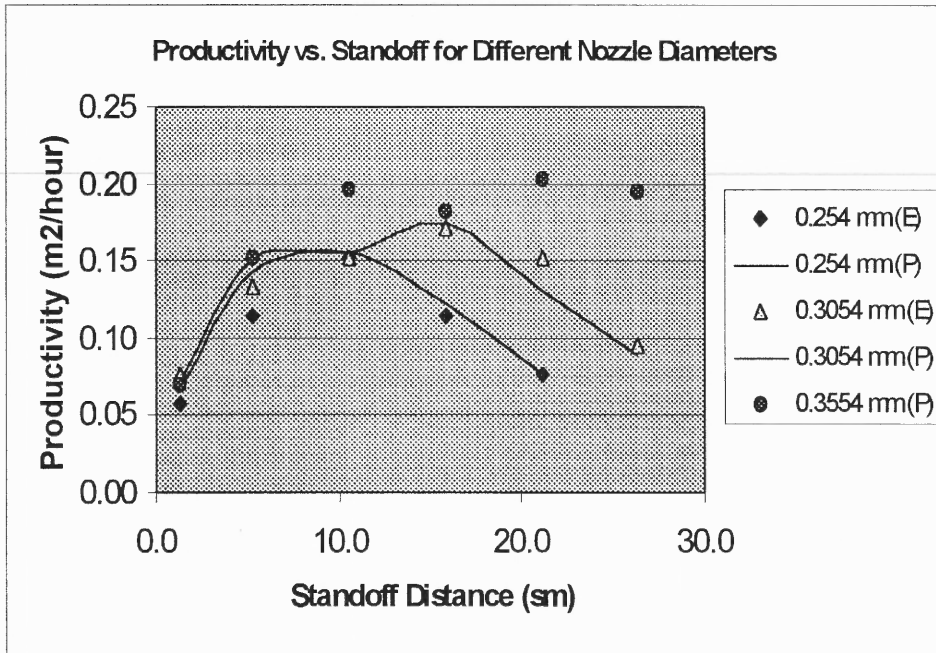
Figure 8.22 Media Assisted Waterjet Paint Removal. E-Experimental, P-Prediction. The data is plotted for Water Pressure 124 MPa, Traverse Rate 635 mm/min, Media Flow 415 g/min, and Paint Layer 0.305 mm.
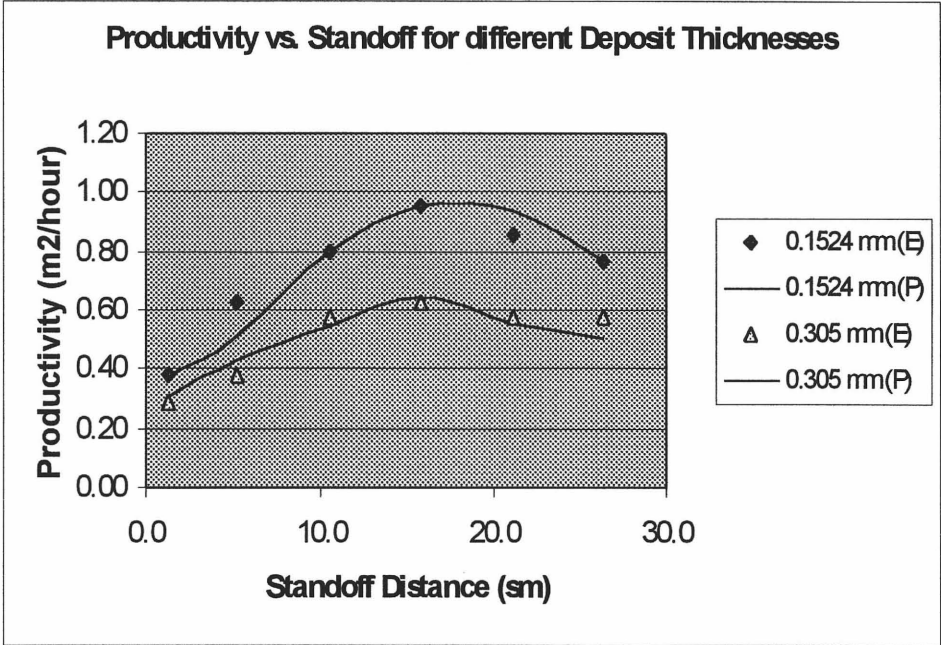
Figure 8.23 Media Assisted Waterjet Paint Removal. E-Experimental, P-Prediction.

The data is plotted for Water Pressure 207 MPa, Traverse Rate 3175 mm/min, Media Flow 415 g/min, and Nozzle Diameter 0.3554 mm.
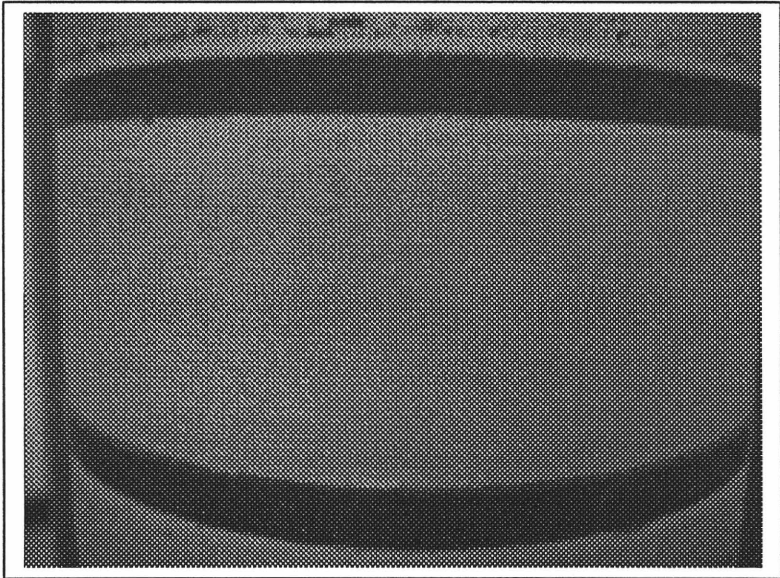
Figure 8.24 Roll cleaned to the " first degree" of cleanliness.
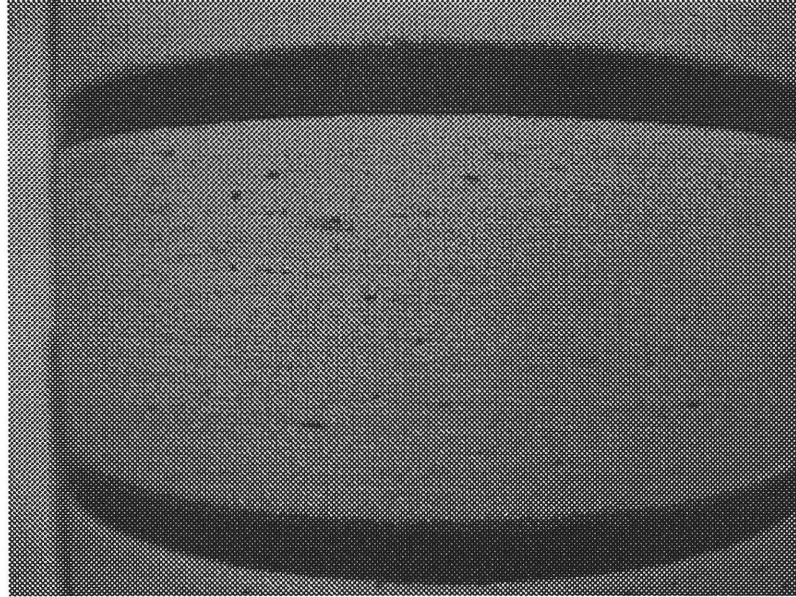
Figure 8.25.Roll cleaned to the " second degree" of cleanliness.
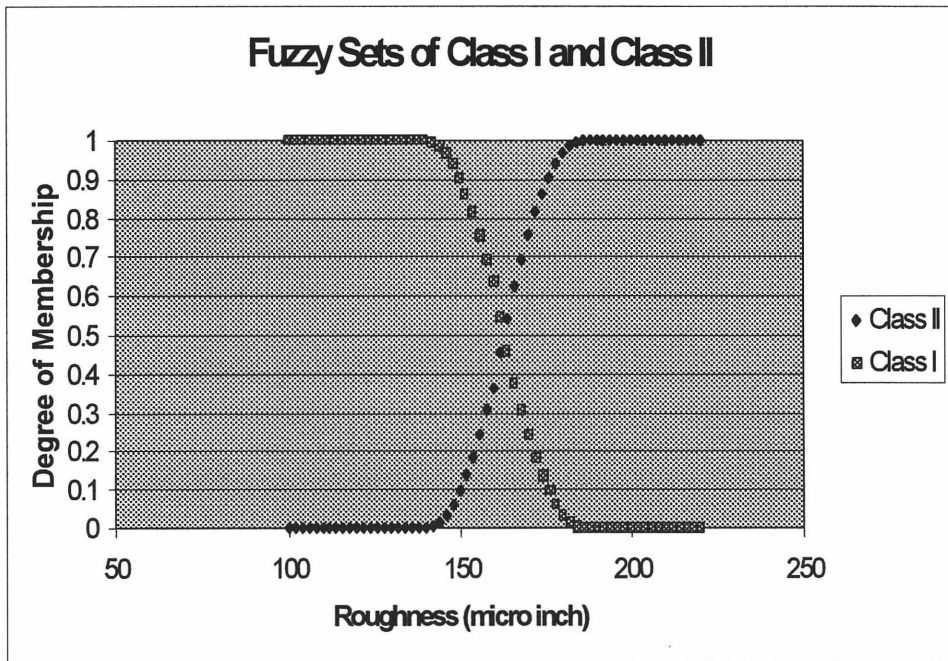
Figure 8.26 Fuzzy Universe for Roughness Classes I and II.
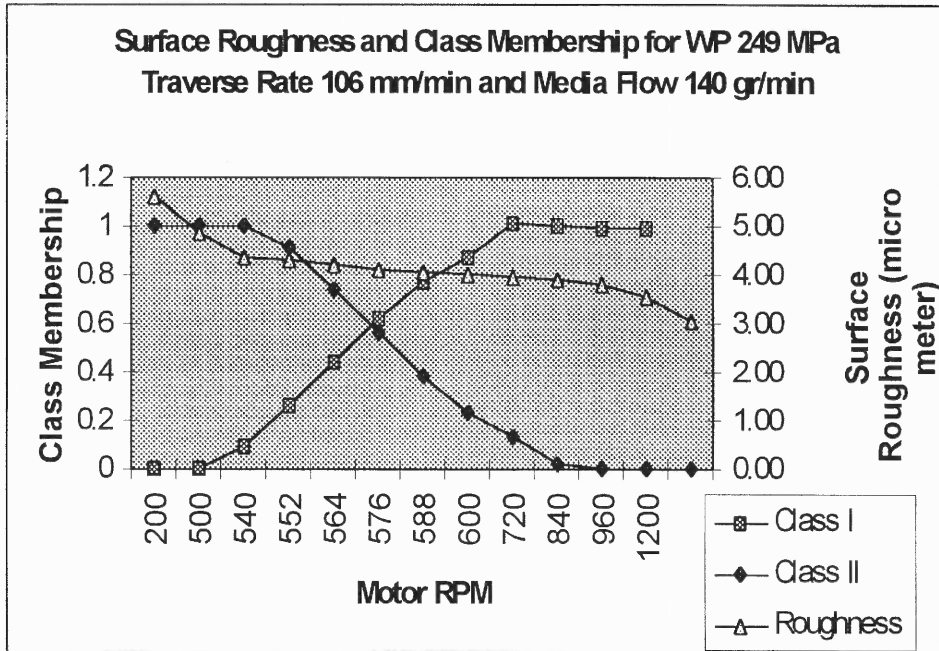
Figure 8.27 Prediction results of the NN- Fuzzy Logic based prediction technique. Class I and Class II series represent the membership values of the corresponding set of waterjet parameters in these classes.
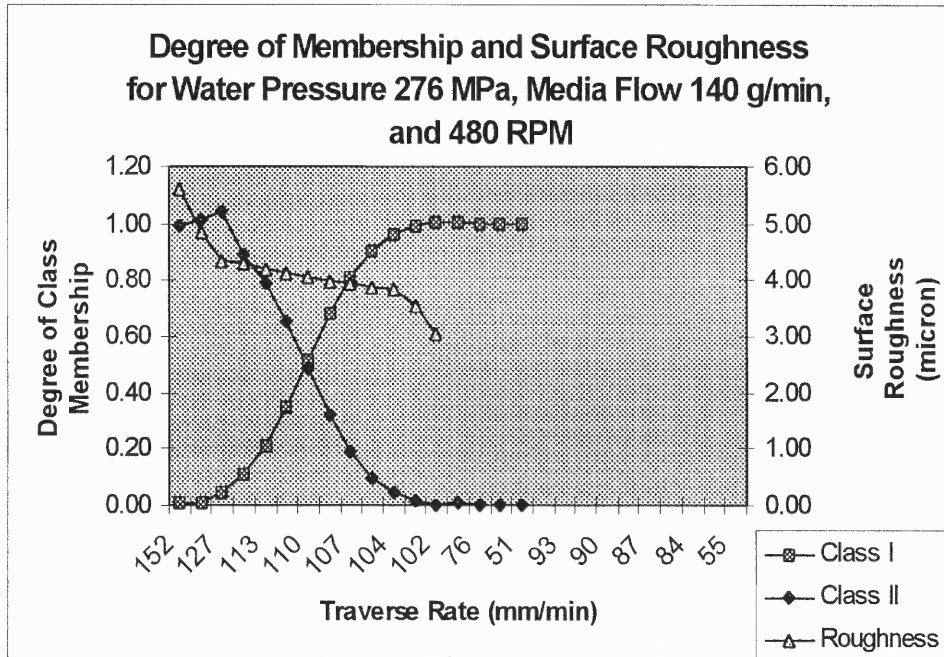
Figure 8.28 Prediction results of the NN- Fuzzy Logic based prediction technique. Class I and Class II series represent the membership values of the corresponding set of waterjet parameters in these classes.
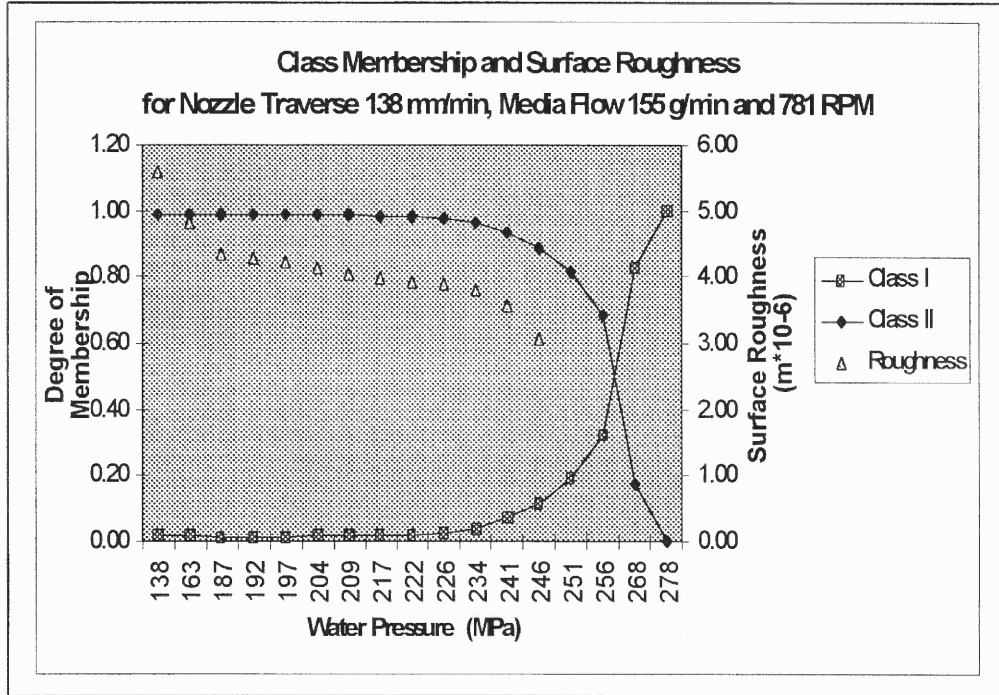
Figure 8.29 Prediction results of the NN- Fuzzy Logic based prediction technique. Class I and Class II series represent the membership values of the corresponding set of waterjet parameters in these classes.
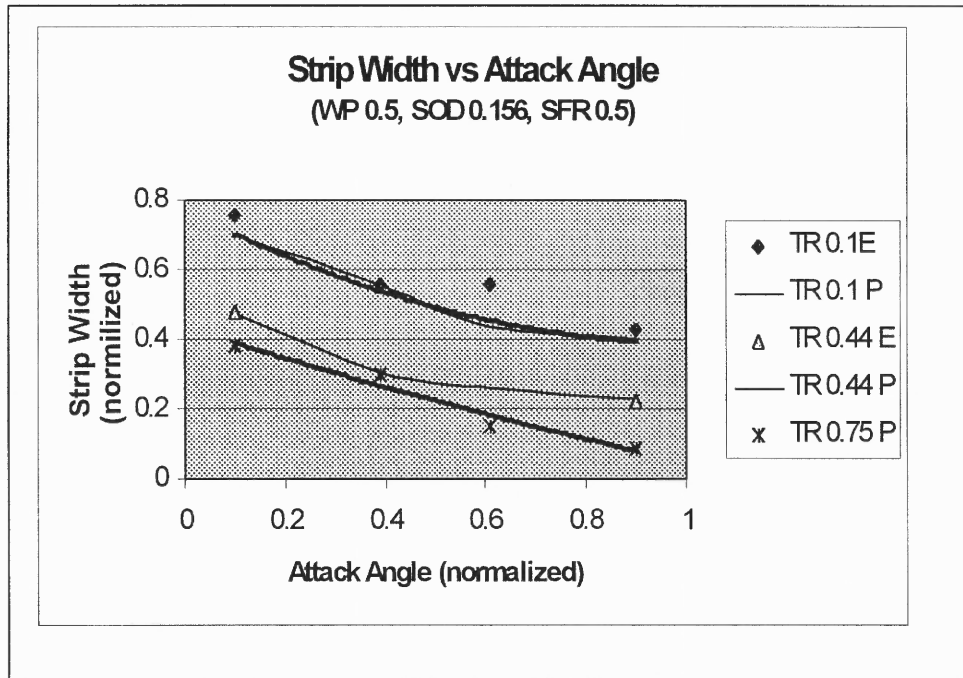
Figure 8.30 Model Prediction (P) and Experimental Data (E), normalized
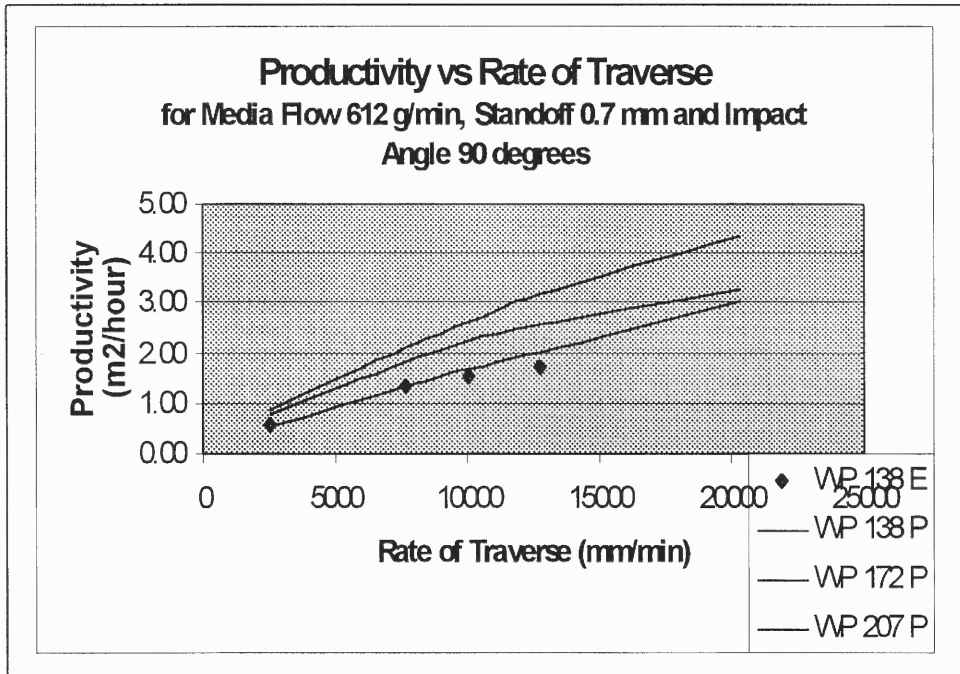
Figure 8.31 Model Prediction (P) and Experimental Data (E).
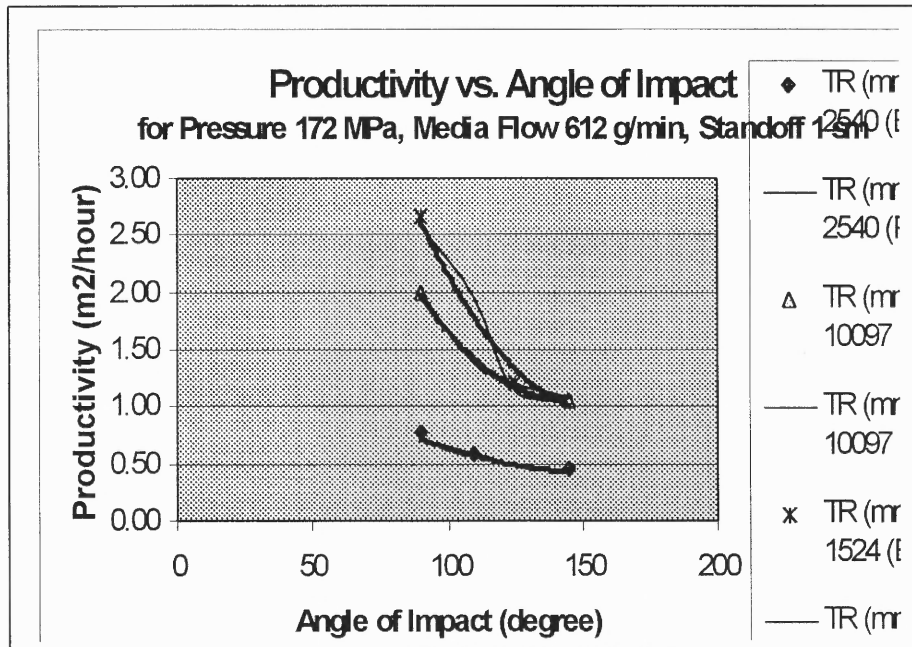
Figure 8.32 Model Prediction (P) and Experimental Data (E)

CHAPTER 9

OPTIMIZATION OF ENERGY UTILIZATION IN THE COURSE OF MATERIAL PROCESSING

9.1 Introduction

Evaluation of the energy consumption for different stages of material processing is one of the major elements of the integration of manufacturing technology. Minimization or at least limitation of the energy consumption for material modification, deformation, addition, removal, etc. to a great extend determines the selection of a route of conversion of raw materials into a product. The process model determines the correlation between the rate of the energy delivery to the tool-workpeace interface and the desired material change. Unfortunately, in the most practical cases this model is unknown. Moreover, a shear number of the various technologies make the construction of a representative model for each individual case impractical. At the same time, at least for traditional technologies, sufficient empirical database representing process is available. Thus, a realistic approach to energy optimization in manufacturing is utilization of the available information about a process in question. However, usually, this information is chaotic, partially crisp (numerical) and partially linguistic (qualitative). Nevertheless, existing techniques of soft computing enable us extract a significant knowledge out of poorly organized information. The objective of this work is to illustrate the application of soft computing for integration of manufacturing technology. We will use waterjet surface decoating in order to demonstrate the application of the proposed technique.

Improvement of the energy constitutes one of the major subjects of the applied physics and engineering. The state of the art in this area is exhaustively discussed in several fundamental works, most by Bejan et al (1996). The specific feature of energy conservation in material processing is the way of energy consumption. In the final analysis material processing results in the destruction of the almost all exergy delivered to the work zone via work and heat fluxes. Thus the most effective way of the optimization of the energy use is the reduction of the entropy production. This approach to energy economy was pioneered by Bejan (1982). In most general way energy is determined by a scalar product

$$T\sigma = JX \tag{9.1}$$

where σ is the specific rate of entropy production, X and J are generalized forces and fluxes , T is the absolute temperature. It is necessary now to express the J and X via identifiable process variables and it is expedient to replace entropy production by more conventional process characteristic, exergy destruction, which in the case of material processing is practically equal to the exergy consumption. However, the exergy consumption, that the energy cost of the process should be related to the technological process results.

Let us determined the energy efficiency of a manufacturing process η_e as the ratio

$$\eta_e = \frac{EX}{B} \tag{9.2}$$

EX=exergy consumption, B=technolological result of the process. Available information should be used to determine EX and B. It is clear that the equation above is applicable only if the technological result can be evaluated by a single number, such as, for example,

reduction of the surface roughness, the length of the welding seam, amount of the deposited material, amount of the material, underwent the phase transition, etc.

Let us limit our analysis to the processes where the result can be determined by a single number, such as, the reduction of the surface roughness, the length of the welding seam, the amount of the deposited material, the amount of the material removed, degree of deformation, etc. The energy efficiency of such processes can be described by the specific exergy consumption that is by the ratio EX/B, where EX is the exergy consumption; B is the technological result of the process. The available information should be used to determine EX and B.

The energy efficiency of the waterjet decoating is determined by the product VP, where V=water consumption for decoating of 1 m^2 of the metal surface, m^3/m^2 and P = water pressure after the pump, MPa. A database representing coating removal was accumulated in order to determine operational conditions (sweeping rate, nozzle diameter, water flow rate, stand off distance) minimizing exergy consumption. Artificial Neural Networks were used for process simulation while the Genetic Algorithm was applied for selection of the optimal strategy. Additional experimental database was acquired in order to validate the results of optimization. Finally, the effectiveness of the use of proposed technique for improvement of the energy utilization, particularly for prediction of the correlation between exergy consumption and process results is discussed. A generic procedure for integration of a manufacturing technology is suggested.

9.2 Optimization of Energy Consumption of Waterjet Rust Removal Process

For the current study the artificial neural network was used to model the waterjet rust removal process (Experimental setup and results are in Chapter 7) The network architecture used in modeling of waterjet derusting process is shown in Figure 8.1. For this problem the four-layer network is chosen. The input layer consists of three neurons, which corresponds to the number of experimental parameters. That is X1 represents the water pressure, X2 represents the traverse rate, and X3 represents the nozzle diameter. The output layer consists of one neuron (T), which corresponds to the process output variable, the strip width. Two hidden layers, 8 neurons each, are used in the current network's architecture.

An experimental database representing waterjet rust removal was acquired and divided into two data sets- training and checking. The training data set was used to train the network to respond correctly to an input pattern. A simple feed forward algorithm with backpropagation of error was used in the training of the network (Chapter 5). The network was trained for 20,000 epochs, at which point the total error reached 0.8%. This error was considered acceptable for the current study. The testing data set was used to verify the network performance. At this point a network is considered trained and can be used as process model, or for optimization.

We are interested in optimizing the specific efficiency of the process, given by Equation 9.3.

Specific Energy (KJ/m2) = Pressure (KPa)*Specific Water Consumption (m3/m2)

(9.3)

The information needed for the application of the GA-based optimization procedure is limited to the knowledge of the possible ranges of process variables, correctly defined objective function (fitness function in this problem), and the process model (not necessarily analytically expressed). In our problem a single bit string incorporated all three input parameters. First we apportioned the number of bits for each variable in a string. This number depends on the maximum value of the variable used. In this study the working pressure did not exceed 310 MPa, the maximal nozzle traverse rate was 12700 mm/min, and the maximal nozzle diameter was 355 microns. Thus for binary representation we needed to apportion 9 bits for water pressure variable, 14 bits for traverse rate variable and 9 bits for strip width. Thus a chromosome for this problem consisted of 32 bits (9+14+9).

This size of the chromosomes (9+14+9) was kept constant in this problem regardless of the actual values of process variables.

100010100 00001001111011 100011000

276 MPa   635mm/min   279mm

We start with first population of chromosomes by generating k random 32-bit chromosomes (bit strings). The number of chromosomes in a population (k) is problem dependent, too few strings will result in a premature convergence, and too many will slow the convergence. Usually the number of bit strings in a population is taken to be equal to 1-1.5 number of bits in a string. Each bit string in a population is then separated into its three components representing encoded process variables, decoded into decimal

$$X_{scaled} = X_{min} + X_{(decimal)} \cdot \frac{X_{max} - X_{min}}{2^n - 1} \qquad (9.4)$$

format, and then scaled within acceptable range according to equation below.

where Xmin and Xmax represent the operating range of a variable, and n is a number of bits in a string apportioned for the variable. Next these decoded and scaled values are fed as an input to a trained artificial neural network to obtain the output (width of strip). The fitness function in this problem is given by (9.3). To estimate whether a chromosome is fit enough for its selection for further genetic operations (process parameters encoded in a chromosome result in adequate energy consumption) we define the Probability of Selection as a ratio of individual chromosome's fitness and the average fitness of the whole population:

Thus for maximization problem the probabiliy of selection is defined as:

$$\text{Probability of Selection} = \text{Fitness} / \text{F avg.} \tag{9.5}$$

However for minimization problem we are interested with inverse probability of selection:

$$\text{Inverse Probability of Selection} = (\text{Fitness} / \text{F avg.})\text{-1}\dots \tag{9.6}$$

If the calculated Probability of Selection of an individual chromosome satisfies earlier set criteria (the value of the Probability of Selection exceeds a cut-off value set by user), the chromosome is selected for further genetic operations. Otherwise the chromosome is discarded.

Table 9.1 shows the manipulations described above for initial randomly generated population consisted of 4 chromosomes. The randomly generated 4 chromosomes are shown in the column 2 of Table 9.1. Here, to save space each chromosome was broken down in three parts, each representing a process variable.

Table 9. 1 GA, Basic Operations

String #	String	Decoded & Scaled Value	Fitness (KJ/m2)	Probability Of Selection	Actual Count
1	010000101 00010000001000 111001011	131.7 MPa 1395 mm/min 331 micron	114,666	0.385	0
2	000110011 10010101100011 010111000	93 MPa 7683.4 mm/min 209 micron	13,312	3.32	1+1
3	000010011 01101010001110 001010111	77 MPa 5641.3 mm/min 165 micron	10,010	4.42	1+1
4	011001100 00101010110101 0001000110	165 MPa 2653.6 mm/min 143.9 micron	38,829	1.138	0
Favg			44,204		

Cut-Off =0.5

Let's consider the string #3 in Table 9.1. The randomly generated string is given by:

String #3= 000010011011010100011100010101111

Here the first 9 digits represent the Water Pressure, next 14 digits represent the Traverse Rate and the last 9 digits represent the Nozzle Diameter, i.e.

Water Pressure = 000010011 MPa

Traverse Rate = 01101010001110 mm/min

Nozzle Diameter = 001010111 micron

Then these binary numbers are converted to the decimal format:

Water Pressure decimal = 19 MPa

Traverse Rate decimal = 6798, mm/min

Nozzle Diameter decimal = 87 micron,

and scaled according to (19) to obtain:

Water Pressure scaled = 77 MPa

Traverse Rate scaled = 5641.279 mm/min

Stand-Off Distance scaled = 165.818 micron

These values are shown in column 3 of Table 9.1. The obtained process parameters were then substituted into the trained Artificial Neural Network to obtain the corresponding output – the Strip Width. This output was used to calculate specific water consumption according to X, or the fitness value. These values are shown in column 4 of Table 9.1. After all chromosomes (column 2) are evaluated and theirs fitness values are calculated the average fitness of the population is found. The ratio of the average fitness of the population to the individual chromosome's fitness yields the Probability of Selection (column 5). This value serves as a criterion according to which we select our chromosomes for the further genetic manipulations or discard unfit chromosomes. Usually this value is compared to predefined Cut-Off value. From the Table 9.1 it follows that chromosome #1 is discarded since its Probability of Selection is less then the Cut-Off value. If the number of chromosomes selected for reproduction is less then the initial population, then some of the chromosomes are selected more then once, ensuring that the "survival of the fittest " rule holds. Thus we select chromosome #3 twice, since its value of Probability of Selection is the highest (actual count in Table 9.1). This new population is then subjected to genetic operations of crossover and mutation. The crossover operator

is basically an exchange of some portion of the chromosome between two randomly selected chromosomes. The number of the chromosomes selected for the crossover depends on the Probability of Crossover. In this example it is taken to be 0.5. Which means that approximately 50% of the population will be selected for crossover. The next genetic operation, mutation, takes place next. Mutation means that the selected (randomly) bit changes its value from 0 to 1 or vice versa. The number of bits selected for mutation depends on the Probability of Mutation. In this example it is taken to be 0.22. Which in turn means that approximately 22% of all bits will mutate. In general the values for Pmutation and Pcrossover are problem dependent and should be varied from run to run to find the optimum ones. Thus we have obtained the final population of the first generation, which represents the initial population for the second generation. The above steps are repeated iteratively until some convergence criteria are met. In the present work several runs with different genetic parameters were made, and the process specific energy consumption was monitored. Then based on the results from several runs the set of the best parameters was identified.

Table 9. 2 Optimization with Genetic Algorithms. Results.

Water Pressure (MPa)	Traverse Rate (mm/min)	Nozzle Diameter (mm)	Productivity m2/hour	Specific Water Consumption (m3/m2)	Specific Energy (KJ/m2)
104.372	11721.30	0.147	0.259	0.075	7841.2
69.0	12500.00	0.127	0.228	0.052	3641.37
76.603	11473.84	0.144	0.236	0.06848	5177.7
111.446	7692.98	0.171	0.227	0.121	13521.38

9.3 Discussion of Results and Recommendations

Table 9.2 shows the results of computations of the optimal cleaning parameters for minimization of the specific energy in the course of waterjet rust removal, with 4 chromosomes in the initial population. It is important to note that this number of chromosomes in the population is extremely low, and was chosen only for the demonstration purposes. Although for the current study the results of the computations are reasonable. All four sets of waterjet parameters result in almost the same productivity of the process, though the specific energy consumption differs significantly. Thus we just choose the set of parameters resulting in lowest specific energy consumption. Here we see that the optimal combination is attained at the minimal water pressure, the maximum traverse rate and minimal diameter of waterjet nozzle. The table shows that the process of the GA-based optimization is stable. As a result of this study we can recommend the above optimal combination of waterjet parameters for any kind of cleaning situation, where the objective function is the minimization of the energy consumption.

9.4 Conclusion

In this work we investigated the application of the AI techniques for description and optimization of waterjet cleaning. The ANN was used to model the nonlinear relationship between process inputs (waterjet pressure, nozzle traverse rate, nozzle diameter) and the process result (the width of the region where the rust was completely removed). The average error of the prediction was 1%. This accuracy is rather adequate. The application of the Genetic Algorithms resulted in the development of a strategy of cleaning. The performed research demonstrated the effectiveness of the use of Artificial Neural

Network and Genetic Algorithms for planning of the Waterjet surface processing. This conclusion constituted the principal result of the presented work.
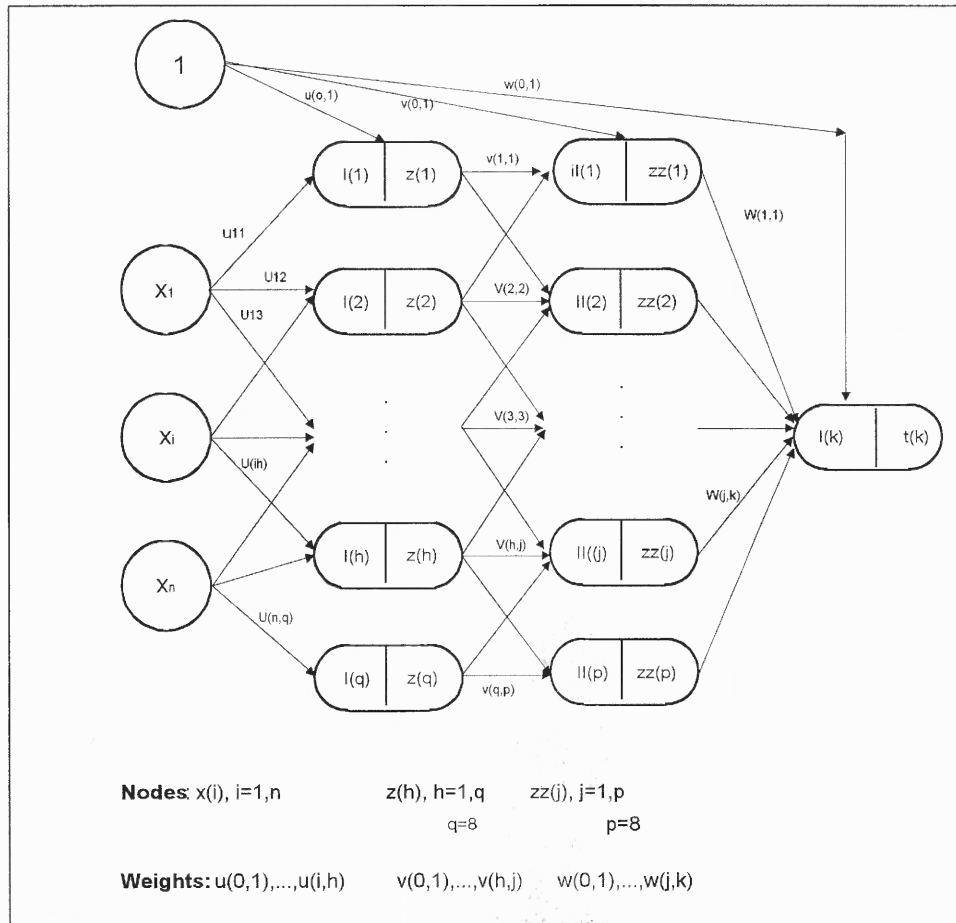
Figure 9. 1 Architecture of Artificial Neural Network for Modeling Waterjet Rust Removal Process
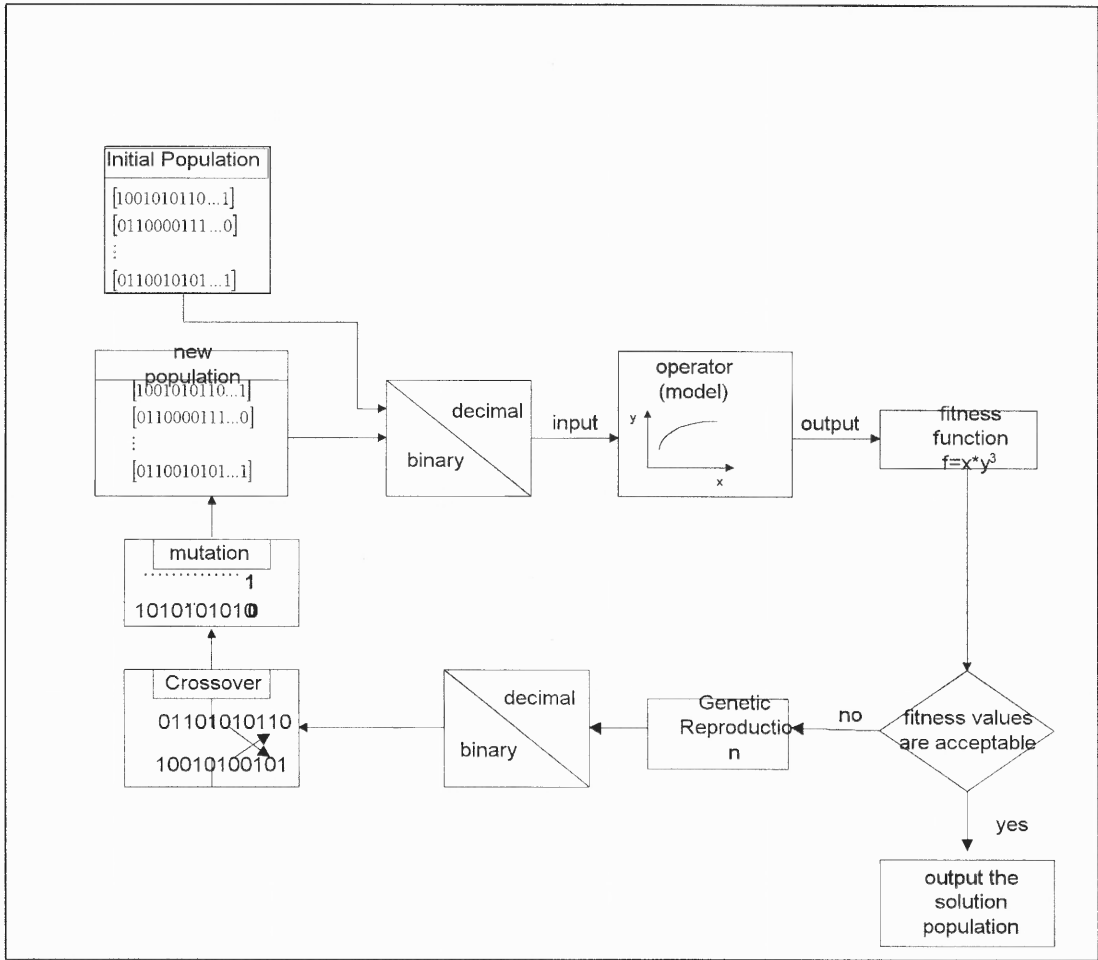
Figure 9. 2 Optimization Scheme with Genetic Algorithms

CHAPTER 10

DEVELOPMENT OF GENERIC APPROACH FOR PREDICTION OF RESULTS AND PARAMETER OPTIMIZATION OF WATERJET - BASED DECOATING PROCESS

10.1 Introduction

As the results of the performed research a formal procedure for planning of the waterjet cleaning was designed and demonstrated. The experimental study enabled us to identify the range of the application of waterjet technology for surface cleaning as well as to acquire a database for development of modeling and optimization techniques. The theoretical study resulted in the development of corresponding algorithms and computer codes. However, the ultimate goal of this research is to provide practitioners with an effective and practical approach for processing all information available to practitioner, regardless of the form and accuracy. This chapter deals with two important issues necessary for implementation of the above posed problem. First, a generic and easily obtainable coefficient characterizing any substrata - to be cleaned - deposit -to be removed must be identified and explained. Second, a generic modeling procedure, utilizing this surface coefficient must be identified and constructed. And, finally the suggested procedure must be tested on several experimental samples with different types of deposits.

10.2 Determination of the Erosion Strength

In our work the following approach was used to obtain a generic coefficient that would characterize any combination of substrata and deposit. Following the results available in the literature (Conn A.F., 1990) we define the area cleaning efficiency E_a as the ratio of area cleaned per unit time and power delivered by the nozzle (10.1).

$$E_a = \frac{\text{Area cleaned per unit time}}{\text{Power delivered by nozzle}} = \frac{\dot{A}}{P} \tag{10.1}$$

where area cleaning rate A is in m2/hour, and

$$P = \Delta p \cdot Q \tag{10.2}$$

where : Δp – pressure drop across nozzle,

   Q – is the flow rate;

Thus Ea has the units of [m2/Kw-hr], that is a unit area cleaned per unit of energy expended by the nozzle.

The idea of characterizing a material's ability to resist erosion is far from new. Thiruvengadam (1967) in his studies of cavitation erosion has suggested a concept of erosion strength that was based on a strain-energy absorption concept. Heymann (1970) has suggested a concept of relative erosion strength. Thus utilizing ideas of both Thiruvengadam and Heymann, Conn A.F., (1990) relates the area cleaning rate, A', an erosion strength for cleaning Sc and an erosive intensity I, for a given waterjet nozzle and

$$\dot{A} = \frac{I}{S_c} \tag{10.3}$$

and fixed set of waterjet parameters (water pressure, traverse rate, angle of impingement, standoff distance, etc.,) as:

Combining expressions 10.1 and 10.3 results in

$$E_a = \frac{I}{P \cdot S_c}$$
(10.4)

or

$$E_a \propto S_c^{-1}$$
(10.5)

The relation 10.5 is the basic relation, used to derive the curves, representing the dependence of the area cleaning efficiency Ea and erosion strength for cleaning Sc (Fig. 10.1).

10.3 Determination of the Erosion Strength based on the Available Cleaning Examples.

The available experimental database reflecting material decontamination with pure waterjet was compiled, and the area cleaning efficiencies were calculated for deposit types given in Table 10.1. The experimental procedures and results for the removal of two types of epoxy paint, rust removal (rust #1 entry in Table 10.1) oil-based paint removal from steel substrata were described in Chapters 7,8. The data in Table 10.1 was used to derive the relationships between area cleaning efficiency Ea and erosion strength for cleaning Sc (Figure 10.1). The point of departure for the line 276 - 310 MPa in Fig. 10.1 was the data for Item 1 from Table 10.1. The calculated cleaning efficiency for removal of deposit Epoxy #1 was assigned an Erosion Strength $Sc=10^3$, relative units. This line, per relation (10.5) was plotted at a slope 1:1 on log-log chart. The rest of the

data points on line 276-310 MPa were located based on calculated Area cleaning efficiencies and working water pressure.

To derive line for 138 MPa (Fig 10.1) items 1 and 2 were compared. Since the Erosion Resistance for the deposit type Epoxy #1 is known (Sc=1000 relative units) and is constant, the first point for line 138 MPa thus could be located. Similarly to derive the line for 70-100 MPa item #6 was located at the 138 MPa line and compared with item #7.

Table 10. 1 Cleaning Examples

Item	Deposit	WP	ND	Flow Rate	Area Cleaning Rate	Power Delivered by Nozzle	Area Clean Effect
	Type *	(MPa)	(mm)	m3/sec	(m2/hour)	Kw	m2/Kw-hr
1	Hard Epoxy	276	0.305	4.610E-05	0.52	12.71	0.0408
2	Hard Epoxy	138	0.305	3.260E-05	0.04	4.50	0.0085
3	Hard Epoxy	103	0.3556	3.837E-05	0.02	3.97	0.0048
4	Rust	310	0.254	3.391E-05	0.99	10.52	0.0938
5	Weak* Rust	310	0.1778	1.662E-05	0.52	5.16	0.1040
6	Oil Based	138	0.254	2.262E-05	0.69	3.12	0.2201
7	Oil Based	69	0.254	1.599E-05	0.17	1.10	0.1541
8	Weak Epoxy*	276	0.3554	6.259E-05	1.04	17.26	0.0603
9	Auto Paint*	138	0.254	2.262E-05	0.14	3.12	0.0434

* Deposits were used for model testing only.
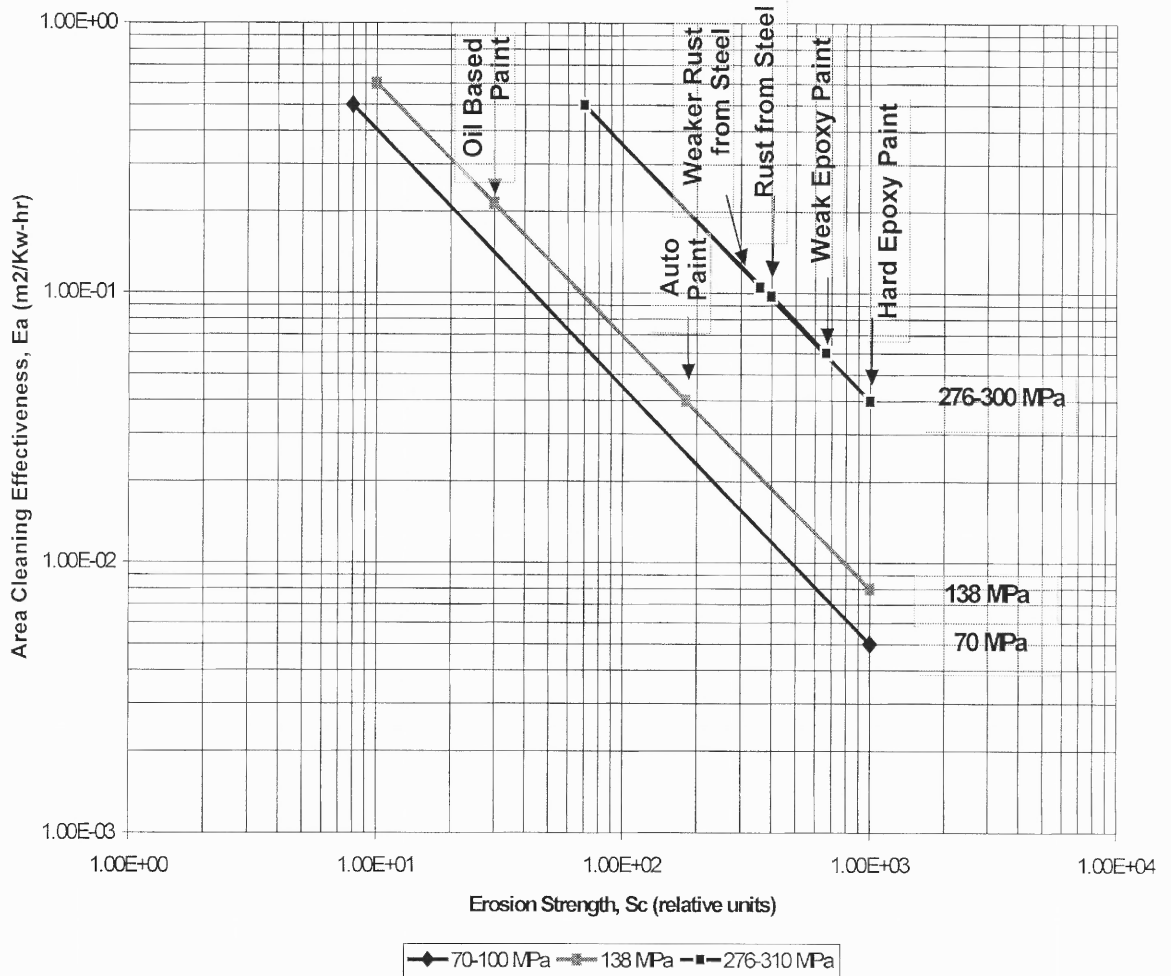
Figure 10. 1 Graphical Relationship Between Ea and Sc

The main result that could be inferred from the Graphical Relationship between the Area

Cleaning Efficiency Ea and Erosion Strength Sc shows that there is a definite relationship

between Ea and Sc and that Erosion Strength for cleaning of similar materials is closely

spaced together, and consequently the Sc coefficient can used to characterize an unknown

deposit-substrata combination. On the other hand, it should be emphasized, that relations

in Fig. 10.1 as was presented by Conn (199) and verified by our experimental studies do

not constitute an exact relation, at best they represent an order of magnitude comparison only.

10.4 Development of Generic Prediction Technique

The problem, that most of the waterjet practitioners face when dealing with an unknown surface is the lack of information about the process or in other words the unavailability of a generic technique that could be used as a first approximation of a process. This section is concerned with the development of such an approach. The idea behind such an approach is to combine the previous knowledge about the process in question and based on that, make an inform decision as to which waterjet parameters to apply, as a first approximation. We are using the notion of Erosion Strength (Sc) developed in the previous section to classify an unknown surface together with Neural Networks Fuzzy Reasoning technique, described in Chapter 5, for information processing.

The prediction technique construction begins with the development of fuzzy universe for Erosion Strength, Sc. The experimental database allows us to construct three fuzzy sets, based on the number of experimental situations available. The items 1,2,3,4,6,7, representing the removal of three basic deposit types (Hard Epoxy, Rust and Oil Based Paint) from Table 1 with corresponding Erosion Strengths 1000, 400 and 30 (from Chart 10.1) were assigned the degrees of membership of unity in either of three sets. Then the working space of the universe for Sc on a semi log scale was equally divided between the tree classes, as shown in Figure 10.2.
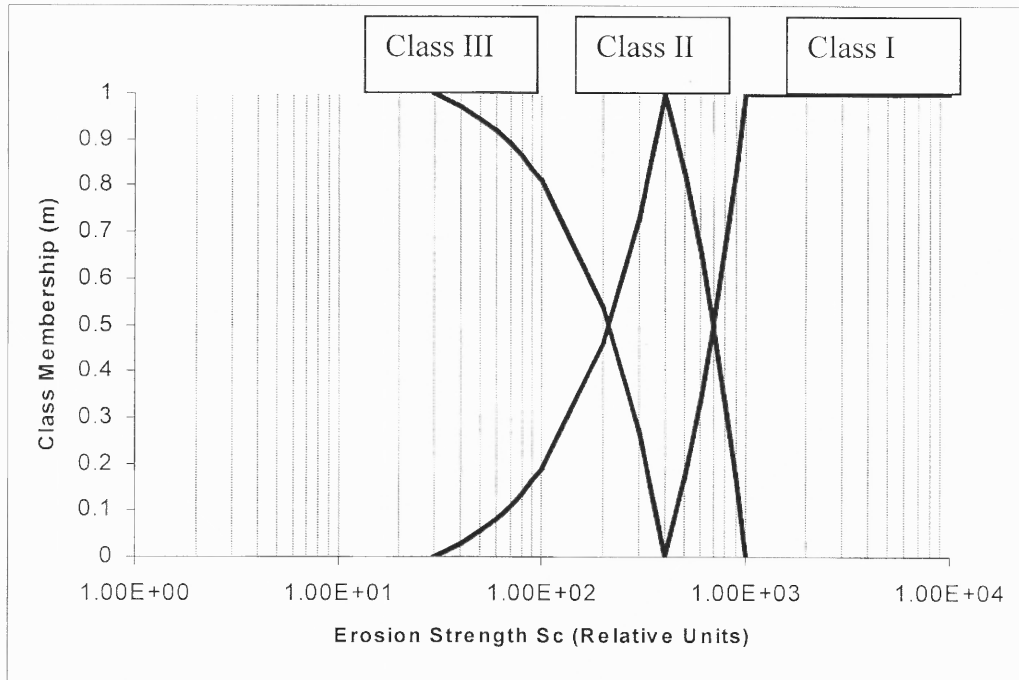
Figure 10. 2 The Fuzzy Universe for Erosion Strength Sc.

Thus each of the classes in Fig. 10.2 is represented (with degree of membership 1) by a specific deposit type available in our experimental database. In other words these three fuzzy sets cover the ranges of all possible values for the materials with erosion strength for cleaning from 1 to 10000 relative units. Similarly, if we identify a deposit substrata combination with some value of erosion strength, Sc, and this value happens to be inside the range [1,10000], then we can identify the degree of membership of such a deposit substrata combination in the three fuzzy sets (Fig. 10.2). This procedure alone can be very useful when trying to classify some unknown deposit-substrata combination.

It should be emphasized that for each of the three basic deposits an extensive experimental study was undertaken, as described in the previous chapters. Since we posses a required empirical knowledge for these processes, the appropriate numerical

representation of each process can now be made with the help of artificial neural networks. The procedure of the application of a neural network for process modeling and optimization was described in details in chapters 5, 7. Thus, after each network has been created, properly trained and tested we have obtained reliable numerical models for the three base deposits, or equivalently three fuzzy base classes of the universe Erosion Strength (Sc). Therefore, it can now be stated, that a process of material cleaning of material with erosion resistance coefficient in the range [1,10000] can now be approximated as some combination of the based models. The computational procedure follows the following steps. For an unknown deposit, a practitioner makes a simple experiment that allows him to calculate Area Cleaning Efficiency for a working water pressure. Then using the computed Ea we can determine the corresponding Erosion Resistance coefficient (Sc) for this surface from the Figure 10.1, for the given water pressure. Once a corresponding Sc coefficient was found, the fuzzy membership in the three classes on Fig. 10.2 can be determined. The above procedure can be described on example of the item number 8, Table 10.1. Separate experiments were made for the auto paint deposit removal with plain waterjet. The computed area cleaning efficiency was calculated as $E_{a\ auto\ paint}$ = 0.04 m2/Kw-Hr. From Figure 10.1 the corresponding coefficient Sc was found to be Sc=180 relative units. And from Figure 10.2, the degree of membership (μ) in the three basic classes can be calculated as $\mu_{(class\ I)}$ =0, $\mu_{(class\ II)}$ =0.4, $\mu_{(class\ III)}$ =0.59. These degrees of membership can be interpreted as follows. The Erosion Resistance of the Auto Paint deposit is approximately midway between that of the Hard Epoxy Paint and rust deposit. Now that the surface was identified we could use the base models given by the neural networks to get a first approximation to the process. We

supply a set of input parameters (Water Pressure, Nozzle Traverse Rate, Nozzle Diameter, and Standoff Distance) as an input into the base models represented by the neural nets. The corresponding output in terms of the single strip width is obtained by each of the network. The final result is obtained by defuzzifing the output according to Eq. 10.6.

$$y_i^* = \frac{\sum_{s=1}^{r} \mu_{A^s}(x_i) \cdot u_S(x_i)}{\sum_{s=1}^{r} \mu_{A^s}(x_i)} \ , i = 1,2 \ldots n \tag{10.6}$$

In equation 10.6 μ - is the membership value of a deposit with Erosion Strength Sc in the three base classes, Us - is the output of the sth neural network, and y* is the final defuzzified output.

The output of the model is the single clean width of the strip produced on the surface by the supplied combination of the input parameters, which then can easily be converted to process productivity. This procedure is sketched on Figure 10.3.

10.5 Experimental Verification of Performance

In order to experimentally verify the suggested modeling approach an additional experimental database was acquired. The experimental samples consisted of the three types of deposits - auto paint, weaker rust, and weak epoxy paint, (items 5,8,9 Table 10.1). Waterjet parameters varied in these additional experiments were limited to the water pressure, nozzle traverse rate, standoff distance, and nozzle diameter. Experimental setup and procedures were similar to those described in the previous chapters. Area

cleaning efficiencies for removal of these deposits was used to identify the corresponding erosion resistance coefficient from Fig. 10.1, and the degrees of belonging of these deposits to the three base classes were identified with the help of Figure 10.2. Table 10.2 shows the results for the test deposits along with the deposits representing the base classes.
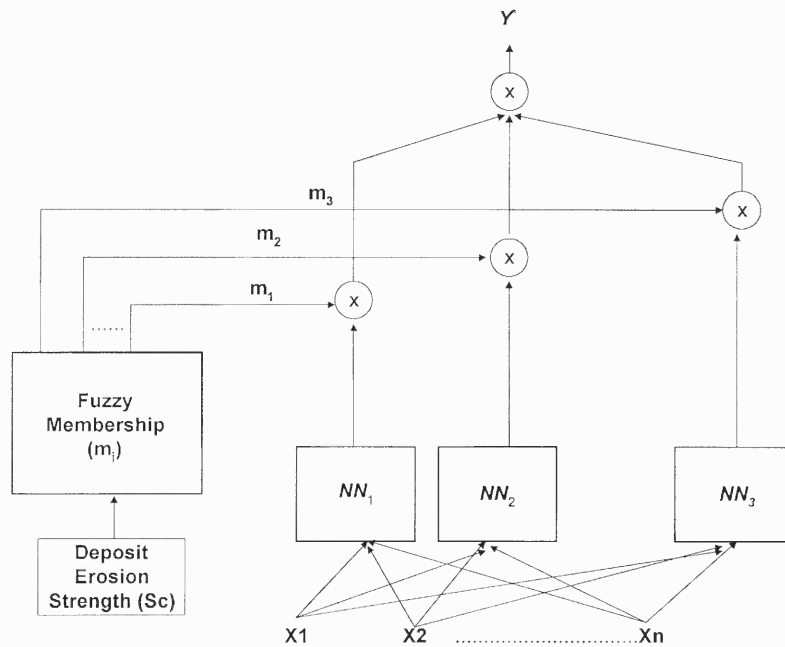
Figure 10. 3 Generic Modeling Approach.
NN1, NN2, NN3 - Artificial Neural Network models for the three base classes.
X1, X2, …, Xn - Process input variables.

The model performance was tested on each of the test deposits by providing the model with a set of waterjet input parameters within the working space (delimited by equipment capabilities), obtaining the corresponding output in terms of the single width of strip and comparing the results with experiments.

Table 10. 2 Cleaning Samples

				Degree of Membership		
N	Deposit	Area Cleaning Efficiency (m2/Kw-hr)	Erosion Strength (Relative Units)	Class I	Class II	Class III
1	Hard Epoxy Paint	0.04	1000	1	0	0
2	Weak Epoxy Paint	0.06	665	0.41	0.58	0
3	Rust from Steel	0.0975	400	0	1	0
4	Weaker Rust from Steel	0.105	360	0	0.89	0.1
5	Auto Paint	0.04	180	0	0.4	0.59
6	Oil Based Paint	0.21	30	0	0	1

10.6 Discussion of Results

The model for prediction of the results of waterjet cleaning described in the previous sections was tested on several additional test deposits. Figures 10.4 - 10.9 present the results of prediction. Analyzing the results, it is clear that the model prediction results are acceptable at both relative error of prediction (~20 %), and at following the trend of the process, which is also important for any cleaning study. Although a relative error of prediction may at the first glance be considered high, it should be kept in mind that standard deviation of experimental measurements was in the vicinity of 25 ~ 30 %, and it really is difficult to expect the model performance to be more accurate then that. Nevertheless, as a first estimation of a cleaning productivity for a given type of deposit, these results constitute a reasonable approximation. Furthermore, since it is shown that the model is also capable of predicting the trend of the process, meaning that the change in one independent input results in, say, increase of the output, allows using this model for the process optimization. We suggest using the Genetic Algorithms for this purpose.

However it should be noted, that at the current stage the prediction technique was tested only in the middle of the problem space. At the outskirts of the problem space the veritable results could not be obtained. The reason for this lies in the limitations in the development of the three base models. Since the ranges of experimental parameters used for the construction of models were different in each case, and there was no coordinated experimental setup, but rather the data was compiled at later stages, there are inconsistencies in choosing the levels of process parameters in case of a test cleaning space. These inconsistencies are due to the poor ability of neural networks to extrapolate. For example, if for a base model development the rate of nozzle traverse was in the range from 1000 mm/min to 2500mm/min, and a test cleaning case was run at 1500~4000 mm/min, the reliable model performance will be in the intersection of these ranges. The way to cure the above problem is to cover all the parameter space (limited by equipment capabilities) for each process variables in all the base models. Of course it results in quite extensive experimentation, but on the good side it needs to be done only once, when developing the base models. Also the current model does not cover the full range of all possible erosion strength of different materials, but by extending the procedure with additional base models for lower or higher degrees of erosion strength for cleaning (Sc), this limitation can be reduced or eliminated.

10.7 Conclusion

The presented modeling approach of results of waterjet cleaning process, allows a user to obtain a reliable process approximation given no or limited information about process condition. For an unknown surface a practitioner needs to determine a single coefficient,

the erosion strength for cleaning (Sc), based on a simple experiment(s). The proposed approach utilizes this coefficient and approximates the cleaning results in terms of process productivity. It is believed that the current work will assist in practical implementation of waterjet cleaning technology, where the information deficiency on process conditions is the main reason of ineffective and low quality results.
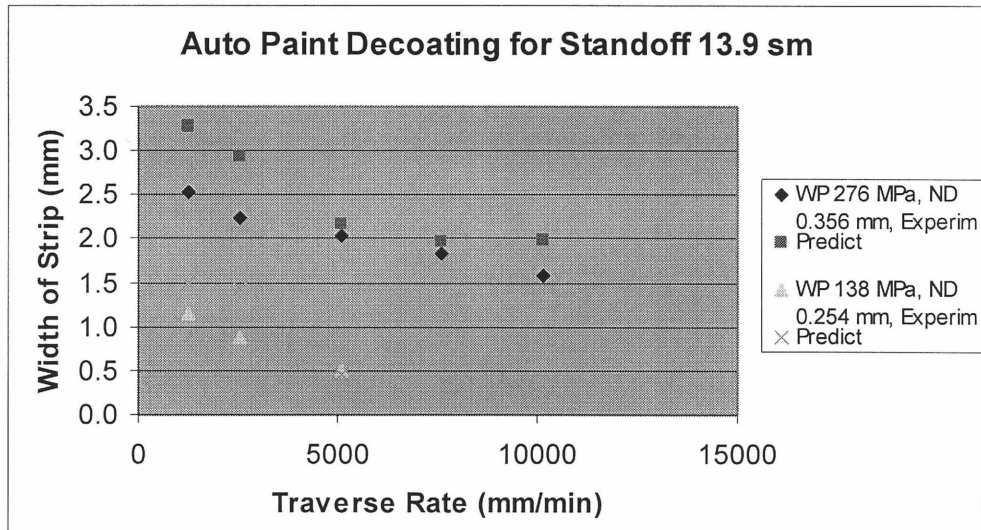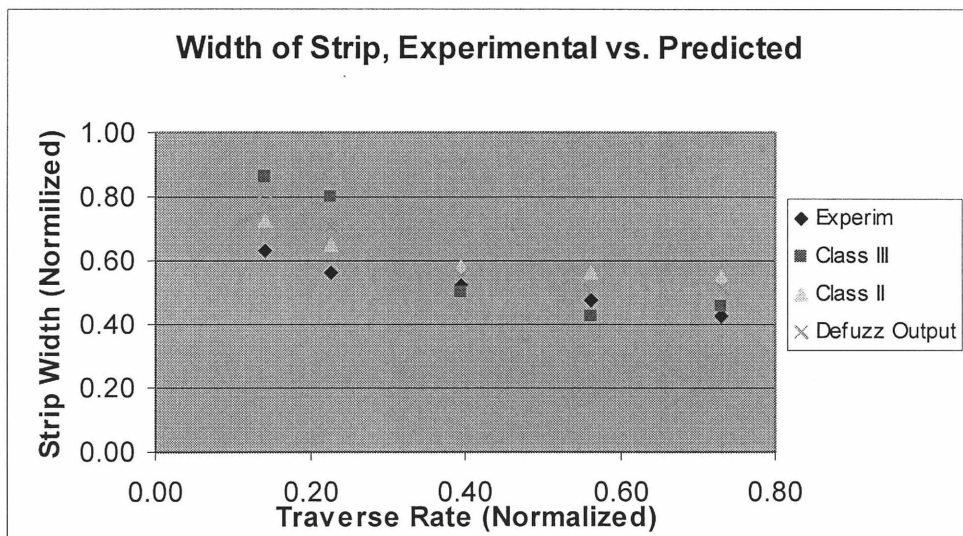
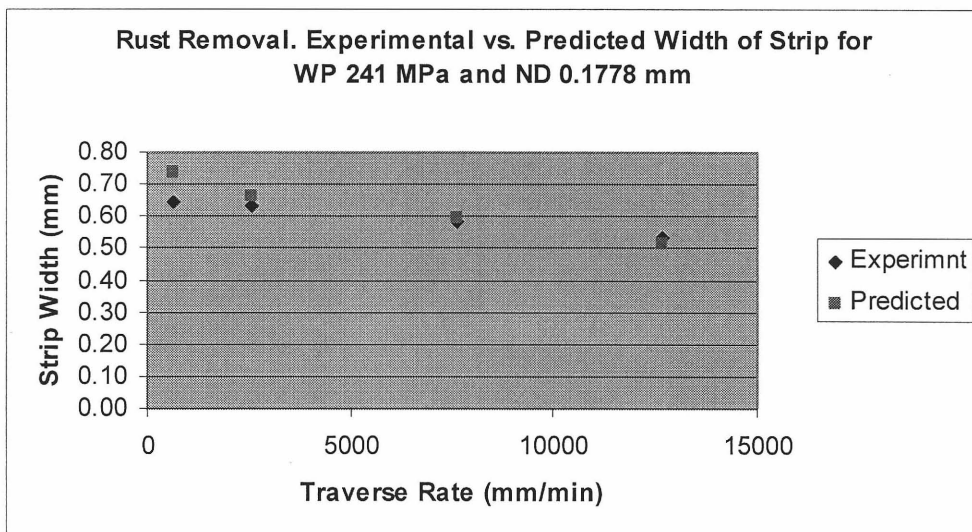**Figure 10.4** Auto Paint Removal

Figure 10. 5 Auto Paint Removal
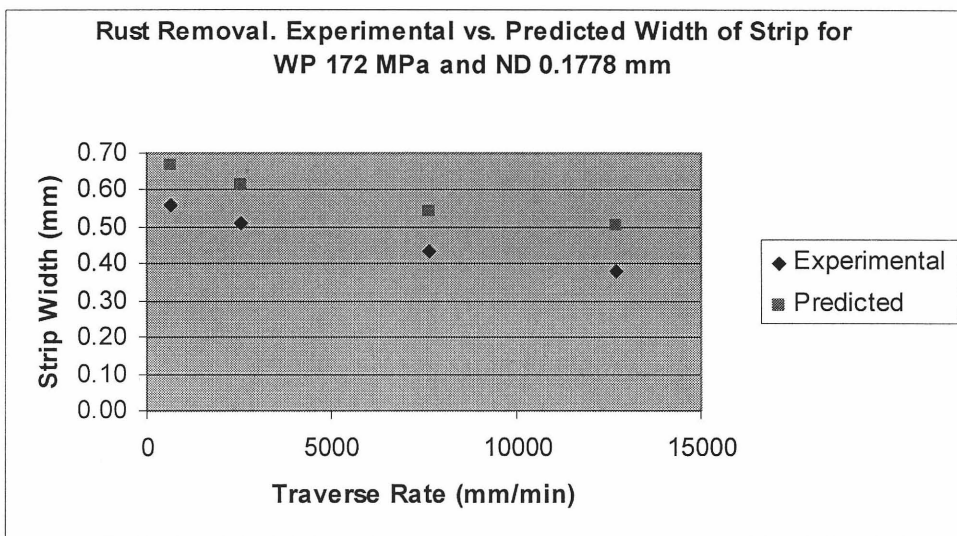
Figure 10.6 Removal of Weak Rust

Figure 10.7 Removal of Weak Rust
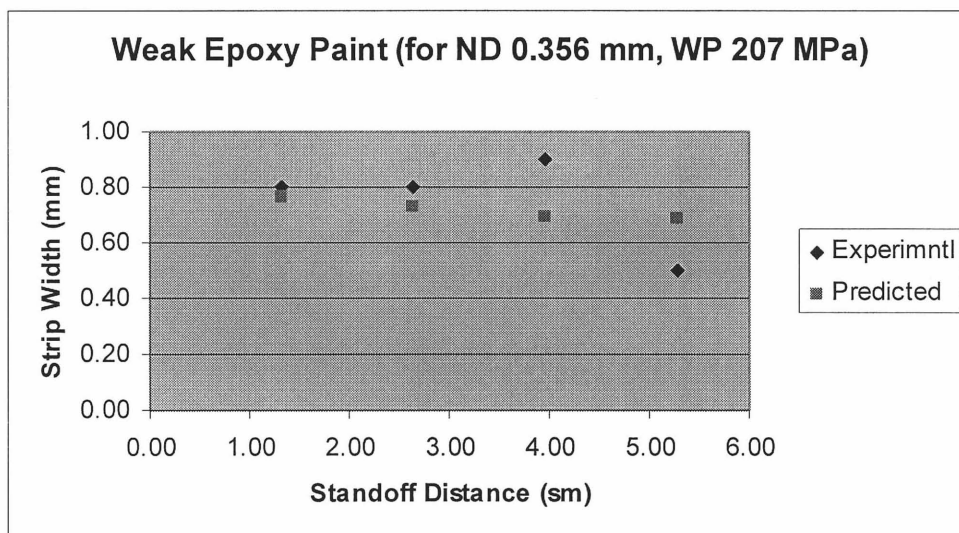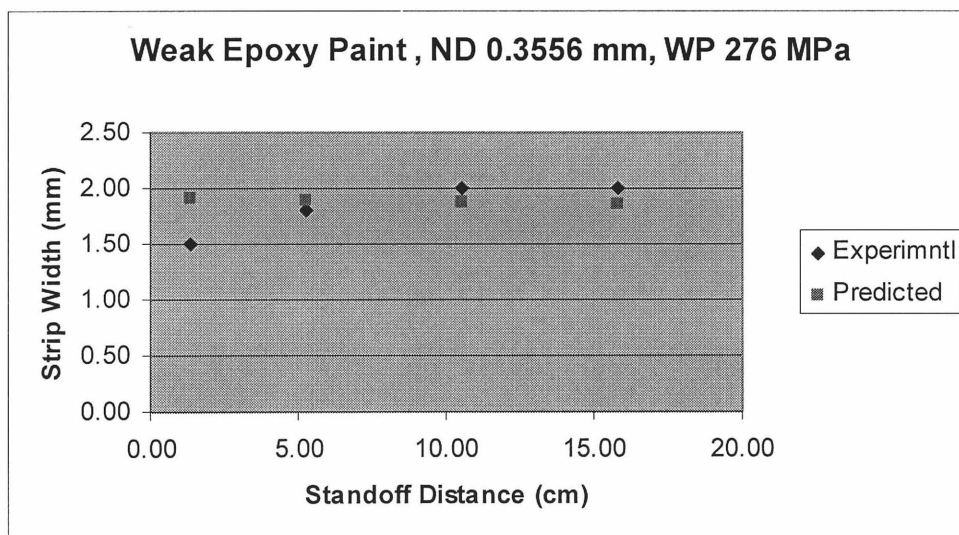
Figure 10.8 Removal of Weak Epoxy

Figure 10.9 Removal of Weak Epoxy

CHAPTER 11

CONCLUSIONS AND RECOMMENDATIONS

11.1 Conclusions

The mission of this study was the investigation of the jet based material decontamination. Our specific objective was to develop a practical numerical procedure for selection of the optimum process parameters at given process constraints and available knowledge about process conditions. This work has pioneered in directing attention on the problems of information utilization in the course of waterjet based material decontamination. The effective methodologies of information processing, with ability to effectively process chaotic, qualitative and quantitative information, were suggested. A practical method for prediction of cleaning results for an unknown surface-substrata combination was suggested. More specifically, the following results and conclusions were obtained as the outcome of this study:

1. The problem of information deficiency and chaotic nature of information about process conditions in the course of material cleaning with high-pressure waterjets was overcome with the help of techniques of Artificial Intelligence (AI). The detailed procedure of application of Fuzzy Logic, Artificial Neural Networks and Genetic Algorithms was presented. The application of these AI techniques was shown to greatly enhance the information utilization in the course of waterjet material cleaning.

2. The generic procedure for modeling and optimization of waterjet cleaning using a single non-dimensional coefficient characterizing an unknown surface was

197

developed. It was shown that the prediction obtained with the developed approach agrees well with experimental results for the tested deposits within defined parametric space of process variables.

3. A feasibility of application of high-pressure waterjet for decontamination of highly sensitive surfaces was demonstrated, and effective ranges of process parameters were identified.

4. An extended database representing removal of various types of industrially important deposits using a high-speed waterjet was compiled. The database included removal of different types of paint (epoxy and oil based), removal of rust from steel surface, removal of viscose deposits (simulated with a roofing tar), by using plain and media assisted waterjets. This database will be used as a reference for wide variety of cleaning cases by industrial practitioners.

5. According to industrial information, the existing practice, at least in the US, rejects the feasibility of pure water for derusting operations. Existing practice of derusting is entirely based on the use of sand blasting, or the use of chemicals. Our experiments demonstrate the feasibility of environmentally friendly jet based derusting operations, while the exploited analytical techniques provided the realistic ranges of operational conditions.

6. Numerical solutions of turbulent flow inside a waterjet nozzle was obtained. Two types of nozzles were considered in the study: primary nozzle and a waterjet nozzle in assembly. The numerical prediction of jet velocity profiles and the interface between the two phases (water - air) inside a nozzle were in a good agreement with

experimental data available in the literature. Thus the current problem setup and the results of simulations can be applied to improvement of the nozzle design.

11.2 Recommendations

For future work we recommend:

1. To extend the available cleaning database for wider ranges of non-dimensional Erosion Resistance coefficient. Incorporating the extended database into the developed modeling technique of waterjet cleaning will result in prediction technique with more flexible practical usage.

2. To develop a software package on the base of the developed modeling technique for facilitation of the practical implementation of waterjet based cleaning technology.

3. To obtain an optimized nozzle design based on the results of the numerical simulations of the flow inside the nozzle presented in this study.

4. To design a practical waterjet based system for precision cleaning of sensitive surfaces.

5. To consider a practical implementation of the environmentally benign cleaning technology as an urgent and achievable task.

BIBLIOGRAPHY

Amano, R.S. and Neusen, K. F. 1982. "A Numerical and Experimental Investigation of High-Velocity Jets Impinging on Flat Plate." 6th *International Symposium on Jet Cutting Technology*. 6: c3.107-c3.122.

Babets, K., Geskin, E. S., Chaudhuri B. 1999. "Neural Network Model of Waterjet Depainting Process", *10th American Waterjet Conference*, Houston, TX.

Babets, K., Geskin, E. S. 1999. "Optimization of Jet Based Material Decontamination", *International Symposium on New Applications of Water Jet Technology*, Ishinomaki, Japan.

Babets K., Geskin, E. S. 2000. "Application of Fuzzy Logic for Modeling of the Waterjet Paint Stripping", *An International Journal of Machining Science and Technology*, Volume 4, Number 1.

Babets, K., Geskin, E.S. 2000. "Optimization of Energy Utilization in the Course of Material Processing", *International Symposium on Advanced Thermodynamics and Energy Utilization*, ECOS 2001.

Conn, A., Johnson, V., Lindenmuth, W., Chahine, G., Frederic, G., 1976. "Some Unusual Applications for Cavitating Waterjets", *Third International Symposium on Jet Cutting Technology*, Chicago, USA.

Conn, A., 1990. "A Relative Cleanability Factor", *Proceedings of 10th International Symposium on Jet Cutting Technology*, BHRG Fluid Engineering.

Conn, A., Chahine, G., 1995. "Ship Hull Cleaning with Self-Resonating Pulsed Waterjets", *Third American Waterjet Conference*, Pittsburgh, USA

Chakravarthy, P., Babu, A., Babu, N. 1998. "A Fuzzy Based Approach for Selection of Process Parameters in Abrasive Waterjet Cutting of Black Granite", *5th Pacific Rim International Conference on Waterjet Technology*, New Delhi, India.

Chen W-L., Geskin E.S. 1990. "Measurements of the Velocity of Abrasive Waterjet by the Use of Laser Transit Anemometer", *Proceedings of 10th International Symposium on Jet Cutting Technology*, BHRG Fluid Engineering.

Chen W-L. 1990. "Correlation Between Particle Velocities And Conditions Of Abrasive Waterjet Formation", *Ph.D. Dissertation*, New Jersey Institute of Technology.

BIBLIOGRAPHY
(Continued)

Cox, E. 1994. "The Fuzzy Systems Handbook: a Practitioner's Guide to Building, Using, and Maintaining Fuzzy Systems", *AP Professional*.

Eddingfield, D. L., Evers, J. L., and Setrok, A. 1981. "Mathematical Modeling of High Velocity Water Jets." *1ˢᵗ U.S. Waterjet Conference*. 1: I-3.1 – I-3.14.

Erdman-Jesnitzer, F., Hassan, A. M., and Louis, H. 1976. "A Study of The Oscillation Effects on The Cleaning And Cutting Efficiency of The High Speed Waterjets", *Proceedings of the Third International Symposium on Jet Cutting Technology*, Chicago, USA.

Erdman-Jesnitzer, F., Louis, H. and Wiedemeier, J. 1978. "Material Behavior, Material Stressing, Principal Aspects in The Application of High Speed Water Jets" *Proceedings of 4ᵗʰ International Symposium of Jet Cutting Technology*, BHRA, Canterbury, England.

Erdman-Jesnitzer, F., Louis, H. and Wiedemeier, J. 1980. "The Action of High Speed Waterjets on Material Measurements Methods and Their Practical Application, a Critical Review." *Proceedings of 5th International Symposium of Jet Cutting Technology*, BHRA Hanover, F.R. Germany.

Galecki, G. and Vickers, G. 1982. "The Development of Ice Blasting for Surface Cleaning." *Proceedings of 6ᵗʰ International Symposium of Jet Cutting Technology*, Guildford, England, pp. 59-80.

Hashish, M. 1991. "Optimization Factors in Abrasive- Waterjet Machining", *Journal of Engineering for Industry*, Vol. 113, pp. 29-37.

Hashish, M. 1993. "Prediction Models for AWJ Machining Operations." *Proceedings of the 7ᵗʰAmerican Water Jet Conference*, Seattle, Washington, pp. 205-216.

Harbaugh, D.J. and Fincher, H. 1993. "Waterjet Nozzle Design for Complex Surfaces.", *Proceedings of 7ᵗʰ American Waterjet Conference*, Seattle, Washington.

ISO 8501 – 1: 1988, Edition 3.

Johnson, S. T. 1993. "Advances in Cleaning and Coating Removal Using Ultra-High Pressure Water Jet Technology." *Proceedings of the 7ᵗʰ American Water Jet Conference*, Seattle, Washington.

Jun, H., 1993. *Proceedings of the 7ᵗʰ American Waterjet Conference*, Volume 2, pp. 643-653, Seattle, Washington.

BIBLIOGRAPHY
(Continued)

Khan, E. 1989. "Investigation of the Dynamics of Abrasive Waterjet Formation." *MS Thesis*, New Jersey Institute of Technology.

Kang, S., Reitter, T., Carlson, G. 1993. "Target Response to the Impact of High-Velocity Non- Abrasive Waterjet." *Proceedings of 7th American Water Jet Conference*, Seattle, Washington.

Kovacevich, R., Hashish, M., Mohan, R., Ramulu, M., Kim, T., Geskin, E.S. 1997 "State of the Art Research in Abrasive Waterjet Machining." *Journal of Manufacturing Science and Engineering*, Vol. 119, pp. 776-785.

Launder, B.E., and Spalding, D.B. 1972. "Lectures in Mathematical Models of Turbulence." *Academic Press*.

Louis, H., Schicorr, W. 1982. "Fundamental Aspects in Cleaning with High Speed Water Jets." *Proceedings of the 6th International Symposium on Jet Cutting Technology*, BHRA, Guildford, England.

Lai, M.K.Y., Vijay, M.M., Zou, C. 1991. "Computational Fluid Dynamics Analysis of Submerged Cavitating Water Jets." *Proceedings of the 6th American Waterjet Conference*, Waterjet Technology Association, St. Louis, Missouri.

Laurinat, A., Louis, H., Meier- Wiechert, G. 1993. "A Model for Milling with Abrasive WaterJets." *Proceedings of the 7th American Water Jet Conference*, Seattle, Washington.

Liu, B., Jia, B., Zhang, D., Wang, C., Li, H., Yao, H. 1993. *Proceedings of the 7th American Waterjet Conference*. Volume 2, pp. 629-643, Seattle, Washington.

Leu, M., Geskin, E., Meng, P., Tismenetskiy, L., Uschitsky, M. 1994. "Waterjet in-Situ Cleaning." *Report to IAB Meeting of the Emission Reduction Research Center*, The Pennsylvania State University, PA.

Li F. 1996. "Experimental and Numerical Investigation of Abrasive Waterjet Polishing Technology." *Ph.D. Thesis*, New Jersey Institute of Technology.

Masters, T. 1993. "Practical Neural Network Recipes in C++." *Academic Press*.

Mabrouki, T., Cornier A., Raissi, K. 1998. "The Study of HP Pure Waterjet Impact as the Primary Mechanism of Paint Decoating Process." *Proceedings of the 14th International Conference on Jetting Technology*. Brugge, Belgium.

BIBLIOGRAPHY
(Continued)

Meng, P., Geskin, E., Tismenetskiy, L and Leu, M. C. 1995. "Improvement of the Waterjet Based Precision Cleaning Technology." *Proceedings of 8t^h American Water Jet Conference*. Houston, Texas.

Meng, P., Geskin, E., Tismenetskiy, L. 1996(a). "Cleaning with High Pressure Directed Waterjets." *Proceedings of Japan-USA Symposium on Flexible Automation*, Boston, MA.

Meng, P., Leu, M.C., Geskin, E.S. and Tismenetskiy, L. 1996(b) "Mathematical Modeling and Experimental Verification of Stationary Waterjet Cleaning Process." *ASME Journal of Manufacturing Science and Engineering*.

Meng, P., Leu, M.C., Geskin, E.S. and Tismenetskiy, L. 1996(c) "An Analytical and Experimental Study of Cleaning with Moving Waterjets." *ASME Journal of Manufacturing Science and Engineering*.

Meng, P. 1996. "Experimental and Analytical Investigation of Water Jet Cleaning Process", *Ph.D. Dissertation*, New Jersey Institute of Technology.

Midden, C., Domann, H. and Aust, E. 1990. "Robot Guided Waterjet Cleaning for Subsea Applications." *Proceedings of the 10th International Symposium on Jet Cutting Technology*, Amsterdam, Holland, Paper E2.

Michalewicz, Zbigniew. 1996. "Genetic Algorithms + Data Structures = Evolution Programs." *Springer*. Third Edition.

Neusen K.F., Alberts, D.G., Gores and Labus T.J. 1990. "Distribution of Mass in a Three-Phase Abrasive Waterjet Using Scanning X-Ray Densitometry." *Proceedings of 10th International Symposium on Jet Cutting Technology*, BHRG Fluid Engineering, Amsterdam, Netherlands.

Neusen K.F., Gores T.J., Labus T.J. 1992. "Measurement of Particle and Drop Velocities in a Mixed Abrasive Waterjet Using a Forward-Scatter LDV System." *Jet Cutting Technology*, Kluwer Academic Publishers.

Osman A.N., Buisine D., Thery B., Houssaye G. 1996. "Measure of Air Flow Rate According to the Mixing Chamber Designs." *Proceedings of 13th International Conference on Jet Cutting Technology*, Sardinia, Italy.

Ross, Timothy J.1995. "Fuzzy Logic With Engineering Applications." McGraw-Hill.

BIBLIOGRAPHY
(Continued)

Raissi K, Cornier A., Kremer D., Simonin O. 1996. "Mixing Tube Geometry Influence On Abrasive Waterjet Flow." *Proceedings of 13th International Conference on Jet Cutting Technology*, Sardinia, Italy.

Singh, P. J., Munoz, J., Chen, W.L. 1992. "Ultra-High Pressure Waterjet Removal of Thermal Spray Coatings." *Proceedings of 11th International Symposium on Jet Cutting Technology* BHRA, Dordrecht, Netherlands.

Saunders, D.H., Barton, R.E.P. 1986. "The Use of Fan-Shaped Water Jets in Preference to Straight Jets to Remove a Paint Coating." *Proceedings of 8th International Symposium on Jet Cutting Technology*, pp. 353-362, Durham, England.

Schicorr, W., Louis, H. 1982. "Fundamental Aspects in Cleaning with High Speed Water Jets." *Proceedings of the 6th International Symposium on Jet Cutting Technology*, pp. 217-228, Guildford, England.

Shegxiong, X., Wangping, H., Sheng, Z., Da-jun. 1993. *Proceedings of the 7th American Waterjet Conference*, Volume 2, pp. 653-663, Seattle, Washington.

Suryanarayana, C., and Norton, M.G. 1998. "X-Ray Diffraction, a Practical Approach." *Plenum Press*, New York.

Sawamura T., Fukunishi Y., Kobayashi R. 1999. "The Effects of the Abrasive Flow Rate on Abrasive and Water Velocities." *Proceedings of the International Symposium on New Applications of Water Jet Technology*, Ishinomaki, Japan.

Thiruvengadam, A. 1966. "The Concept of Erosion Strength." *Erosion by Cavitation or Impingement*, American Society for Testing and Materials, ASTM.

Takagi H, Hayashi I. 1991. "NN-Driven Fuzzy Reasoning." *International Journal of Approximate Reasoning*, Vol. 5, No. 3, pp. 191 – 212.

Tazib A., Schmitt A., Parsy F., Abriak N., Thery B. 1994. "Effect of Air on Acceleration Process in AWJ Entrainment System." *Proceedings of 12th International Symposium on Jet Cutting Technology*, Rouen, France.

Tsoukalas, L., Uhrig, Robert E. 1997 'Fuzzy and Neural Approaches in Engineering." *John Wiley & Sons*.

United States Environmental Protection Agency, Office of Research and Development. 1994. "Guide to Cleaner Technologies." *EPA/625/R-93/015*,Washington DC 20460.